NASA TECHNICAL NOTE

NASA TN D-5107

c. 1

NASA TN D-5107

TECH LIBRARY KAFB, NM

0131836

LOAN COPY: RETURN TO
AFWL (WLIL-2)
KIRTLAND AFB, N MEX

ON LATERAL CABLE OSCILLATIONS OF CABLE-CONNECTED SPACE STATIONS

by Willard W. Anderson

Langley Research Center
Langley Station, Hampton, Va.

NATIONAL AERONAUTICS AND SPACE ADMINISTRATION • WASHINGTON, D. C. • MARCH 1969

TECH LIBRARY KAFB, NM

0131836

ON LATERAL CABLE OSCILLATIONS OF CABLE-CONNECTED SPACE STATIONS

By Willard W. Anderson

Langley Research Center
Langley Station, Hampton, Va.

NATIONAL AERONAUTICS AND SPACE ADMINISTRATION

For sale by the Clearinghouse for Federal Scientific and Technical Information
Springfield, Virginia 22151 – CFSTI price $3.00

ON LATERAL CABLE OSCILLATIONS OF CABLE-CONNECTED SPACE STATIONS

By Willard W. Anderson
Langley Research Center

SUMMARY

The influence of lateral cable oscillations on a spinning cable-connected space station is defined in terms of steady-state and transient response to torques acting on the space station. The system is defined by using linear rigid-body equations and a dual formulation of the cable modes. Damping is included in the dual formulation and estimates of this damping are provided. The analysis allows a determination of the required depth of modeling for a given system in terms of the system parameters and the expected disturbances. Energy flow within the system is discussed by using a system bond graph.

INTRODUCTION

The equations of motion of a rotating cable—counterweight—space-station system in a gravitational field gradient are extremely complex and nonlinear. A complete solution of these equations is therefore not feasible and thus the requirement exists that assumptions be made which reduce the mathematical problem to a level where solution is possible.

This paper represents an attempt to define one aspect of the system, namely the lateral oscillation of the connecting cable and in particular the effect of this oscillation on the dynamic response of the space station and counterweight. Coupling between lateral and longitudinal oscillation is not included. The influence of the gravitational field and of the angular momentum of the system is not directly included. The variation of cable tension is neglected and only linear equations are used in defining the solutions. Low cable curvature arises from high-velocity lateral cable waves. Cable lengths are assumed to be less than 2 statute miles (3.2 km) and space-station and counterweight mass, geometry, and inertia are assumed to be of equal order of magnitude. These are important simplifications (refs. 1 and 2) which can influence the results, but they have been made in order to define clearly the basic character of the interaction between lateral cable modes and the space station and counterweight and in particular the effect of lateral cable forces on the attitude of the space station and counterweight. The analysis and description are presented in terms of easily calculable frequency parameters which refer

to uncoupled-cable and massless-cable systems. The dual modal formulation is required, rather than the formulations of earlier papers.

SYMBOLS

A	cable cross-sectional area (see eq. (8))
A,B,C	X-, Y-, and Z-axis rigid-body inertias
A,B,C,D,E,F	steady-state parameters
A_1,A_2	cable attachment lengths
c	cable phase velocity
E	cable complex modulus
E'	cable storage modulus
E''	cable loss modulus
e	power bond effort
e	base of natural logarithms (see, for example, eqs. (C6) and (D4))
F_1,F_2	Z-direction disturbance forces
f	power bond flow
g_n	cable mode spatial functions
h_n,h_n^*,h_n^{**}	cable mode time functions
I	cable area inertia
I_1,I_2	system inertias
$i = \sqrt{-1}$	

J_1, J_2	system inertias (see eqs. (D2))
K_1, K_2	system stiffnesses
k	cable wave number
L, N, P, Q	steady-state parameters
l	cable length
M_c	cable bending moment
M_o, M_1, M_2, M_x, M_z	disturbance torques
m	bond graph modulus
m_1, m_2	system masses
n	modal index
P_1, P_2	X-direction disturbance forces
r	cable damping parameter
r_c	cable radius
s	cable coordinate
T	cable tension
T_1, T_2	disturbance torques
t	time
U_1, U_2, U_3, U_T	system energies
$u_s(t)$	unit step function

u_1, u_2	system translations
V	cable shear force
v_o, v_1, v_2, v^*	system translations
X, Y, Z	system axes
x, y, z	system coordinates
$\alpha_x, \alpha_y, \alpha_z$	rigid-body attitudes
$\gamma_1, \gamma_2, \gamma_3, \gamma_4$	steady-state phase angles
ϵ	cable ratio parameter
η	lateral cable displacement
$\theta_o, \theta_1, \theta_2, \theta_3$	system attitudes
ρ_n	cable modal damping coefficient
ρA	cable mass per unit length (ρ in this case denotes mass density)
σ	cable tensile stress
$\varphi_1, \varphi_2, \varphi_3$	system attitudes
ψ	lateral cable displacement
Ω_o	spin frequency or velocity
Ω_1, Ω_2	uncoupled system frequencies (see eqs. (D2))
ω	forcing function frequency
ω_n	cable mode frequencies

Subscript:

max maximum

Dots over symbols indicate derivatives with respect to time. Primes indicate derivatives with respect to distance.

DESCRIPTION OF PHYSICAL SYSTEM

The basic configuration of the physical system is shown in figure 1. The three portions of the system are the space station $\left(\text{mass} = m_1,\ \text{inertia} = I_1\right)$, the counterweight $\left(\text{mass} = m_2,\ \text{inertia} = I_2\right)$, and the cable (mass per unit length = ρA, damping parameter = r, tension = T). The X,Y,Z axes system is also shown. A cable coordinate s is assumed to be approximately equal to y. The axes system rotates approximately with the physical system about the Z (spin) axis at the angular velocity Ω_0. System geometry is defined by the cable length l and the distances A_1 and A_2 from space-station and counterweight centers of mass to cable attachment points. The space-station and counterweight inertias about the X- and Z-axis are assumed to be approximately equal, within the stability assumptions of appendix A.

Crew-motion disturbances are defined by the X- and Z-direction forces P_1, P_2, F_1, and F_2 and by the torques M_1, M_2, T_1, and T_2. Space-station and counterweight attitudes and translations are φ_1, φ_2, u_1, and u_2 for the XY plane (fig. 2) and θ_1, θ_2, v_1, and v_2 for the YZ plane (fig. 3). Lateral cable displacements are $\psi(s,t)$ for the XY plane and $\eta(s,t)$ for the YZ plane.

The system is further described in a later section in terms of effort and flow power variables by using bond graph techniques.

DISCUSSION OF EQUATIONS OF MOTION

If the effects of cable mass and cable damping are negligible, the equations required to define the motion of two rigid bodies (space station and counterweight) connected by a cable contain 12 variables (if positive cable tension is assumed and constraints are neglected). The 12 variables represent six degrees of freedom for two rigid bodies. These equations would be highly coupled and nonlinear. However, if the motion of the bodies relative to the rotating axes system of figure 1 is small and the system rotates slowly, the nonlinearity and coupling can be neglected. With this simplified system description the effects of cable mass and damping can be easily added. This constitutes the approach used in developing the system equations presented herein.

In appendix A the rigid-body Euler or low-frequency characteristics of the system are discussed and basic inertial requirements are placed on the system from stability and "stiffness" considerations. The conclusions of appendix A are that the rigid-body constant-spin-velocity assumption is valid, that the Z-axis rigid-body coupling rate is small, and that the rigid-body X-axis attitude can be described with a stable second-order equation.

Appendix B contains derivations of the system equations of motion where the cable lateral forces are considered in a general form. The derivation for the YZ plane begins with the rigid-body equation for X-axis attitude, the first of equations (A4). Disturbances and equations of motion for the Y-axis are not included since they do not directly influence the lateral cable motion. The equations of motion for the XY (spin) plane are shown to be identical to those for the YZ plane for high-frequency response, for systems where the flexible-body mode frequencies are well above the spin frequency Ω_o.

Appendix C contains a derivation of the cable equations of motion and a dual formulation of these equations in modal form, including equations for predicting the damping parameters for the modes as functions of the cable geometry and material. The final linear equations for the YZ plane which constitute a linear mathematical description of the physical system are

$$\left.\begin{aligned}
m_1\ddot{v}_1 &= F_1 + T\frac{\partial\eta}{\partial s}(0,t) \\
m_2\ddot{v}_2 &= F_2 - T\frac{\partial\eta}{\partial s}(\ell,t) \\
I_1\ddot{\theta}_1 + TA_1\theta_1 &= M_1 + TA_1\frac{\partial\eta}{\partial s}(0,t) \\
I_2\ddot{\theta}_2 + TA_2\theta_2 &= M_2 + TA_2\frac{\partial\eta}{\partial s}(\ell,t)
\end{aligned}\right\} \tag{1}$$

$$\left.\begin{aligned}
\eta(0,t) &= v_1 + A_1\theta_1 \\
\eta(\ell,t) &= v_2 - A_2\theta_2 \\
\eta(\ell,t) - \eta(0,t) &= \ell\theta_3
\end{aligned}\right\} \tag{2}$$

$$
\left.
\begin{aligned}
& T \frac{\partial^2 \eta}{\partial s^2}(s,t) + r \frac{\partial^3 \eta}{\partial s^2 dt}(s,t) = \rho A \frac{\partial^2 \eta}{\partial t^2}(s,t) \\
& \text{or} \\
& \frac{\partial \eta}{\partial s}(0,t) = \theta_3 - \sum_{n=1}^{\infty} \dot{h}_n^{**} \\
& \frac{\partial \eta}{\partial s}(l,t) = \theta_3 - \sum_{n=1}^{\infty} (-1)^n \dot{h}_n^{**} \\
& \ddot{h}_n^{**} + 2\rho_n \omega_n \dot{h}_n^{**} + \omega_n^2 h_n^{**} = \frac{2}{l}\left[\dot{\eta}(0,t) + (-1)^{n+1} \dot{\eta}(l,t)\right] \qquad (n = 1, 2, \ldots)
\end{aligned}
\right\} \quad (3)
$$

Equations (1) represent the space station and countweight; equations (2), the conditions at the cable attachment points (no cable shear being assumed); and equations (3), the cable itself, both as a partial differential equation and as an infinite series of ordinary differential equations (modal description).

The following sections present response data for steady-state and transient disturbances for the YZ plane only. These data are valid for the XY plane also, for the frequency range where lateral cable oscillations are important, but are not valid for the XY plane for disturbances of extremely low frequency. For example, the resonance at $\omega = \Omega_o$ in evidence in the following steady-state data for the YZ plane is not present in the XY plane; but the resonances at $\omega = \Omega_1, \Omega_2, \omega_1$, and so forth are present.

Steady-State Response

The dynamic equations of motion in the YZ plane, equations (1) to (3), have been solved for a harmonic input moment $M_1 = M_o \sin \omega t$ acting on the space station. This disturbance was chosen for two reasons. First, it directly causes large space-station attitude response and thus would influence pointing accuracies of any experiment (telescope, tracking experiment, etc.); secondly, it yields representative vehicle gain plots for any attitude-control-system analysis. The solution is summarized in appendix D, and a digital program listing and explanation for calculation of response information are included in appendix E. The program calculates vehicle gain only but can be easily modified to calculate phase in order to obtain more control-system information by using the phase equations of appendix D. Vehicle gain is given in figures 4 to 12 in terms of the four dimensionless amplitudes: θ_1/θ_o, v_1/v_o, θ_2/θ_o, and v_2/v_o where

$$\theta_o = \frac{M_o}{TA_1} \qquad v_o = \frac{M_o}{T}$$

as functions of the eight dimensionless variables ω/Ω_1, ρ_1, ω_1/Ω_1, Ω_2/Ω_1, m_1/m_2, I_1/I_2, A_2/l, and I_2/J_2 where

$$\Omega_1 = \left(\frac{TA_1}{I_1}\right)^{1/2}$$

$$\Omega_2 = \left(\frac{TA_2}{I_2}\right)^{1/2}$$

$$c = \left(\frac{T}{\rho A}\right)^{1/2}$$

$$\omega_1 = \frac{\pi c}{l}$$

$$\rho_1 = \frac{\pi r c}{2Tl}$$

$$J_2 = m_2 A_2^{\ 2}$$

The first dimensionless variable is the ratio of the disturbance frequency ω to the uncoupled resonant frequency Ω_1. Plots of steady-state response data indicate that the basic flexible-body attitude response of the space station resembles the response of a second-order system, with the resonant frequency Ω_1. The second variable ρ_1 is the damping coefficient for the first flexible-body cable mode. Appendix C contains a derivation of this coefficient, and a discussion is presented later in this section. The third dimensionless variable ω_1/Ω_1 is the ratio of the fundamental uncoupled cable frequency ω_1 to the uncoupled space-station resonant frequency Ω_1. The separation of these two frequencies in the frequency domain is a measure of the coupling between space-station attitude and lateral cable oscillation. Appendix C also contains a derivation of ω_1. The fourth variable Ω_2/Ω_1 is the ratio of the uncoupled counterweight resonant frequency Ω_2 to the uncoupled space-station resonant frequency Ω_1. The four remaining variables are ratios of mass, inertia, and geometry.

The interrelationship between these variables and the system response characteristics is quite extensive in terms of possible data generation. For example, $4(3^7)$ or approximately 8800 response plots would be required for only three values each for the last seven dimensionless variables. For this reason, only the main characteristics of

the system are presented and a program listing and explanation are included in appendix E for systems other than those presented. Also, to avoid symbol repetition, the values of the last seven variables will be given as a set of values where, for example, the set (0, 50, 1, 1, 1, 0.01, 0.333) indicates that

$$\rho_1 = 0$$

$$\frac{\omega_1}{\Omega_1} = 50$$

$$\frac{\Omega_2}{\Omega_1} = 1$$

$$\frac{m_1}{m_2} = 1$$

$$\frac{I_1}{I_2} = 1$$

$$\frac{A_2}{l} = 0.01$$

$$\frac{I_2}{J_2} = 0.333$$

Figure 4 contains space-station and counterweight response data plotted as functions of the forcing frequency ratio ω/Ω_1 for the preceding set of variables representing a symmetrical system of the indicated geometry and with lateral cable modes of very high frequency. Coupling between lateral cable oscillation and space-station and counterweight oscillation is therefore negligible. The space-station attitude response is seen to resemble the response of a single-degree-of-freedom system, with a resonant frequency Ω_1 and an additional resonance at the spin frequency Ω_o. The spin-frequency effect is not a true resonance but represents a rotation or tilting of the actual spin plane. This effect is a rigid-body characteristic of the system for YZ-plane oscillation. It occurs at the spin frequency Ω_o, where the input moment M_1 is in phase with the rotation, becoming equivalent to a moment fixed in inertial space and therefore continuously rotating the system. The linear mathematics used in generating these steady-state response plots are not valid at the resonance but are valid near the resonance if the resulting amplitudes are small. Counterweight steady-state response is relatively small, with maximum amplitudes near $\omega = \Omega_o$ and $\omega = \Omega_1 = \Omega_2$. Figure 4(b) is a plot

of space-station and counterweight translations, which are equal for this case since cable mass is negligible $(\omega_1 >> \Omega_1)$. The low-frequency rigid-body response can be expressed mathematically by the equations of appendix A and the relation

$$|v_1| \sim |v_2| \sim (l + A_1 + A_2)\alpha_x$$

The high-frequency response indicates a resonance at $\omega = \Omega_1$; but for frequencies other than this, amplitudes are small.

Figure 5 contains four space-station and counterweight attitude plots which can be used to demonstrate the influence of the dimensionless variables on the separation between spin frequency and uncoupled resonance frequency. The equation that relates the two frequencies is

$$\left(\frac{\Omega_o}{\Omega_1}\right)^2 = \frac{I_2}{J_2}\frac{A_2}{l}\left(1 + \frac{m_2}{m_1}\right)\left(\frac{\Omega_2}{\Omega_1}\right)^2 \left\{\frac{1}{1 + \frac{A_2}{l}\left[1 + \left(\frac{\Omega_1}{\Omega_2}\right)^2 \frac{I_1}{I_2}\right]}\right\} \tag{4}$$

Equation (4) is the result of an algebraic manipulation of the following equation for cable tension (where cable mass is neglected):

$$T = \frac{m_1 m_2}{m_1 + m_2}(l + A_1 + A_2)\Omega_o^2 \tag{5}$$

Equation (4) illustrates the dependence of the spin ratio on the variables I_2/J_2, A_2/l, m_1/m_2, Ω_2/Ω_1, and, to a lesser degree, I_1/I_2. The plots of figure 5 illustrate that changing these variables will affect the lower resonance, according to equation (4), without appreciably changing the basic high-frequency character of the system, when the fundamental cable frequency ω_1 is high and the spin ratio is sufficiently small $(\Omega_o << \Omega_1)$. Figure 5(a) is a response plot for the system (0, 50, 1, 1, 1, 0.01, 0.0333). The plot illustrates that a decrease in the inertia ratio I_2/J_2 results in a decrease in spin ratio without affecting the response near $\omega \sim \Omega_1$. Figure 5(b) is a response plot for the system (0, 50, 1, 1, 1, 0.1, 0.333). The increase in A_2/l from the system of figure 4 increases the spin ratio, but again the response near $\omega \sim \Omega_1$ is not affected. Figure 5(c) is for the system (0, 50, 1, 4, 1, 0.1, 0.333). The decrease in spin ratio relative to the results of figure 5(b) is a result of the increase in the ratio m_1/m_2. Figure 5(d) is for the system (0, 50, 2, 1, 1, 0.1, 0.333). The increase in the ratio Ω_2/Ω_1 is reflected not only by the increase in Ω_o/Ω_1 but also by the additional resonance at $\omega \sim \Omega_2$. This additonal resonance has a pronounced effect on counterweight response but only a small effect on space-station response. Figure 5 indicates

that if the spin ratio Ω_o/Ω_1 calculated by equation (4) is small, the system response can be considered as the uncoupled superposition of flexible-body motion on rigid-body motion (appendix A) near $\omega \sim \Omega_1 \sim \Omega_2$ $\left(\text{when } \omega_1 >> \Omega_1\right)$.

Figure 6 is an attitude response plot for the system (0, 50, 0.5, 1, 1, 0.01, 0.0333). This system deviates from symmetry by having $\frac{\Omega_2}{\Omega_1} = 0.5$, this condition being reflected by the strong counterweight resonance at $\omega \sim \Omega_2$. The influence of this third resonance on space-station attitude is not appreciable. Figure 7 is an attitude response plot for the system (0, 50, 2, 1, 1, 0.01, 0.0333). The counterweight uncoupled resonance Ω_2 is twice the space-station uncoupled resonance Ω_1. Again the effect of the additional resonance is not appreciable for the space-station response.

The previous data are for systems where the cable fundamental mode frequency ω_1 is well above Ω_o, Ω_1, and Ω_2. This is a required condition if a cable is to be modeled as a massless string, with no degrees of freedom of its own. Figure 8 contains plots for the system (0, 2, 1, 1, 1, 0.1, 0.333), where $\frac{\omega_1}{\Omega_1} = 2$. The decrease in ω_1/Ω_1 implies the addition to the system of an infinite number of degrees of freedom and therefore, for an undamped system, an infinite number of cable resonances. However, when the fundamental uncoupled cable frequency is sufficiently high, the coupling, although in existence, will not appreciably alter response, other than to superimpose the cable modes at nearly the uncoupled cable frequencies ω_n. This is very nearly the case for figures 8(a) and 8(b), although two new resonant peaks now appear on either side of the resonance at $\omega \sim \Omega_1$. Space-station and counterweight translations are plotted in figures 8(c) and 8(d). The two resonances near $\omega \sim \Omega_1$ are clearly defined, as is the resonance associated with ω_1. The response for the higher cable resonances is too low to appear in the figures. The space-station and the counterweight translations exhibit a response at several frequencies near Ω_1 and greater than Ω_1, where one translation (v_1) is zero and the other (v_2) is finite. This condition seems more descriptive than significant.

Figures 9 and 10 contain the same response information as figure 8, but for the systems (0, 1, 1, 1, 1, 0.1, 0.333) and (0, 0.5, 1, 1, 1, 0.1, 0.333), or for systems with $\frac{\omega_1}{\Omega_1} = 1$ and $\frac{\omega_1}{\Omega_1} = 0.5$, respectively. The figures illustrate how cable-to-counterweight and cable-to-space station coupling increases as the fundamental uncoupled cable frequency decreases. This result reflects more influence of the cable mass on the system response. The point is made that the system is quite involved dynamically if the uncoupled cable frequencies ω_n are near the uncoupled space-station and counterweight frequencies Ω_1 and Ω_2; therefore, any simulation of such a system would require the inclusion of the effects of cable lateral motion when the ratio ω_1/Ω_1 is not large.

Cable damping has been assumed to be small for all previous response data. This assumption is valid if the variable ρ_1 is small. The following order-of-magnitude analysis shows that for systems where the cable length is long, the damping coefficient ρ_1 will be negligibly small. In appendix C the modal damping of equations (C13) is expressed as

$$\rho_n = \frac{r\omega_n}{2T} \tag{6}$$

Substituting equation (C10) yields

$$\rho_1 = \frac{E''I}{2T}\left(\frac{\pi}{l}\right)^2 \tag{7}$$

For a cable of circular cross section, the area inertia is given as

$$I = \left(\frac{r_c}{2}\right)^2 A \tag{8}$$

where r_c is the cable radius and A is the cable cross-sectional area. Substitution of equation (8) into equation (7) yields

$$\rho_1 = \frac{\pi^2}{8}\frac{E''}{\sigma}\left(\frac{r_c}{l}\right)^2 \tag{9}$$

where $\sigma = \frac{T}{A}$ is the tensile stress in the cable. It is assumed a priori that E'' is of the same order of magnitude as σ, this assumption being valid for most metallic cables. Therefore, the order-of-magnitude relation exists that

$$\rho_1 \sim \left(\frac{r_c}{l}\right)^2 \tag{10}$$

This equation clearly supports the assumption of small damping since cable radius r_c is several orders of magnitude lower than cable length l. The data presented are thus justified.

Figure 11 is included for the system (0.1, 0.5, 1, 1, 1, 0.1, 0.333), for which it was assumed that another mechanism was available to provide cable damping and that this cable damping was mathematically similar to the damping ρ_n. This system is identical to that for figure 10, with the exception that $\rho_1 = 0.1$. Rigid-body space-station and counterweight responses are identical near $\omega \sim \Omega_o$. The absence of flexible-body vehicle motion in this frequency region is thus substantiated. For the frequency range where

$\omega > \Omega_0$, response is increasingly altered as resonant amplitudes for the frequencies near $\omega \sim \Omega_1$ become smaller, until, for the high cable modes, resonances no longer exist. This effect is caused by the increasingly greater damping in each higher cable mode (eq. (6)).

Transient Response

Equations (1), (2), and (3) have been digitally integrated for two transient disturbance moments acting on the space station. The first moment $M_1 = 100u_s(t)$ represents the disturbance caused by a crew member who moves relative to the artificial gravity field in the Z-direction and then remains at a new position. The second moment $M_1 = 100u_s(t)\cos(1.1t)$ represents the disturbance caused by a crew member who moves continuously between two positions after an initial motion similar to that of the first case. These disturbances act on a symmetrical vehicle defined by the following coefficients:

$$m_1 = m_2 = 700 \text{ slugs } (10\ 216 \text{ kg})$$

$$I_1 = I_2 = 40\ 000 \text{ slug-ft}^2 \ (54\ 232 \text{ kg-m}^2)$$

$$A_1 = A_2 = 10 \text{ feet } (3.048 \text{ meters})$$

$$l = 2500 \text{ feet } (762 \text{ meters})$$

$$\left.\begin{array}{l} \rho A = 0.015 \text{ slug/ft } (0.718 \text{ kg/m}) \\ T = 10\ 000 \text{ pounds } (44\ 482 \text{ N}) \end{array}\right\} c = 817 \text{ ft/sec } (249 \text{ m/sec})$$

$$\rho_1 = 10^{-6}$$

These coefficients are expressed in steady-state notation as $\left(10^{-6}, 0.649, 1, 1, 1, 0.004, 0.571\right)$. Figure 12 contains steady-state plots for attitude and translation of the space station and counterweight. These plots illustrate the close proximity of the station, counterweight, and cable lower resonances in the frequency domain. The general character of these plots is similar to that of the plots previously described.

Figure 13 contains time domain plots of space-station and counterweight response for the step moment $M_1 = 100u_s(t)$. These plots contain transient motion superimposed on the steady-state motion predicted by figure 12 for a zero frequency or constant input.

Figure 13(a) illustrates the transient overshoot of space-station attitude by a factor of two times the steady-state displacement $\theta_o = \frac{M_1}{TA_1} = 10^{-3}$ radian and then subsequent

oscillation at the frequency $\Omega_1 = \left(\frac{TA_1}{I_1}\right)^{1/2} = 1.58$ rad/sec. The space station then begins to radiate energy through the cable to the counterweight, with accompanying loss in amplitude.

Figure 13(b) is a plot of counterweight attitude. An initial delay in response $\Delta t = \frac{l}{c} = 3.06$ seconds is required for any energy to propagate from the space station along the cable to the counterweight. The counterweight then begins to oscillate at the uncoupled frequency $\Omega_2 = \Omega_1 = 1.58$ rad/sec, with increasing attitude, until a complete exchange of available energy has taken place between the space station and the counterweight. The energy exchange then reverses. This process would repeat until damping had absorbed the available energy and the system had reached the steady state. (For the low damping of the system in fig. 13, this absorption requires significant time and therefore is not a noticeable effect.)

Figure 13(c) is a plot of space-station translation v_1. The low-frequency oscillation is that predicted by the first of equations (A4)

$$\ddot{\alpha}_x + \Omega_o^2 \alpha_x = \frac{M_x}{A}$$

namely

$$\alpha_x = \frac{M_x}{A\Omega_o^2}(1 - \cos \Omega_o t)$$

where

$$\left.\begin{aligned} M_x &= 100u_s(t) \text{ ft-lb } \left(M_x = 136u_s(t) \text{ N-m}\right) \\ A &= I_1 + I_2 + \frac{m_1 m_2}{m_2 + m_2}(l + A_1 + A_2)^2 = 0.222 \times 10^{10} \text{ slug-ft}^2 \left(0.301 \times 10^{10} \text{ kg-m}^2\right) \\ \Omega_o &= \left(T \frac{m_1 + m_2}{m_1 m_2} \frac{1}{A_1 + A_2 + l}\right)^{1/2} = 0.106 \text{ rad/sec} \end{aligned}\right\} \quad (11)$$

or

$$\left.\begin{aligned} v_1 &= -v^*(1 - \cos \Omega_o t) \\ v_2 &= v^*(1 - \cos \Omega_o t) \end{aligned}\right\} \quad (12)$$

where

$$v^* = \frac{l + A_1 + A_2}{2} \frac{M}{A\Omega_o^2} = 0.005 \text{ foot } (0.0015 \text{ meter})$$

The value of v^* can also be found from figure 12; $v^* \sim 0.5v_o = 0.005$ foot (0.0015 meter).

Equations (12) describe the low-frequency oscillation of figure 13(d) as well. The time lag $\Delta t = 3.06$ seconds for counterweight motion to begin and the low-amplitude high-frequency oscillations illustrate small flexible-body motion and coupling effects superimposed on the rigid-body motion.

The first example dealt with a simplified crew motion of constant magnitude and therefore the transient response of the system could be interpreted easily. The second example deals with an oscillatory crew motion, which yields a more complicated superposition of transient and steady-state response.

Figure 14 contains time domain plots of system response for the oscillatory input $M_1 = 100u_s(t)\cos(1.1t)$. Figure 14(a) contains space-station attitude. This response indicates two oscillations, one at the space-station frequency $\Omega_1 = 1.58$ rad/sec and one at the forcing frequency $\omega = 1.1$ rad/sec. The oscillation at the space-station frequency appears to be similar to that shown in figure 13(a), while the oscillation at the forcing frequency maintains a constant magnitude. The steady-state magnitude as found from figure 12(a) is $\theta_1 = 1.7\theta_o = 1.7 \times 10^{-3}$ radian, which is approximately the oscillation magnitude found for $100 < t < 120$ seconds, where the steady state was reached temporarily for the system of figure 13.

Figure 14(b) also indicates two oscillations, the steady-state oscillation at the forcing frequency having the lower magnitude $\theta_2 = 0.22\theta_o = 0.22 \times 10^{-3}$ radian (fig. 12(a)), in evidence for $190 < t < 210$ seconds. Therefore it may be seen that the oscillation at $\Omega_2 = \Omega_1 = 1.58$ rad/sec is more dominant than in figure 14(a). The same energy transfer between the space station and the counterweight occurs until system damping absorbs all available energy and the response is entirely steady state.

Figures 14(c) and 14(d) are quite similar if the basic energy lag time $\Delta t = 3.06$ seconds is neglected. The high-frequency oscillation occurs approximately at the forcing frequency. The low-frequency beat may indicate the proximity of the forcing frequency $\omega = 1.1$ rad/sec and the lowest cable mode $\omega_1 = 0.649\Omega_1 = 1.027$ rad/sec. The steady-state oscillation amplitude can be found from figure 12 to be $v_1 \sim v_2 \sim 0.1v_o = 0.001$ foot (0.0003 meter), which is approximately the average amplitude shown in figures 14(c) and 14(d).

This discussion of transient response was included in order to examine, for some forcing functions, the deviation of actual response from that predicted by the steady-state nondimensional plots previously presented. Since all types of disturbance inputs are theoretically possible and since the system is an infinite-degree-of-freedom system, no positive conclusion about transient response is possible. However, it appears from the data, including that presented, that orders of magnitude of maximum attitudes and translations can usually be estimated by approximating the disturbance as a harmonic function (or series of functions) and doubling the steady-state maximum response. Also the effect of energy flow between the space station and the counterweight will cause a transient oscillation of similar magnitude to appear when the steady-state prediction for that portion of the system is small. A second conclusion about the transient behavior is that the effect of the cable lag time Δt is not, in itself, critical for systems typical of those presently conceived.

Bond Graph Representation

A bond graph for the system described by equations (1) to (3) is included (fig. 15) to provide additional description and to serve as a graphical tool for the discussion of energy flow within the system. References (3) to (5) contain detailed discussion of the elements of a bond graph. A simplified discussion is also included in appendix F.

Energy enters the system at the effort sources of bonds 1, 5, 13, and 16. These effort sources represent the space-station and counterweight forcing functions M_1, F_1, M_2, and F_2 which arise from crew motion, aerodynamic drag, and so forth. This energy then flows from the space station or counterweight into the cable, causing the dynamic motion of the system and the interaction between the cable, space station, and counterweight.

Figure 16 contains time plots of the energy of the space station, cable, and counterweight and the total energy for the system of figure 13. The total energy, plotted in figure 16(a), has a maximum value of $\frac{TA_1(2\theta_o)^2}{2} = 0.2$ ft-lb (0.27 joule), which occurs initially and represents a loss of artificial gravitational field potential energy when the crew member changes position in the field at time $t \doteq 0$. This energy enters the system at bond 1 and appears as space-station kinetic and potential energy (fig. 16(b)). It then flows through bond 4 to other elements of the system until at $100 < t < 120$ seconds the counterweight energy (fig. 16(c)) is equal to the space-station energy. At this point the available space-station energy $\left(\text{energy above the steady-state energy } \frac{TA_1\theta_o^2}{2} = 0.05 \text{ ft-lb } (0.068 \text{ joule})\right)$ is zero and the counterweight begins to radiate its energy through the cable

to the space station, the energy exchange thus being reversed. It is interesting to note that the maximum energy contained in the cable (fig. 16(d)) is only 4 percent of the maximum energy present in the system. Also the magnitude of the total system energy is extremely low. This result indicates that a probable low-power attitude control system could provide active damping for the space station (for crew-motion magnitudes discussed herein).

CONCLUDING REMARKS

In the preceding analysis, equations for the dynamic system have been developed and solved. The results of this analysis allow certain concluding remarks concerning the behavior of the system, within the boundaries of all connected simplifying assumptions.

First, the basic attitude response of the space station is that of an undamped second-order system, with a resonant frequency Ω_1. Coupled to this basic response are rigid-body characteristics, usually in evidence at frequencies lower than Ω_1, and cable lateral mode effects, usually in evidence at frequencies higher than Ω_1. The entire system can be considered to be the superposition of uncoupled rigid-body, flexible-body, and "heavy string" motion when $\frac{\Omega_o}{\Omega_1} << 1$ and $\frac{\omega_1}{\Omega_1} >> 1$ where $\frac{\Omega_o}{\Omega_1}$ is the ratio of spin frequency to uncoupled space-station frequency and $\frac{\omega_1}{\Omega_1}$ is the ratio of fundamental cable mode frequency to uncoupled space-station frequency. However, the example system does not meet these conditions. Damping from mechanisms involved with the viscoelastic bending of the cable is extremely small because of the low dynamic curvature of the cable. The low cable curvature arises from the high velocity of cable lateral waves.

The counterweight has a weak effect on the steady-state response of the space station. However, for any real situation where the transient response will usually dominate, the counterweight is seen to absorb energy from the space station and then radiate this energy through the cable back to the space station. Therefore, in this sense, the contribution of the counterweight is in no way negligible.

Finally, the orders of magnitude of the maximum attitudes and translations of the space station and counterweight could be estimated, in the cases considered, by approximating the disturbance in question as a harmonic function (or series of functions) and doubling the steady-state maximum response.

Langley Research Center,
National Aeronautics and Space Administration,
Langley Station, Hampton, Va., November 22, 1968,
125-19-03-10-23.

APPENDIX A

RIGID-BODY CHARACTERISTICS OF THE ROTATING SYSTEM

This appendix presents a solution of Euler's equations for the system, where the cable length is large and the overall system inertias are constant (fig. 17). If the system is assumed to have only low-frequency disturbances ($\omega << \Omega_1$) acting on it, it will behave as a rigid rotating body. If, in addition to the rigid-body motion, the total disturbance profile is assumed to cause only small flexible-body displacements relative to the spacecraft dimensions, the rigid-body inertias will be essentially constant and the total spacecraft motion will consist of the superposition of small linear flexible-body motion on rigid-body motion.

Euler's equations are

$$\left.\begin{aligned} M_X &= A\ddot{\alpha}_X + (C - B)\dot{\alpha}_Y\dot{\alpha}_Z \\ O &= B\ddot{\alpha}_Y + (A - C)\dot{\alpha}_X\dot{\alpha}_Z \\ M_Z &= C\ddot{\alpha}_Z + (B - A)\dot{\alpha}_X\dot{\alpha}_Y \end{aligned}\right\} \tag{A1}$$

where $\dot{\alpha}_X$, $\dot{\alpha}_Y$, and $\dot{\alpha}_Z$ refer to the rigid-body rates, α_X and α_Y are small attitudes of the system about the x- and y-axis, and A, B, and C refer to the X-, Y-, and Z-axis rigid-body inertias. Torques M_X and M_Z are assumed to be small and to act along the X- and Z-axis, respectively.

These equations are simplified by the assumption that the cable is long and therefore Y-axis inertia B is small, and that A and C are approximately equal. Also the spin velocity $\dot{\alpha}_Z$ is assumed to be nearly constant and of magnitude Ω_0. Direct substitution of these assumptions into equations (A1) is not possible, however, since it would violate the physical necessity that

$$\left.\begin{aligned} A + B &> C \\ A + C &> B \\ B + C &> A \end{aligned}\right\} \tag{A2}$$

The inequalities (A2) can be rewritten as

$$-1 < \frac{C - A}{B} < 1 \qquad (A + C > B) \quad (A3)$$

Equations (A1) are now rewritten with simplifying assumptions as

$$\left.\begin{aligned} \ddot{\alpha}_x + \frac{C - A}{B}\,\Omega_o{}^2\alpha_x &= \frac{M_x}{A} \\ \dot{\alpha}_y &= \frac{C - A}{B}\,\Omega_o\alpha_x \\ \ddot{\alpha}_z &= \frac{M_z}{A} + \frac{C - A}{B}\,\Omega_o\dot{\alpha}_x\alpha_x \end{aligned}\right\} \qquad (A4)$$

where all initial values other than $\dot{\alpha}_z = \Omega_o$ are zero and the quantity $\frac{C - A}{B}$ is bounded between 1 and -1.

The stability of the system is now apparent (and well known), namely $C > A$. If maximum stability is assumed the condition that must be met is obviously

$$\frac{C - A}{B} = 1$$

which reflects the system maximum stiffness under the disturbance torque M_x. This condition is used in the derivation of the equations of the flexible system.

The magnitude of the Y-axis rate as given by the second of equations (A4) is seen to depend on the X-axis displacement and the Z-axis rate. For long cable systems the displacement α_x is small and therefore the Y-axis rate is also small relative to Ω_o. Also the Z-axis acceleration is seen by the third of equations (A4) to be second-order small since the quantity M_z/A is small. This result substantiates the constant-spin-velocity assumption.

APPENDIX B

LINEAR SYSTEM EQUATIONS

The linearized Euler equation for rigid-body motion in the YZ plane (the first of eqs. (A4)) for a condition of maximum YZ-plane stiffness is

$$\ddot{\alpha}_x + \Omega_o{}^2\alpha_x = \frac{M_x}{A} \tag{B1}$$

This equation can also be derived from conservation of angular momentum according to figure 17(a) where the system is shown as a rigid body and the body forces from the artificial gravity field acting on the space station and counterweight are equal in magnitude to the tension T and directed normal to the spin axis. The equation is

$$\ddot{\alpha}_x + \frac{T(l + A_1 + A_2)}{A}\alpha_x = \frac{M_x}{A} \tag{B2}$$

where

$$A = \frac{m_1 m_2}{m_1 + m_2}(l + A_1 + A_2)^2 \tag{B3}$$

$$I_1 + I_2 << A$$

Equation (5) defines the tension as

$$T = \frac{m_1 m_2}{m_1 + m_2}(l + A_1 + A_2)\Omega_o{}^2$$

Substitution of equations (B3) and (5) into equation (B2) will yield equation (B1) and thus verify the uncoupled rigid-body assumptions of figure 17(a) and equation (B2).

In a manner analogous to that for the derivation of equation (B2), equations for the complete system in the YZ plane can be derived. According to figure 3, conservation of lateral momentum requires that

$$\left.\begin{aligned} F_1 + T\frac{\partial\eta}{\partial s}(0,t) &= m_1\ddot{v}_1 \\ F_2 - T\frac{\partial\eta}{\partial s}(l,t) &= m_2\ddot{v}_2 \end{aligned}\right\} \tag{B4}$$

while conservation of angular momentum requires that

$$\left.\begin{aligned} M_1 + TA_1\left[\frac{\partial\eta}{\partial s}(0,t) - \theta_1\right] &= I_1\ddot{\theta}_1 \\ M_2 + TA_2\left[\frac{\partial\eta}{\partial s}(l,t) - \theta_2\right] &= I_2\ddot{\theta}_2 \end{aligned}\right\} \tag{B5}$$

Also the constraints exist that

$$\left.\begin{aligned} \eta(0,t) &= v_1 + A_1\theta_1 \\ \eta(l,t) &= v_2 - A_2\theta_2 \\ \eta(l,t) - \eta(0,t) &= l\,\theta_3 \end{aligned}\right\} \tag{B6}$$

A comparison of figures 2 and 3 shows the similarity of the XY- and YZ-plane configurations, the exception being the direction of the body forces T (fig. 17) and thus the incorporation of a rigid-body oscillation at the spin frequency Ω_o. The response in the XY plane is therefore identical to that in the YZ plane for disturbances at frequencies much greater than the spin frequency Ω_o.

APPENDIX C

CABLE EQUATIONS AND MODAL DESCRIPTION

The differential equation of motion for the cable is derived by considering conservation of lateral momentum for each incremental identified cable mass point. The cable is an infinite-degree-of-freedom system since there are an infinite number of mass points. An arbitrary mass point is shown in figure 18. The D'Alembert loading $\rho A \frac{\partial^2 \eta}{\partial t^2} ds$, the cable tension T, the cable shear force V, and the cable bending moment M_c are also shown in the figure. From lateral (η-direction) equilibrium, for small η,

$$\left(\frac{\partial}{\partial s} T \frac{\partial \eta}{\partial s} + \frac{\partial V}{\partial s}\right) ds = \rho A \frac{\partial^2 \eta}{\partial t^2} ds \tag{C1}$$

From rotational equilibrium (the rotary inertia being neglected), for small η,

$$\frac{\partial M_c}{\partial s} ds = -V\, ds$$

or

$$\frac{\partial V}{\partial s} = -\frac{\partial^2 M_c}{\partial s^2} \tag{C2}$$

Substitution of equation (C2) into equation (C1), for constant tension T, yields

$$T \frac{\partial^2 \eta}{\partial s^2} - \frac{\partial^2 M_c}{\partial s^2} = \rho A \frac{\partial^2 \eta}{\partial t^2} \tag{C3}$$

The cable moment M_c is small but is included to introduce damping (energy dissipation) into the system. This moment is related to curvature by the equation

$$M_c = EI \frac{\partial^2 \eta}{\partial s^2} \tag{C4}$$

If the material is assumed to be viscoelastic, the modulus is complex, or

$$M_c = \left(E' + \frac{E''}{\omega} \frac{\partial}{\partial t}\right)\left(I \frac{\partial^2 \eta}{\partial s^2}\right) \tag{C5}$$

where E'' represents the viscous portion of the complex modulus (loss modulus), E' is the elastic portion of the modulus, I is the area moment of inertia for the cable cross section, and ω is the oscillation frequency for η, which is necessary for use of the complex modulus but is not a true material property. The effect of bending energy storage E' will not be included hereafter since damping only is the desired second-order effect.

The solution of equation (C3) with the cable moment described by equation (C5) is an undesirably complex way to introduce cable damping. Therefore, an alternative way, valid for small damping only, is presented. It is noted that this approximation deals mainly with the second term M_c in equation (C3).

A wave traveling in the cable could have the form

$$\eta(s,t) \sim e^{i(\omega t - ks)} \tag{C6}$$

where ω is the oscillation frequency and k is the wave number. Substituting equations (C6) and (C5) into equation (C3) and neglecting E' required that

$$k = \pm \left[\frac{-1 \pm \left(1 + \frac{4\epsilon\omega^2}{c^4}\right)^{1/2}}{2\epsilon/c^2} \right]^{1/2} \tag{C7}$$

where

$$c = \left(\frac{T}{\rho A}\right)^{1/2}$$

$$\epsilon = i\,\frac{E''I}{\rho A}$$

The modulus of the complex quantity ϵ/c^2 is small and can equal zero. Therefore, equation (C7) is not in a desirable form for computation. A more acceptable form, which considers ϵ/c^2 as a small number is

$$\left.\begin{aligned} k &= \pm \frac{\omega}{c}\left(1 + \frac{\epsilon\omega^2}{c^4}\right)^{-1/2} \\ k &= \pm i \frac{c}{\epsilon^{1/2}} \end{aligned}\right\} \tag{C8}$$

These four approximate solutions are necessary to meet the four required boundary conditions of equation (C3) when the moment M_c is defined by equation (C5). However, for small ϵ the second two solutions result in a very local exponential correction of the equation of motion of the cable near the cable attachment point. The length of this region is given by the equation (ref. 6)

$$l_\epsilon \sim \left|\frac{\epsilon^{1/2}}{c}\right|$$

Therefore, by assuming the condition $l_\epsilon/l << 1$ is satisfied, only two boundary conditions are sufficient. The wave-number equation is therefore taken as

$$k = \pm \frac{\omega}{c}\left(1 + \frac{ir\omega}{T}\right)^{-1/2} \tag{C9}$$

where $r\omega$, defined by the equation

$$r\omega = E''I\frac{\omega^2}{c^2} = \frac{E''I\rho A\omega^2}{T} \tag{C10}$$

is a pseudo-damping parameter. The choice of r is somewhat arbitrary since E'' is a cable parameter which varies with cable tension (i.e., strain level) T, cable mass per unit length ρA, and frequency ω.

The definition given by equation (C10) of the damping parameter r also is convenient if a modal-equation approach is used. The reason is that equation (C3) assumes the form

$$T\frac{\partial^2\eta}{\partial s^2} + r\frac{\partial^3\eta}{\partial s^2\partial t} = \rho A\frac{\partial^2\eta}{\partial t^2} \tag{C11}$$

which has a separable solution. (Substitution of equation (C6) into equation (C11) will yield the wave-number equation (C9) and thus verify equation (C11).) Solving equation (C11) by using cable modes is standard and will be outlined only.

APPENDIX C

A separable solution for $\eta(s,t)$ is assumed to be of the form

$$\eta_n(s,t) = g_n(s)h_n(t) \tag{C12}$$

Substitution of equation (C12) into equation (C11) yields the two separated equations

$$\left.\begin{aligned} &\ddot{h}_n + 2\rho_n\omega_n\dot{h}_n + \omega_n^2 h_n = 0 \\ &g_n'' + \left(\frac{\omega_n}{c}\right)^2 g_n = 0 \end{aligned}\right\} \tag{C13}$$

where

ω_n mode frequency

ρ_n mode damping coefficient, $\frac{r\omega_n}{2T}$

c undamped phase velocity, $\left(\frac{T}{\rho A}\right)^{1/2}$

For the boundary condition at the cable extremities ($s = 0$ and $s = l$) of zero lateral force or

$$T\frac{\partial\eta}{\partial s}(0,t) = T\frac{\partial\eta}{\partial s}(l,t) = 0$$

the solution of the s-dependent function becomes

$$g_n(s) = \cos\frac{n\pi s}{l} \tag{C14}$$

with the condition that

$$\omega_n = \frac{n\pi c}{l}$$

The following lateral forces at the cable extremities (numerically designated according to fig. 15) are introduced:

$$e_8 = -T \frac{\partial \eta}{\partial s}(0,t)$$

$$e_9 = T \frac{\partial \eta}{\partial s}(l,t) \tag{C15}$$

Equation (C11) is then rewritten by using the δ-function $\delta(x)$ and becomes

$$T \frac{\partial^2 \eta}{\partial s^2} + r \frac{\partial^3 \eta}{\partial s^2 \partial t} - \rho A \frac{\partial^2 \eta}{\partial t^2} = -e_8 \delta(0) - e_9 \delta(l) \tag{C16}$$

The solution is assumed to be expressible as a series of normal modes of the form

$$\eta(s,t) = \sum_{n=0}^{\infty} h_n(t) \cos \frac{n\pi s}{l} \tag{C17}$$

Substitution of equation (C17) into equation (C16) and use of the orthogonality of the modes yields the following uncoupled equations for $h_n(t)$:

$$\left.\begin{aligned}
&\ddot{h}_0 = \frac{e_8 + e_9}{\rho A l} && (n = 0) \\
&\ddot{h}_n + 2\rho_n \omega_n \dot{h}_n + \omega_n{}^2 h_n = \frac{e_8 + (-1)^n e_9}{\rho A l/2} && (n = 1, 2, \ldots) \\
&\dot{\eta}(0,t) = f_8 = \dot{h}_0 + \sum_{n=1}^{\infty} \dot{h}_n \\
&\dot{\eta}(l,t) = f_9 = \dot{h}_0 + \sum_{n=1}^{\infty} (-1)^n \dot{h}_n
\end{aligned}\right\} \tag{C18}$$

The preceding mathematical description of the cable is standard and normally adequate. However, the requirement exists in any computer solution of a system that variables must be integrated and not differentiated with respect to time. In this specific case a dual formulation of the cable mathematics is thus required, where flow variables (velocities) are integrated and summed to yield effort variables (forces). The dual formulation of the equations can be found by an algebraic inversion of equations (C18) in Laplace

notation, where all initial conditions are set equal to zero. References 7 and 8 contain more specific information on the dual formulation for elastodynamic problems. Reference 9 discusses the inversion problem. The algebra of the inversion is omitted and the formulation is given as

$$\left.\begin{aligned}
&\ddot{h}_0^* = \frac{T}{l}(f_8 - f_9) && (n = 0)\\
&\ddot{h}_n^* + 2\rho_n\omega_n\dot{h}_n^* + \omega_n{}^2 h_n^* = \frac{2T}{l}\left[f_8 - (-1)^n f_9\right] && (n = 1, 2, \ldots)\\
&e_8 = \dot{h}_0^* + \sum_{n=1}^{\infty} \dot{h}_n^*\\
&e_9 = -\dot{h}_0^* - \sum_{n=1}^{\infty} (-1)^n \dot{h}_n^*
\end{aligned}\right\} \quad \text{(C19)}$$

Equations (C19) can be rewritten, where cable slopes are functions of attachment-point velocities and positions, as

$$\left.\begin{aligned}
&\frac{\partial\eta}{\partial s}(0,t) = \theta_3 - \sum_{n=1}^{\infty} \dot{h}_n^{**}\\
&\frac{\partial\eta}{\partial s}(l,t) = \theta_3 - \sum_{n=1}^{\infty} (-1)^n \dot{h}_n^{**}\\
&\ddot{h}_n^{**} + 2\rho_n\omega_n\dot{h}_n^{**} + \omega_n{}^2 h_n^{**} = \frac{2}{l}\left[\dot{\eta}(0,t) + (-1)^{n+1}\dot{\eta}(l,t)\right] && (n = 1, 2, \ldots)\\
&\theta_3 = \frac{\eta(l,t) - \eta(0,t)}{l}
\end{aligned}\right\} \quad \text{(C20)}$$

These equations are an equally valid description for XY-plane lateral cable motion where $\eta \rightarrow \psi$ and $\theta \rightarrow \varphi$.

APPENDIX D

STEADY-STATE EQUATIONS

The governing equations for the space station and counterweight, equations (B4), (B5), and (B6), are rewritten as two boundary-condition equations for the cable. If $F_1 = F_2 = M_2 = 0$ these equations are

$$\left.\begin{aligned}
\frac{\ddot{M}_1}{K_1} &= \frac{1}{\Omega_1^2}\frac{\ddddot{\eta}}{A_1}(0,t) - \left(1 + \frac{I_1}{J_1}\right)\frac{\partial\ddot{\eta}}{\partial s}(0,t) + \frac{\ddot{\eta}}{A_1}(0,t) - \Omega_1^2\frac{I_1}{J_1}\frac{\partial\eta}{\partial s}(0,t) \\
0 &= \frac{1}{\Omega_2^2}\frac{\ddddot{\eta}}{A_2}(l,t) + \left(1 + \frac{I_2}{J_2}\right)\frac{\partial\ddot{\eta}}{\partial s}(l,t) + \frac{\ddot{\eta}}{A_2}(l,t) + \Omega_2^2\frac{I_2}{J_2}\frac{\partial\eta}{\partial s}(l,t)
\end{aligned}\right\} \tag{D1}$$

where

$$\left.\begin{aligned}
\Omega_n^2 &= \frac{TA_n}{I_n} \\
K_n &= TA_n \\
J_n &= m_n A_n^2
\end{aligned}\right\} \qquad (n = 1,2) \tag{D2}$$

For a harmonic disturbance torque

$$M_1 = M_o \sin \omega t \tag{D3}$$

a solution for cable lateral displacement η which satisfies equations (D1) as well as equation (C9) will be of the form

$$\begin{aligned}
\eta(s,t) = {} & a_1 e^{k_2 s}\sin(\omega t + k_1 s) + b_1 e^{-k_2 s}\sin(\omega t - k_1 s) \\
& + a_2 e^{k_2 s}\cos(\omega t + k_1 s) + b_2 e^{-k_2 s}\cos(\omega t - k_1 s)
\end{aligned} \tag{D4}$$

where

$$k_1 = \mathrm{Re}(k)$$

$$k_2 = -\mathrm{Im}(k)$$

APPENDIX D

The coefficients a_1, a_2, b_1, and b_2 are found by substitution of equations (D3) and (D4) into equations (D1), which yields the matrix equation

$$\begin{bmatrix} 1 + B & 1 - B & -A & A \\ A & -A & 1 + B & 1 - B \\ 1 - D + CF & (1 + D + CF)E & C - (1 - D)F & (-C + (1 + D)F)E \\ -C + (1 - D)F & (C - (1 + D)F)E & 1 - D + CF & (1 + D + CF)E \end{bmatrix} \begin{Bmatrix} a_1/l \\ b_1/l \\ a_2/l \\ b_2/l \end{Bmatrix} = \begin{Bmatrix} C_1/l \\ 0 \\ 0 \\ 0 \end{Bmatrix}$$

where

$$A = D_1 k_1 = \frac{D_1}{l} k_1 l$$

$$B = D_1 k_2 = \frac{D_1}{l} k_2 l$$

$$C = D_2 k_1 = \frac{D_2}{l} k_1 l$$

$$D = D_2 k_2 = \frac{D_2}{l} k_2 l$$

$$E = e^{-2k_2 l}$$

$$F = \tan k_1 l$$

$$C_1 = \frac{M_o A_1}{K_1\left(1 - \frac{\omega^2}{\Omega_1^2}\right)}$$

$$D_1 = -\frac{A_1\left(1 + \frac{I_1}{J_1} - \frac{\Omega_1^2 I_1}{\omega^2 J_1}\right)}{1 - \frac{\omega^2}{\Omega_1^2}}$$

$$D_2 = -\frac{A_2\left(1 + \frac{I_2}{J_2} - \frac{\Omega_2^2 I_2}{\omega^2 J_2}\right)}{1 - \frac{\omega^2}{\Omega_2^2}}$$

APPENDIX D

The displacements of the space station and the counterweight can now be written as solutions of the preceding differential equations as follows:

$$\theta_1 = \frac{M_o/K_1}{1 - \frac{\omega^2}{\Omega_1^2}} \sin \omega t + \frac{1}{1 - \frac{\omega^2}{\Omega_1^2}} \frac{\partial \eta}{\partial s}(0,t)$$

$$v_1 = -\frac{\Omega_1^2}{\omega^2} A_1 \frac{\partial \eta}{\partial s}(0,t)$$

$$\theta_2 = \frac{1}{1 - \frac{\omega^2}{\Omega_2^2}} \frac{\partial \eta}{\partial s}(l,t)$$

$$v_2 = \frac{\Omega_2^2}{\omega^2} A_2 \frac{\partial \eta}{\partial s}(l,t)$$

By introducing the notation

$$\frac{\partial \eta}{\partial s}(0,t) = L \sin \omega t + N \cos \omega t$$

$$\frac{\partial \eta}{\partial s}(l,t) = P \sin \omega t + Q \cos \omega t$$

the displacements can be rewritten in dimensionless form in terms of maximum amplitudes and phase angles. Therefore

$$\frac{\theta_1 TA_1}{M_o} = \left(\frac{\theta_1 TA_1}{M_o}\right)_{max} \sin\left(\omega t + \gamma_1\right)$$

where

$$\left(\frac{\theta_1 TA_1}{M_o}\right)_{max} = \frac{\sqrt{\left(1 + \frac{TA_1}{M_o} L\right)^2 + \left(\frac{TA_1}{M_o} N\right)^2}}{1 - \frac{\omega^2}{\Omega_1^2}}$$

$$\gamma_1 = \tan^{-1}\left(\frac{\frac{TA_1}{M_o} N}{1 + \frac{TA_1}{M_o} L}\right)$$

$$\frac{v_1 T}{M_o} = -\left(\frac{v_1 T}{M_o}\right)_{max} \sin\left(\omega t + \gamma_2\right)$$

where

$$\left(\frac{v_1 T}{M_o}\right)_{max} = \frac{\Omega_1{}^2\sqrt{\left(\frac{TA_1}{M_o} L\right)^2 + \left(\frac{TA_1}{M_o} N\right)^2}}{\omega^2}$$

$$\gamma_2 = \tan^{-1} \frac{N}{L}$$

$$\frac{\theta_2 TA_1}{M_o} = \left(\frac{\theta_2 TA_1}{M_o}\right)_{max} \sin\left(\omega t + \gamma_3\right)$$

where

$$\left(\frac{\theta_2 TA_1}{M_o}\right)_{max} = \frac{\sqrt{\left(\frac{TA_1}{M_o} P\right)^2 + \left(\frac{TA_1}{M_o} Q\right)^2}}{1 - \frac{\omega^2}{\Omega_1{}^2}}$$

$$\gamma_3 = \tan^{-1} \frac{Q}{P}$$

and

$$\frac{v_2 T}{M_o} = \left(\frac{v_2 T}{M_o}\right)_{max} \sin\left(\omega t + \gamma_4\right)$$

where

$$\left(\frac{v_2 T}{M_o}\right)_{max} = \frac{\Omega_2{}^2\sqrt{\left(\frac{TA_2}{M_o} P\right)^2 + \left(\frac{TA_2}{M_o} Q\right)^2}}{\omega^2}$$

$$\gamma_4 = \tan^{-1} \frac{Q}{P} = \gamma_3$$

and where L, N, P, and Q are defined as

$$L = k_2\left(a_1 - b_1\right) - k_1\left(a_2 - b_2\right)$$

$$N = k_1\left(a_1 - b_1\right) + k_2\left(a_2 - b_2\right)$$

$$P = \sin k_1 l\left[-\left(a_1k_1 + a_2k_2\right)e^{k_2 l} - \left(b_1k_1 + b_2k_2\right)e^{-k_2 l}\right]$$
$$+ \cos k_1 l\left[\left(a_1k_2 - a_2k_1\right)e^{k_2 l} - \left(b_1k_2 - b_2k_1\right)e^{-k_2 l}\right]$$

$$Q = \cos k_1 l\left[\left(a_1k_1 + a_2k_2\right)e^{k_2 l} - \left(b_1k_1 + b_2k_2\right)e^{-k_2 l}\right]$$
$$+ \sin k_1 l\left[\left(a_1k_2 - a_2k_1\right)e^{k_2 l} + \left(b_1k_2 - b_2k_1\right)e^{-k_2 l}\right]$$

There are eight basic independent dimensionless variables required to define the system maximum amplitudes. These variables are $r\omega/T$, $\omega l/c$, A_1/l, ω/Ω_1, I_1/J_1, A_2/l, ω/Ω_2, and I_2/J_2. The required program input must be in terms of the following eight dimensionless variables, written here as functions of the preceding eight equation variables:

$$\frac{\omega}{\Omega_1} = \frac{\omega}{\Omega_1}$$

$$\rho_1 = \frac{\pi}{2}\frac{r\omega}{T}\frac{c}{\omega l}$$

$$\frac{\omega_1}{\Omega_1} = \pi\frac{c}{\omega l}\frac{\omega}{\Omega_1}$$

$$\frac{\Omega_2}{\Omega_1} = \frac{\Omega_2}{\omega}\frac{\omega}{\Omega_1}$$

$$\frac{m_1}{m_2} = \frac{J_1}{I_1}\frac{I_2}{J_2}\left(\frac{\Omega_2}{\omega}\right)^2\left(\frac{\omega}{\Omega_1}\right)^2\frac{A_2}{l}\frac{l}{A_1}$$

$$\frac{I_1}{I_2} = \left(\frac{\omega}{\Omega_1}\right)^2\left(\frac{\Omega_2}{\omega}\right)^2\frac{A_1}{l}\frac{l}{A_2}$$

$$\frac{A_2}{l} = \frac{A_2}{l}$$

$$\frac{I_2}{J_2} = \frac{I_2}{J_2}$$

The required output are the four dimensionless maximum amplitudes $\left(\theta_1 TA_1/M_o\right)_{max}$, $\left(v_1T/M_o\right)_{max}$, $\left(\theta_2 TA_1/M_o\right)_{max}$, and $\left(v_2T/M_o\right)_{max}$.

APPENDIX E

COMPUTER PROGRAM FOR STEADY-STATE SOLUTION

The computer program for steady-state solution of the system equations for an input moment M_1 acting on the space station is listed herein.* Eight input variables are required for solution of the problem. These variables, in terms of the equation variables defined in the analysis, are

$$DP\ (1) = \frac{\omega}{\Omega_1}$$

$$DP\ (2) = \rho_1$$

$$DP\ (3) = \frac{\omega_1}{\Omega_1}$$

$$DP\ (4) = \frac{\Omega_2}{\Omega_1}$$

$$DP\ (5) = \frac{m_1}{m_2}$$

$$DP\ (6) = \frac{I_1}{I_2}$$

$$DP\ (7) = \frac{A_2}{l}$$

$$DP\ (8) = \frac{I_2}{J_2}$$

The results are printed out as the following dimensionless maximum amplitudes:

$$VAR\ (1) = \left(\frac{\theta_1 T A_1}{M_o}\right)_{max}$$

$$VAR\ (2) = \left(\frac{v_1 T}{M_o}\right)_{max}$$

---

*The program discussion and listing which appear in this appendix were supplied by Cohoon and Heasley, Inc., consulting engineers, Cambridge, Massachusetts, under contract to Langley Research Center.

APPENDIX E

$$\text{VAR (3)} = \left(\frac{\theta_2 TA_1}{M_o}\right)_{max}$$

$$\text{VAR (4)} = \left(\frac{v_2 T}{M_o}\right)_{max}$$

The program is arranged flexibly to permit solution of the problem for many values of any or all of the variables in a single run. Specified in the input for each variable are the number of equally spaced values it is to have and the smallest and largest of those values. The program will solve the equations for each of the given values of DP (1) by using the first value of the other input variables. It then indexes to the second value of DP (2) and repeats the solution for all the values of DP (1). This process is repeated until the complete set is finished. Note that although this is a very simple way to obtain results, it is also a very easy way to generate a tremendous amount of data.

The following discussion and program listing should be sufficient to permit anyone familiar with the computer to use this program.

Input

The input variables are read in on eight cards, each of which has four numbers on it. The numbers on the cards are read with the format (12, E15.8, 14, E15.8). The first number on the card specifies the variable. The other numbers on the card specify, in sequence, the initial value of the variable, the total number of values of the variable which are to be considered, and the final value of the variable. The following is an example:

1	0.10000000E0	11	10.0000000E0
DP (1)	Initial value	Number of values	Final value

Data must be fed in with the first numbers in ascending order. If this is not done, a statement is made and the program does not continue.

Output

The printout of the input variables and the results is in the following form with an E15.8 format:

DP (1) =	DP (2) =	DP (3) =
DP (4) =	DP (5) =	DP (6) =
DP (7) =	DP (8) =	

VAR (1) =	VAR (2) =
VAR (3) =	VAR (4) =

A line is skipped whenever such a set is printed out.

There are a number of checks in the program that have certain printouts associated with them as follows:

(A) DATA CARDS ARE NOT IN ORDER. This statement is printed out if the input cards are not in the correct sequence. When this is printed out, the program stops.

(B) DP (3,4,5,6) CANNOT BE ZERO. This is printed out if the input DP (3), DP (4), DP (5), or DP (6) is zero or becomes exactly zero during the run. The program does not stop but rather continues to the next index. If the variable is still zero, the statement will be printed out again and the program will index again.

(C) WITH DP (1) = 1 EQUATION BECOMES INFINITE. This is printed out if DP (1) is equal to 1. This condition would set some of the equations in the program equal to infinity. When this is printed out, the program indexes and continues.

(D) WITH EV (7) = 1 EQUATION BECOMES INFINITE. This is printed out if EV (7) is equal to 1. This condition would set some of the equations in the program equal to infinity. When this is printed out, the program indexes and continues.

(E) MATRIX IS NOT SOLVABLE IN THIS FORM. This statement refers to the solution of the set of simultaneous equations in the program and may occur if the program is asked to calculate a resonant amplitude with insufficient damping. If the divisor is smaller than a test value, this statement will be printed out. Since computation error is increased with division by small numbers, this is a check to inform the person who analyzes the data that numbers in the solution matrix are getting small. The test value in the program is 0.00000001. When this statement is printed out, the program indexes and continues.

APPENDIX E

Program Listing

```
      PROGRAM CPH(INPUT,OUTPUT,TAPE5=INPUT,TAPE6=OUTPUT)
C  PROGRAM FOR MAX. DEFLECTIONS FOR NASA 1  FORTRAN 4  C+H
      DIMENSION RINI(8),JACK(8),RFIN(8),DR(8),DELT(8)
      DIMENSION DP(8),EV(8),GO(4,5),COF(4),AT(4,4),VAR(4),ER(4)
 1111 DO 301 I=1,8
      READ (5,302) JOE,RINI(I),JACK(I),RFIN(I)
  302 FORMAT(I2,E15.8,I4,E15.8)
      IF(JOE-I)303,304,303
  303 WRITE (6,305)
  305 FORMAT(28H DATA CARDS ARE NOT IN ORDER)
      GO TO 300
  304 CONTINUE
  301 CONTINUE
      DO 306 I=1,8
      IF(JACK(I)-1)307,308,307
  308 DELT(I)=0.
      GO TO 306
  307 DR(I)=JACK(I)-1
      DELT(I)=(RFIN(I)-RINI(I))/DR(I)
  306 CONTINUE
      DP(8)=RINI(8)
      JACK8=JACK(8)
      DO 319 J8=1,JACK8
      DP(7)=RINI(7)
      JACK7=JACK(7)
      DO 317 J7=1,JACK7
      DP(6)=RINI(6)
      JACK6=JACK(6)
      DO 316 J6=1,JACK6
      DP(5)=RINI(5)
      JACK5=JACK(5)
      DO 315 J5=1,JACK5
      DP(4)=RINI(4)
      JACK4=JACK(4)
      DO 314 J4=1,JACK4
      DP(3)=RINI(3)
      JACK3=JACK(3)
      DO 313 J3=1,JACK3
      DP(2)=RINI(2)
      JACK2=JACK(2)
      DO 312 J2=1,JACK2
      DP(1)=RINI(1)
```

```
      JACK1=JACK(1)
      DO 311 J1=1,JACK1
      TEST=.00000001
C     BEGINNING OF SOLUTION WITH ABOVE INPUT VARIABLES
      DO 1 I=3,6
      IF(DP(I))1,2,1
    2 WRITE (6,4)
    4 FORMAT(42H DP(3,4,5,6) CANNOT BE ZERO LOOK AT PAGE 2)
      GO TO 100
    1 CONTINUE
      PI=3.14159
      EV(1)=DP(1)*DP(2)*2./DP(3)
      EV(2)=PI*DP(1)/DP(3)
      EV(3)=DP(6)*DP(7)/DP(4)**2
      EV(4)=DP(1)
      EV(5)=DP(8)*DP(4)**4/(DP(5)*DP(6))
      EV(6)=DP(7)
      EV(7)=DP(1)/DP(4)
      EV(8)=DP(8)
      FE=.5*ATAN (EV(1))
      CO1=EV(2)*(1./(1.+EV(1)**2)**.25)*COS (FE)
      CO2=EV(2)*(1./(1.+EV(1)**2)**.25)*SIN (FE)
      IF(1.-EV(4)**2) 5,6,5
    6 WRITE(6,77)
   77 FORMAT(34H WITH DP(1)=1 EQ. BECOMES INFINITE)
      GO TO 100
    5 CONTINUE
      CON=EV(3)*(1./(1.-EV(4)**2))
      DON=-EV(3)*(1.+EV(5)-(1./DP(1)**2)*EV(5))/(1.-EV(4)**2)
      IF(1.-EV(7)**2)20,21,20
   21 WRITE(6,67)
   67 FORMAT(34H WITH EV(7)=1 EQ. BECOMES INFINITE)
      GO TO 100
   20 CONTINUE
      DOR=-DP(7)*((1.+DP(8)-(1./EV(7))**2*DP(8))/(1.-EV(7)**2))
      A=DON*CO1
      B=DON*CO2
      C=DOR*CO1
      D=DOR*CO2
      ELN=2.71828183
      E=ELN**(-2.*CO2)
      F=SIN (CO1)/COS (CO1)
      GO(1,1)=1.+B
```

```
      GO(2,1)=A
      GO(3,1)=1.-D+C*F
      GO(4,1)=-C+(1.-D)*F
      GO(1,2)=1.-B
      GO(2,2)=-A
      GO(3,2)=(1.+D+C*F)*E
      GO(4,2)=(C-(1.+D)*F)*E
      GO(1,3)=-A
      GO(2,3)=1.+B
      GO(3,3)=C-(1.-D)*F
      GO(4,3)=1.-D+C*F
      GO(1,4)=A
      GO(2,4)=1.-B
      GO(3,4)=(-C+(1.+D)*F)*E
      GO(4,4)=(1.+D+C*F)*E
      GO(1,5)=CON
      GO(2,5)=0.0
      GO(3,5)=0.0
      GO(4,5)=0.0
C     BEGINNING SOLUTION OF MATRIX
      AT(1,1)=GO(1,1)
      IF(ABS (AT(1,1))-TEST)40,40,16
   40 WRITE(6,11)
   11 FORMAT(36H MATRIX IS NOT SOLVABLE IN THIS FORM)
      GO TO 100
   16 CONTINUE
      AT(2,1)=GO(2,1)
      AT(3,1)=GO(3,1)
      AT(4,1)=GO(4,1)
      H12=GO(1,2)/AT(1,1)
      AT(2,2)=GO(2,2)-AT(2,1)*H12
      IF(ABS (AT(2,2))-TEST)40,40,17
   17 CONTINUE
      AT(3,2)=GO(3,2)-AT(3,1)*H12
      AT(4,2)=GO(4,2)-AT(4,1)*H12
      H13=GO(1,3)/AT(1,1)
      H23=(GO(2,3)-AT(2,1)*H13)/AT(2,2)
      AT(3,3)=GO(3,3)-AT(3,1)*H13-AT(3,2)*H23
      IF(ABS (AT(3,3))-TEST)40,40,18
   18 CONTINUE
      AT(4,3)=GO(4,3)-AT(4,1)*H13-AT(4,2)*H23
      H14=GO(1,4)/AT(1,1)
      H24=(GO(2,4)-AT(2,1)*H14)/AT(2,2)
```

```
      H34=(GO(3,4)-AT(3,1)*H14-AT(3,2)*H24)/AT(3,3)
      AT(4,4)=GO(4,4)-AT(4,1)*H14-AT(4,2)*H24-AT(4,3)*H34
      IF(ABS (AT(4,4))-TEST)40,40,19
   19 CONTINUE
      CR1=GO(1,5)/AT(1,1)
      CR2=(GO(2,5)-AT(2,1)*CR1)/AT(2,2)
      CR3=(GO(3,5)-AT(3,1)*CR1-AT(3,2)*CR2)/AT(3,3)
      CR4=(GO(4,5)-AT(4,1)*CR1-AT(4,2)*CR2-AT(4,3)*CR3)/AT(4,4)
      GO(4,5)=CR4
      GO(3,5)=CR3-H34*GO(4,5)
      GO(2,5)=CR2-H24*GO(4,5)-H23*GO(3,5)
      GO(1,5)=CR1-H14*GO(4,5)-H13*GO(3,5)-H12*GO(2,5)
C     END OF MATRIX SOLUTION
      COF(1)=CO2*(GO(1,5)-GO(2,5))-CO1*(GO(3,5)-GO(4,5))
      COF(2)=CO1*(GO(1,5)-GO(2,5))+CO2*(GO(3,5)-GO(4,5))
      X1=(GO(1,5)*CO1+GO(3,5)*CO2)*ELN**CO2
      X2=(-GO(2,5)*CO1-GO(4,5)*CO2)*ELN**(-CO2)
      X3=(GO(1,5)*CO2-GO(3,5)*CO1)*ELN**CO2
      X4=(GO(2,5)*CO2-GO(4,5)*CO1)*ELN**(-CO2)
      COF(3)=SIN (CO1)*(-X1+X2)+COS (CO1)*(X3-X4)
      COF(4)=COS (CO1)*(X1+X2)+SIN (CO1)*(X3+X4)
      CL1=1.-DP(1)**2
      CL2=(1.+COF(1))**2
      CL3=(COF(2))**2
      VAR(1)=(SQRT (CL2+CL3))/CL1
      VAR(2)=(EV(5)/DP(1)**2)*SQRT ((COF(1))**2+CL3)
      COL=1.-EV(7)**2
      DL1=(COF(3))**2
      DL2=(COF(4))**2
      VAR(3)=(SQRT (DL1+DL2))/COL
      DL3=((DP(7)/EV(3))*COF(3))**2
      DL4=((DP(7)/EV(3))*COF(4))**2
      VAR(4)=DP(8)*(1./EV(7))**2*SQRT (DL3+DL4)
      WRITE (6,600) DP(1),DP(2),DP(3)
  600 FORMAT(7H DP(1)=,E15.8,7H DP(2)=,E15.8,7H DP(3)=,E15.8)
      WRITE (6,601) DP(4),DP(5),DP(6)
  601 FORMAT(7H DP(4)=,E15.8,7H DP(5)=,E15.8,7H DP(6)=,E15.8)
      WRITE (6,602) DP(7),DP(8)
  602 FORMAT(7H DP(7)=,E15.8,7H DP(8)=,E15.8)
      WRITE (6,603) VAR(1),VAR(2)
  603 FORMAT(10H   VAR(1)=,E15.8,9H  VAR(2)=,E15.8)
      WRITE (6,604) VAR(3),VAR(4)
  604 FORMAT(10H   VAR(3)=,E15.8,9H  VAR(4)=,E15.8/)
```

```
100 CONTINUE
    DP(1)=DP(1)+DELT(1)
311 CONTINUE
    DP(2)=DP(2)+DELT(2)
312 CONTINUE
    DP(3)=DP(3)+DELT(3)
313 CONTINUE
    DP(4)=DP(4)+DELT(4)
314 CONTINUE
    DP(5)=DP(5)+DELT(5)
315 CONTINUE
    DP(6)=DP(6)+DELT(6)
316 CONTINUE
    DP(7)=DP(7)+DELT(7)
317 CONTINUE
    DP(8)=DP(8)+DELT(8)
319 CONTINUE
    GO TO 1111
300 STOP
    END
```

APPENDIX F

DISCUSSION OF SIMPLIFIED BOND GRAPH NOTATION

This short discussion is intended to define the symbols used in figure 15 only and is in no way a definition of the complete notation of bond graphs.

The power bond is defined with the symbol $\frac{e}{f}\rightharpoonup$ where the product of the signal pair e and f describes the power passing through the bond in the direction of the half arrow. For the system of figure 15 the effort e and the flow f are either the pair torque and angular speed or the pair force and linear speed. The signal pairs are not shown in figure 15 but are implied. A power bond number is assigned such that the effort associated with bond 1 is e_1 and the flow f_1.

The effort sources $\left(\text{e.g., } E\overset{1}{\rightharpoonup}\right)$ of figure 15 denote that effort $\left(\text{e.g., } e_1\right)$ is a specified function of time. The symbol 0 denotes a point of common effort; the symbol 1, a point of common flow. The storage element for potential energy has the symbol $\rightharpoonup C$; that for kinetic energy, the symbol $\rightharpoonup I$; that for energy loss, the symbol $\rightharpoonup R$. The final element of figure 15 is the transformer $\overset{a}{\rightharpoonup} TF \overset{b}{\rightharpoonup}$, which implies the relations

$$e_a = me_b$$

$$f_a = \frac{f_b}{m}$$

where m is the transformer modulus.

REFERENCES

1. Targoff, Walter P.: On the Lateral Vibration of Rotating, Orbiting Cables. AIAA Paper No. 66-98, Jan. 1966.

2. Liu, Frank C.: On Dynamics of Two Cable-Connected Space Stations. NASA TM X-53650, 1967.

3. Paynter, Henry M.: Analysis and Design of Engineering Systems. M.I.T. Press, 1961.

4. Paynter, H. M.; and Karnopp, D. C.: Design and Control of Multiport Engineering Systems. Reprinted from Proceedings of IFAC Tokyo Symposium on Systems Engineering for Control System Design, 1965, pp. 443-454.

5. Rosenberg, Ronald Carl: Computer-Aided Teaching of Dynamic System Behavior. Sc. D. Thesis, Massachusetts Inst. Technol., 1965.

6. Anderson, Willard W.: The Dynamics of Moving Filaments and Tapes. Sc. D. Thesis, Massachusetts Inst. Technol., 1966.

7. Karnopp, Dean: Coupled Vibratory-System Analysis, Using the Dual Formulation. J. Acoust. Soc. Amer., vol. 40, no. 2, Aug. 1966, pp. 380-384.

8. Karnopp, Bruce H.: Application of the Legendre Transformation to the Formulation of Linear Problems in Elastodynamics. Tensor, new ser., vol. 18, no. 2, May 1967, pp. 141-149.

9. Karnopp, D. C.: Computer Representation of Continuous Vibratory Systems Using Normal Modes and Bond Graph Techniques. Simulation, vol. 10, no. 3, Mar. 1968, pp. 129-135.

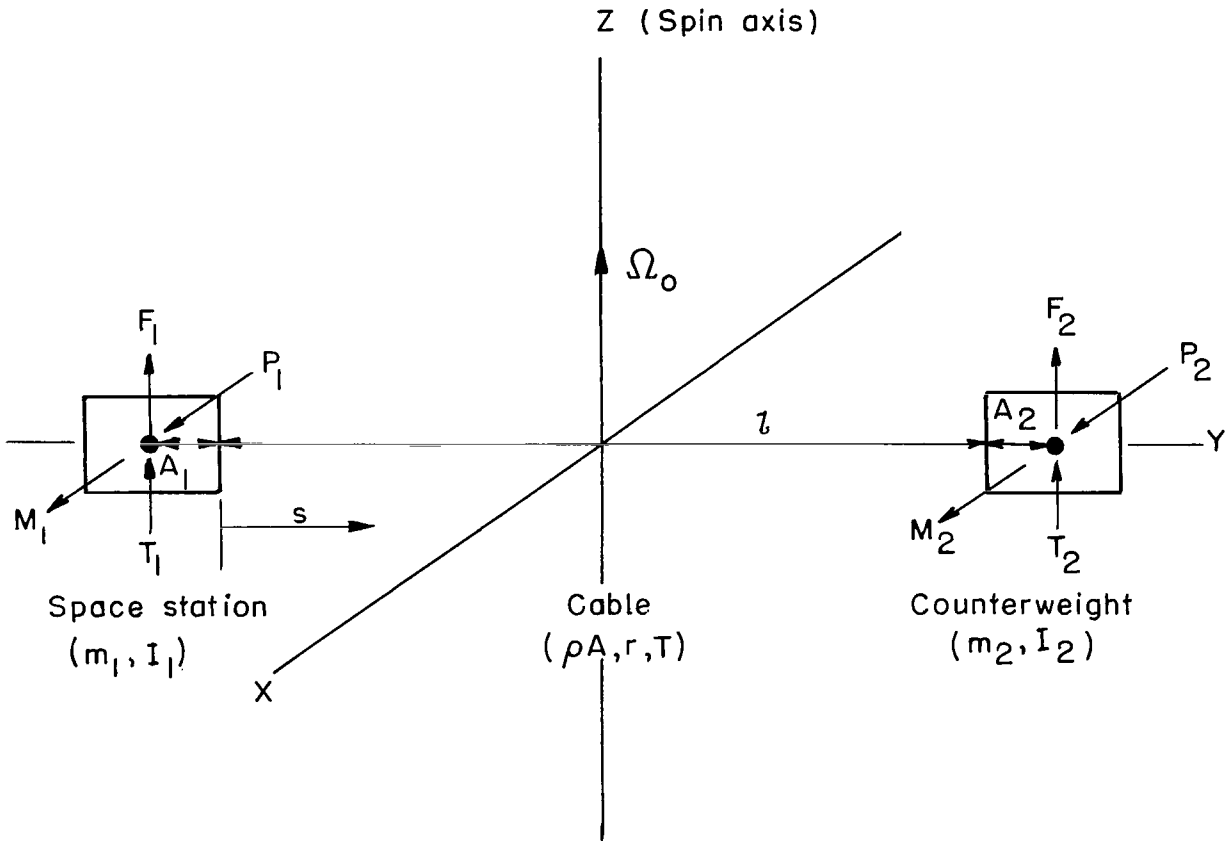

Figure 1.- Spinning system configuration.

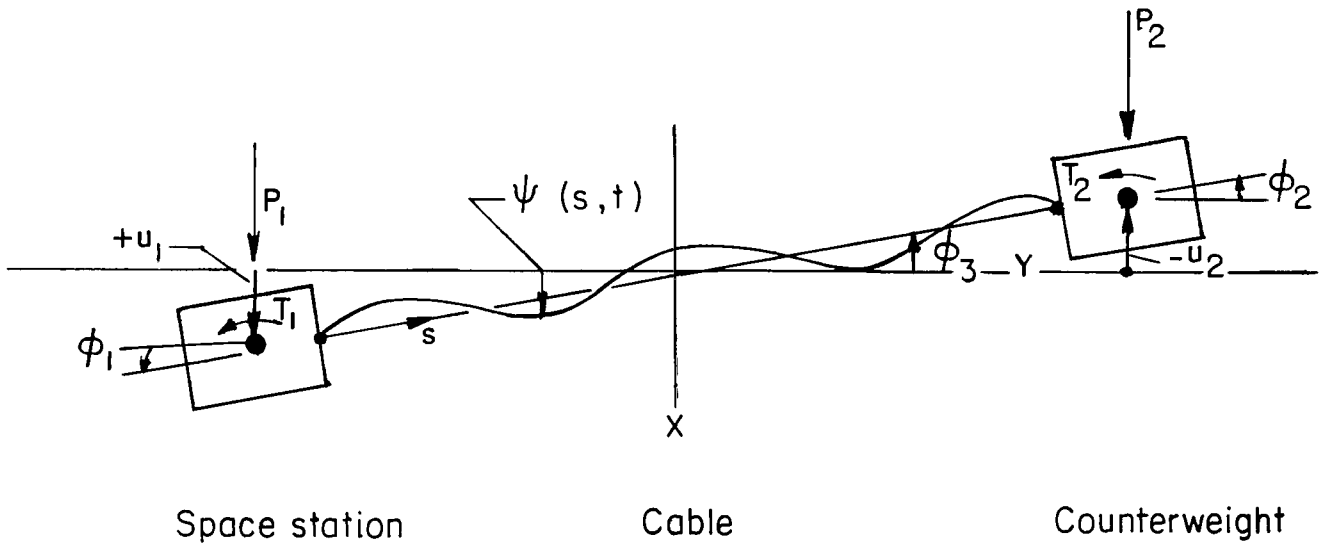

Figure 2.- Configuration in XY (spin) plane.

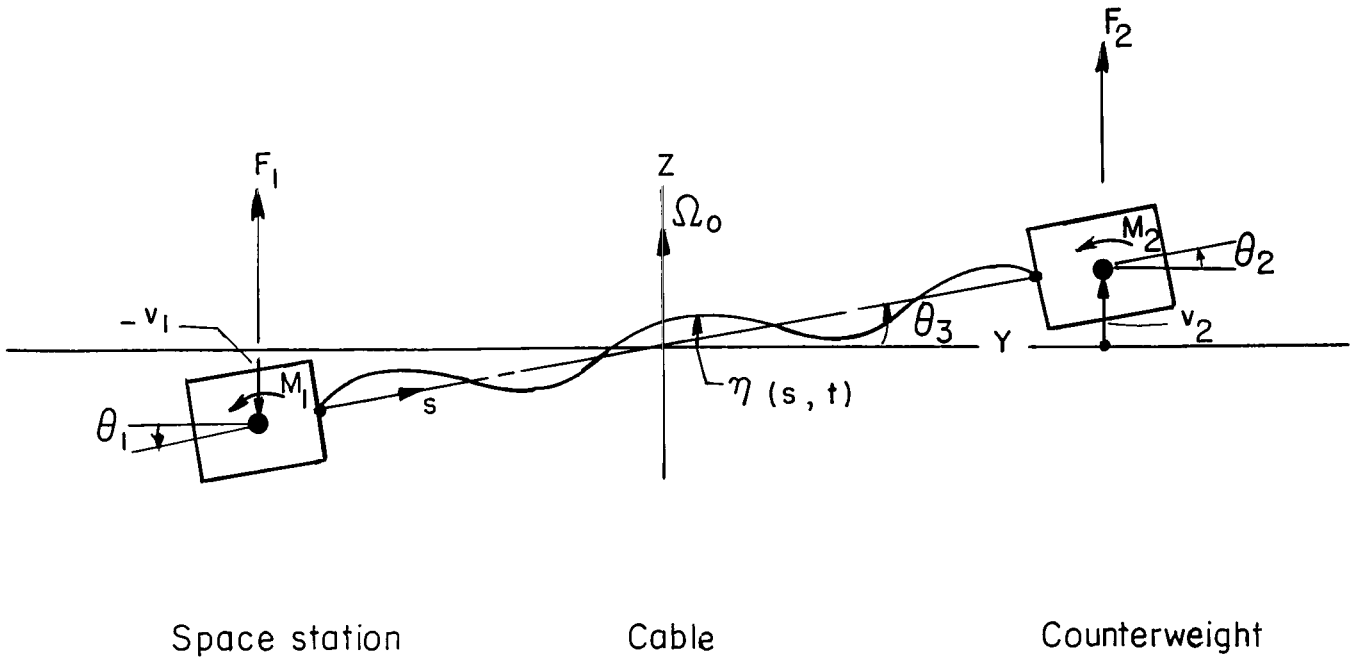

Figure 3.- Configuration in YZ plane.

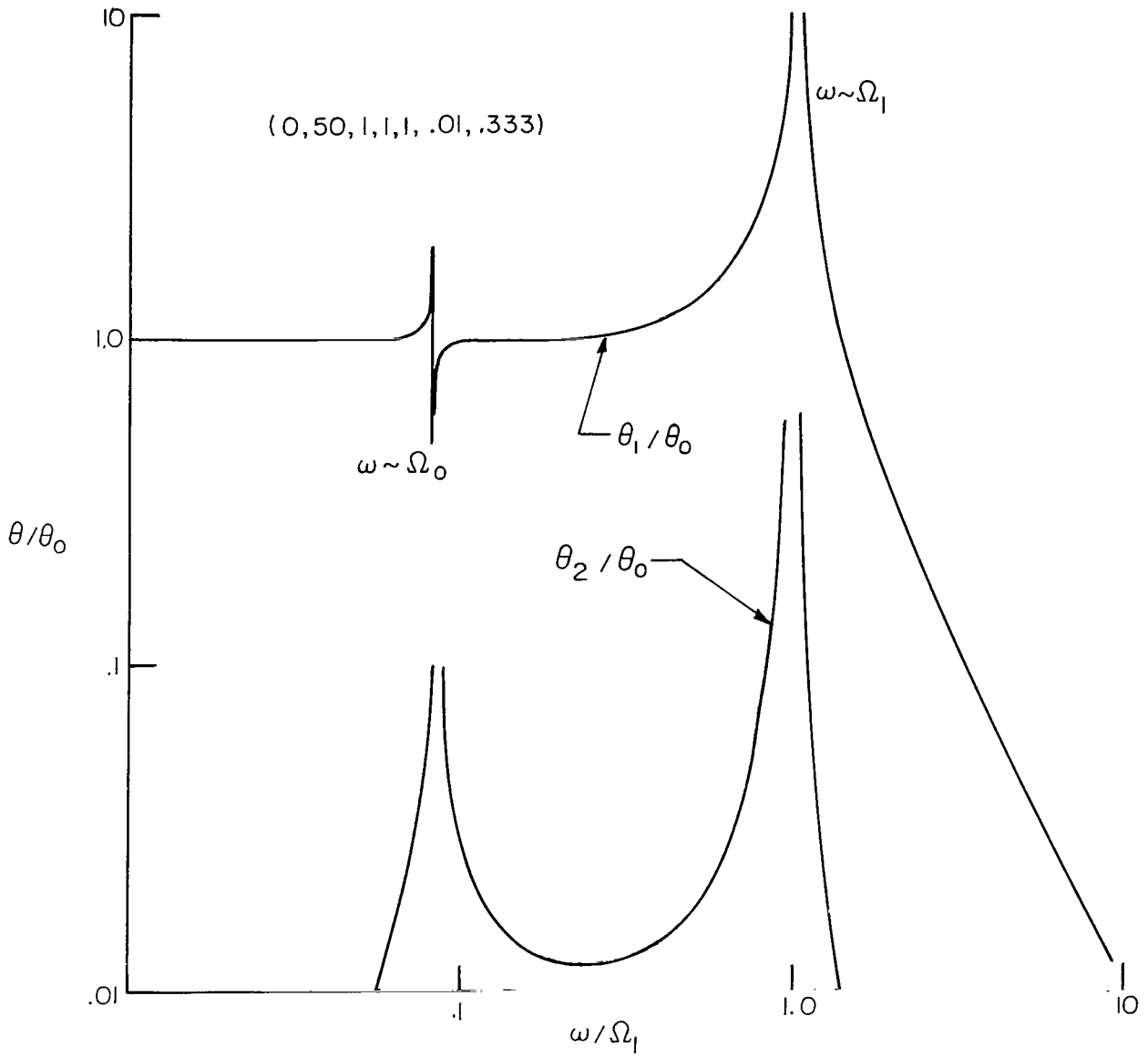

(a) Space-station and counterweight attitude.

Figure 4.- Basic steady-state response.

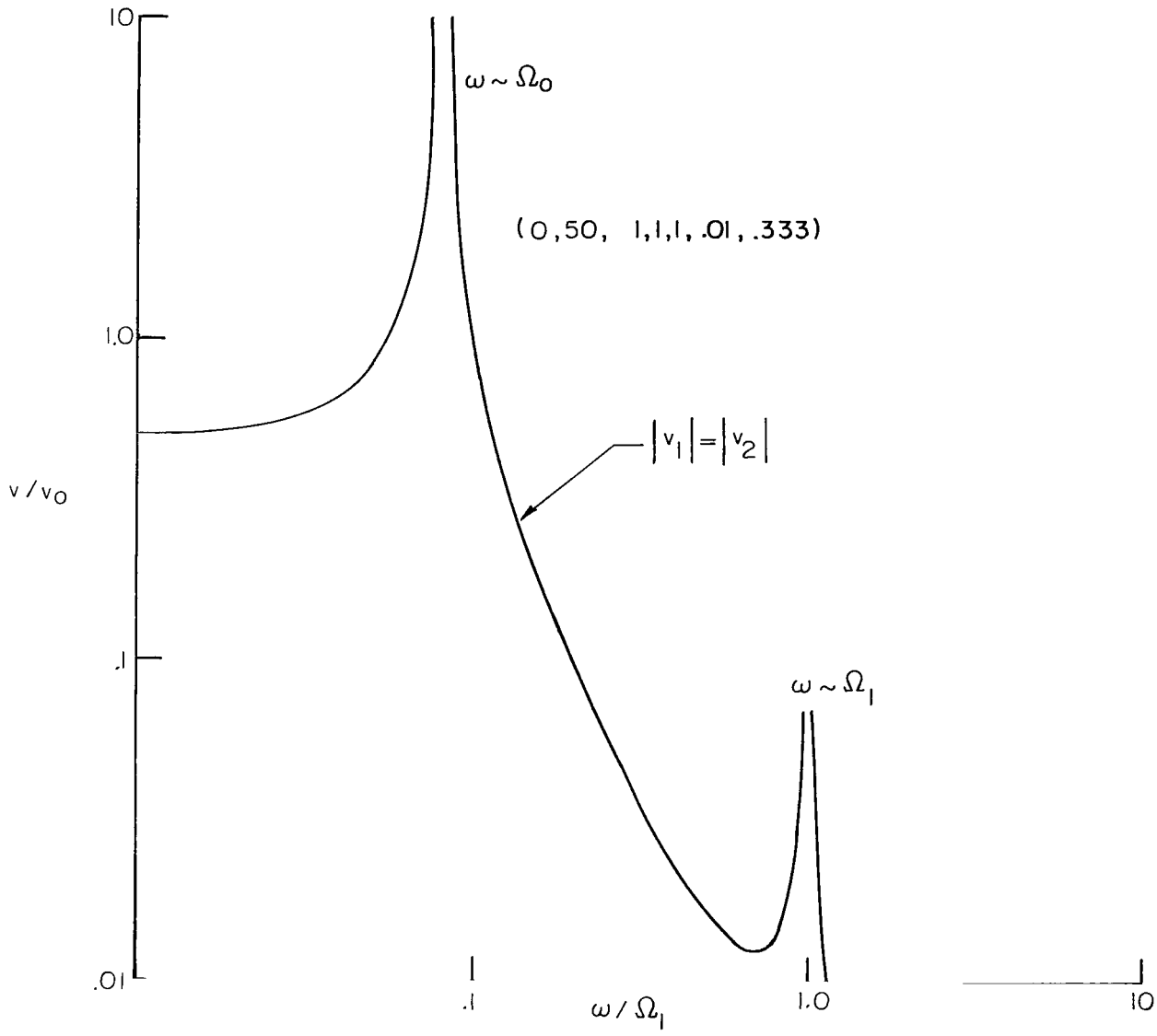

(b) Space-station and counterweight translation.

Figure 4.- Concluded.

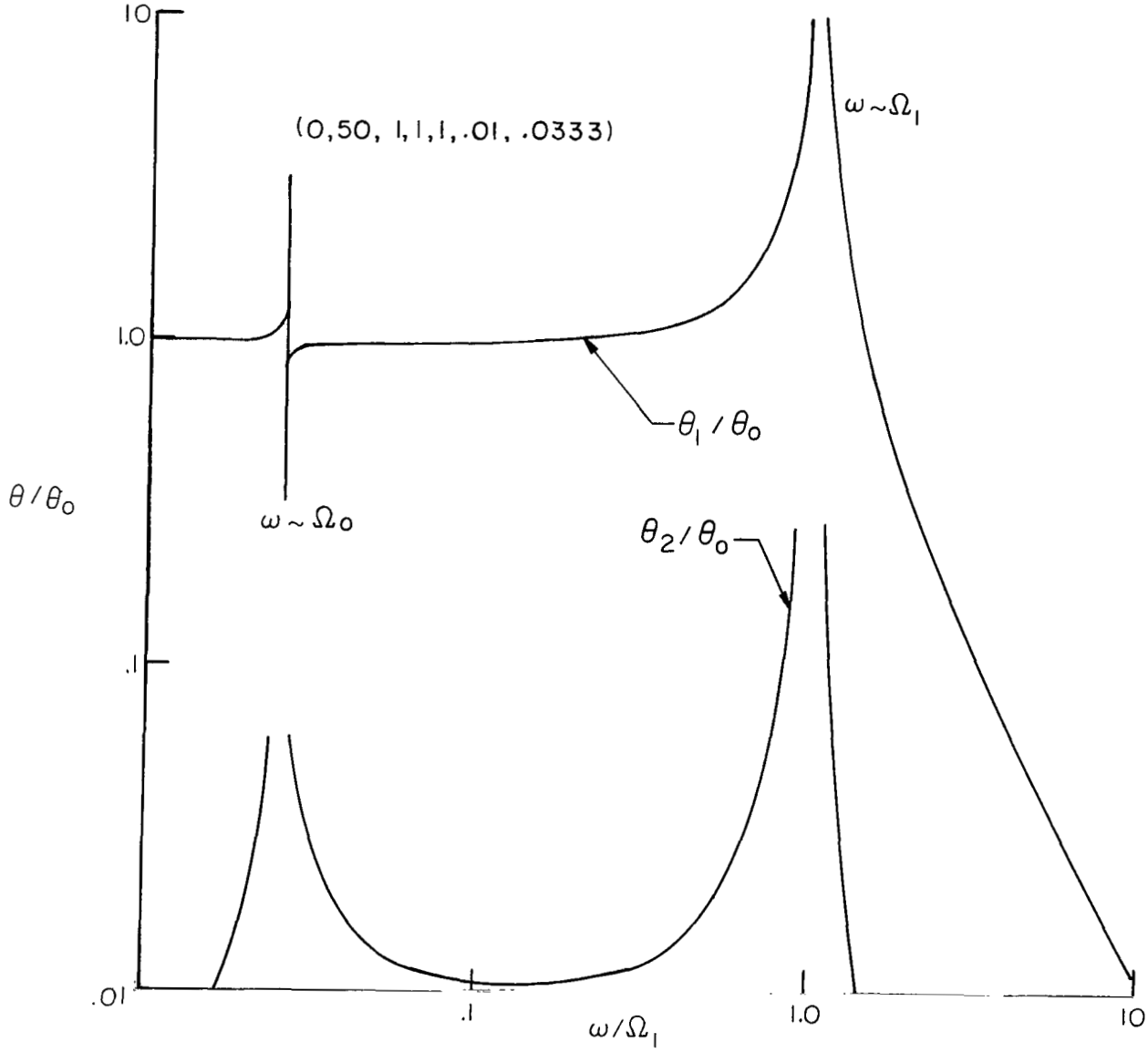

(a) Low inertia ratio, I_2/J_2.

Figure 5.- Variable-spin steady-state response.

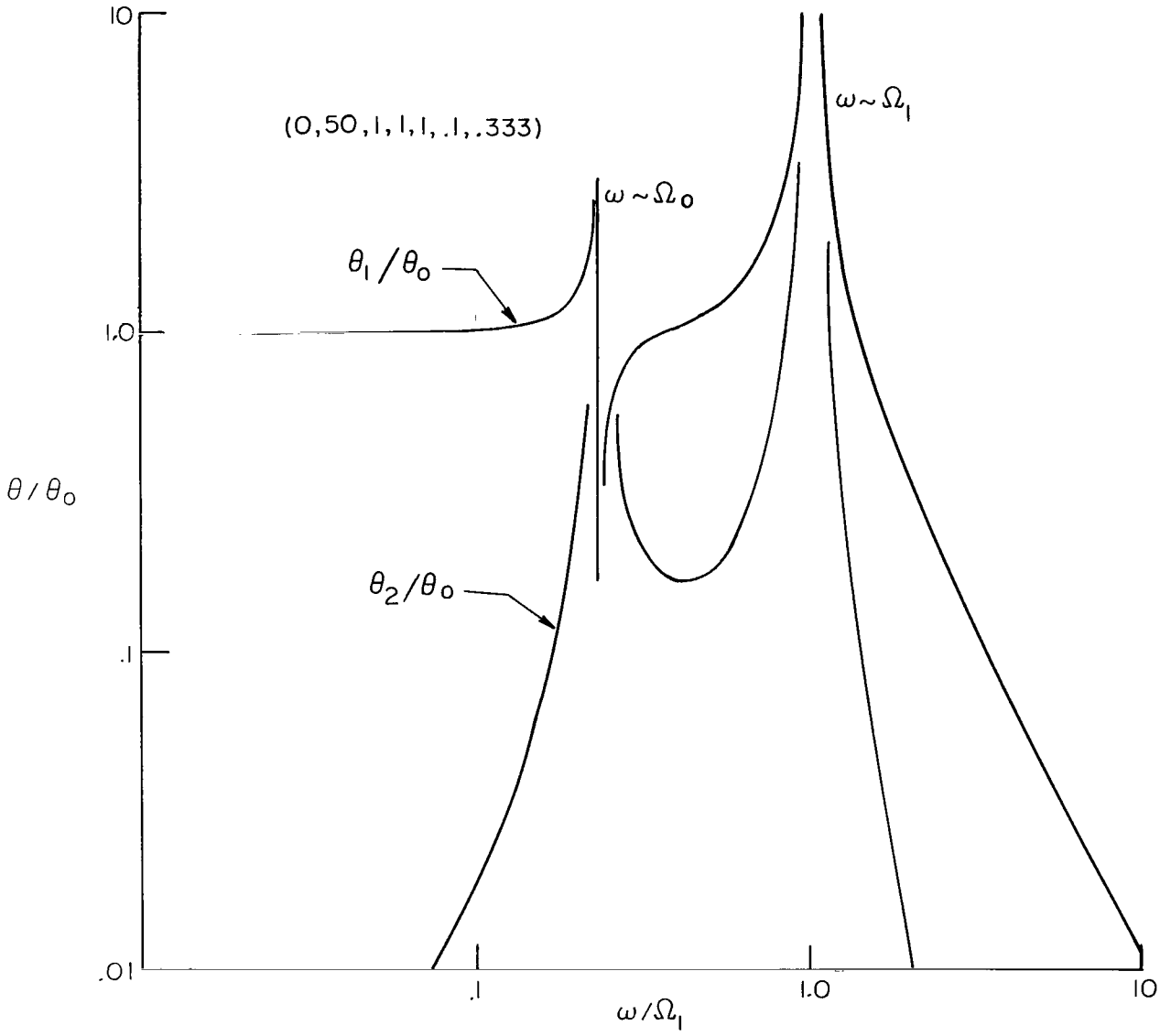

(b) Increased A_2/l.

Figure 5.- Continued.

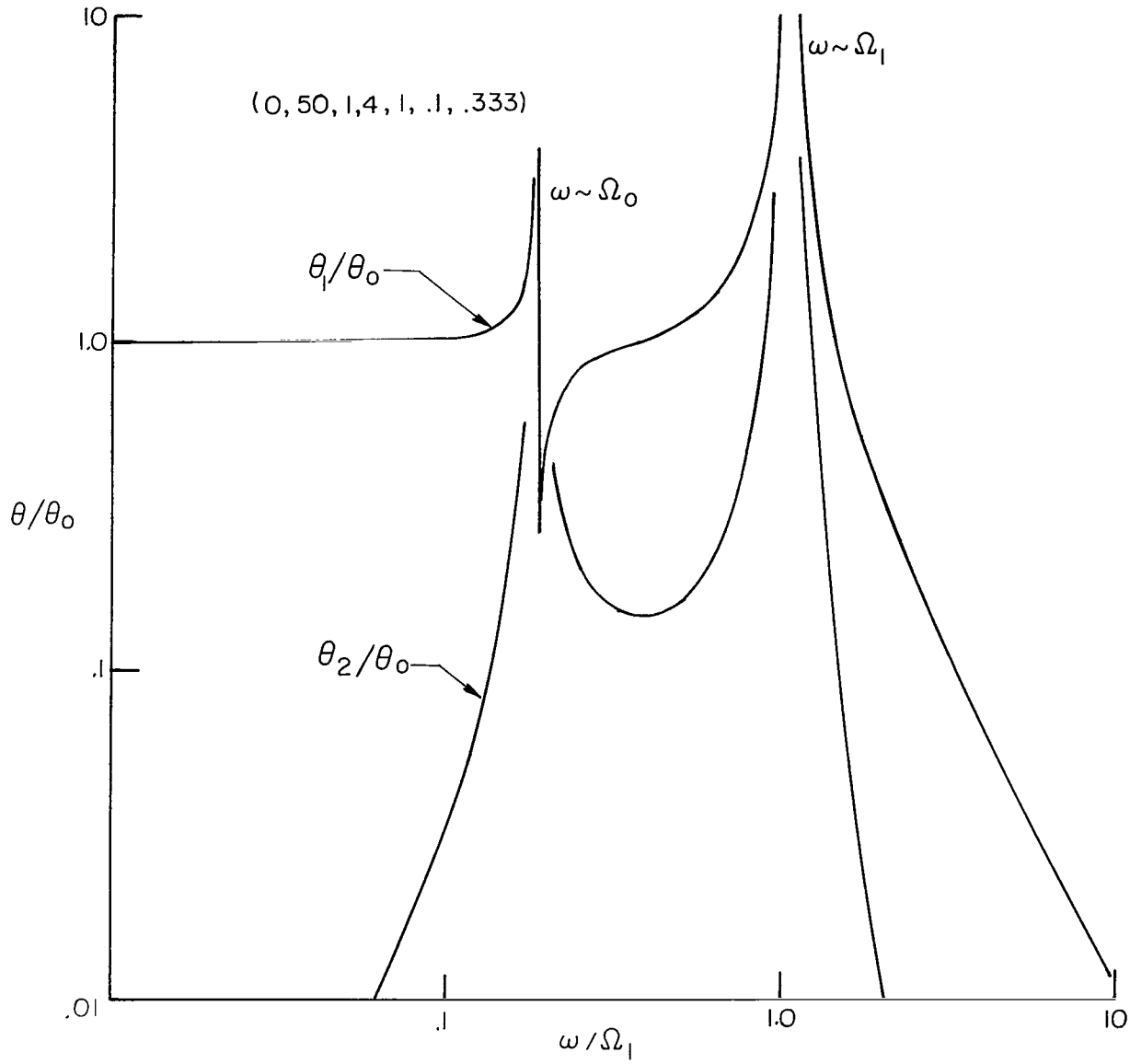

(c) High mass ratio, m_1/m_2.

Figure 5.- Continued.

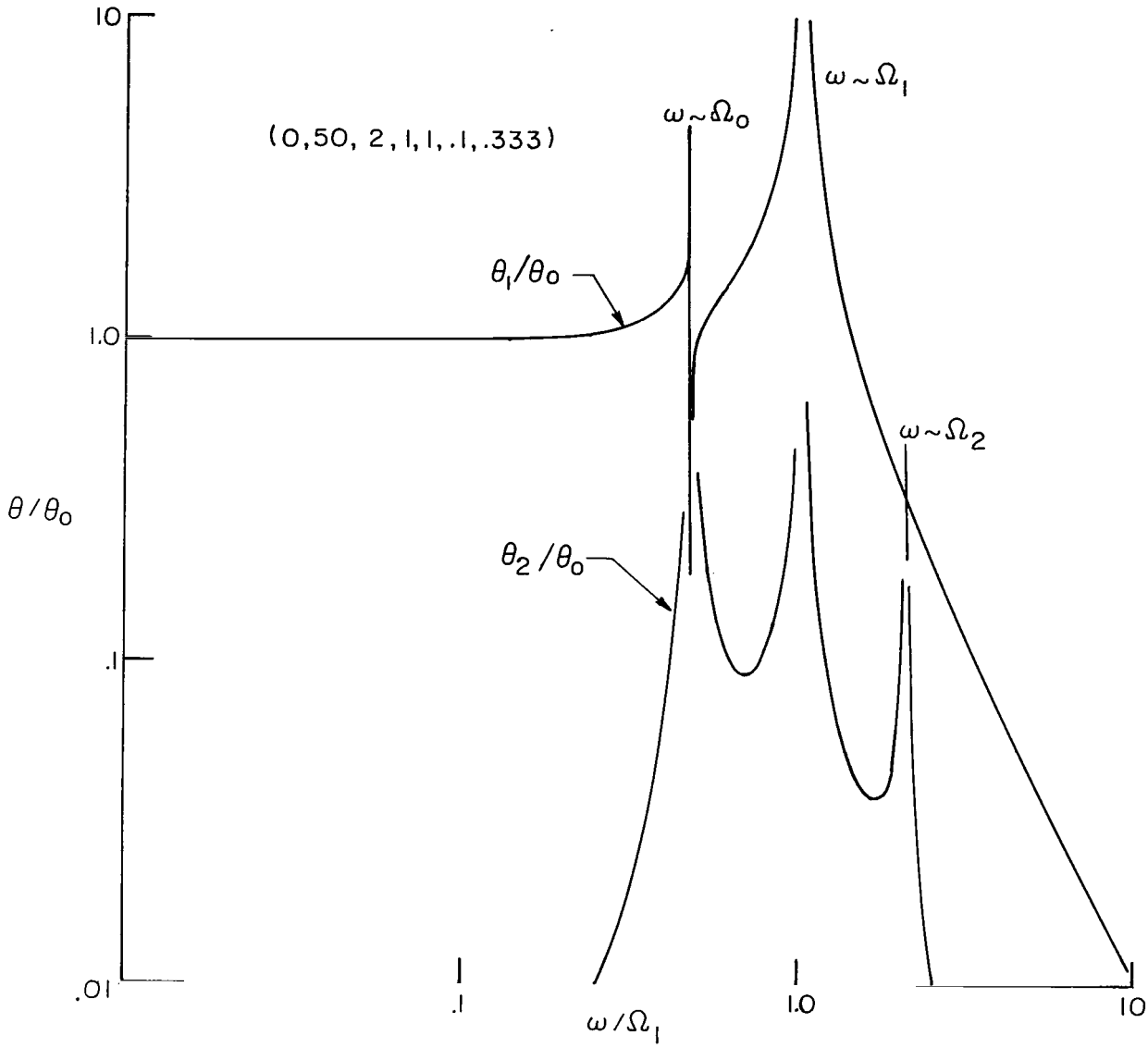

(d) Increased uncoupled frequency ratio, Ω_2/Ω_1.

Figure 5.- Concluded.

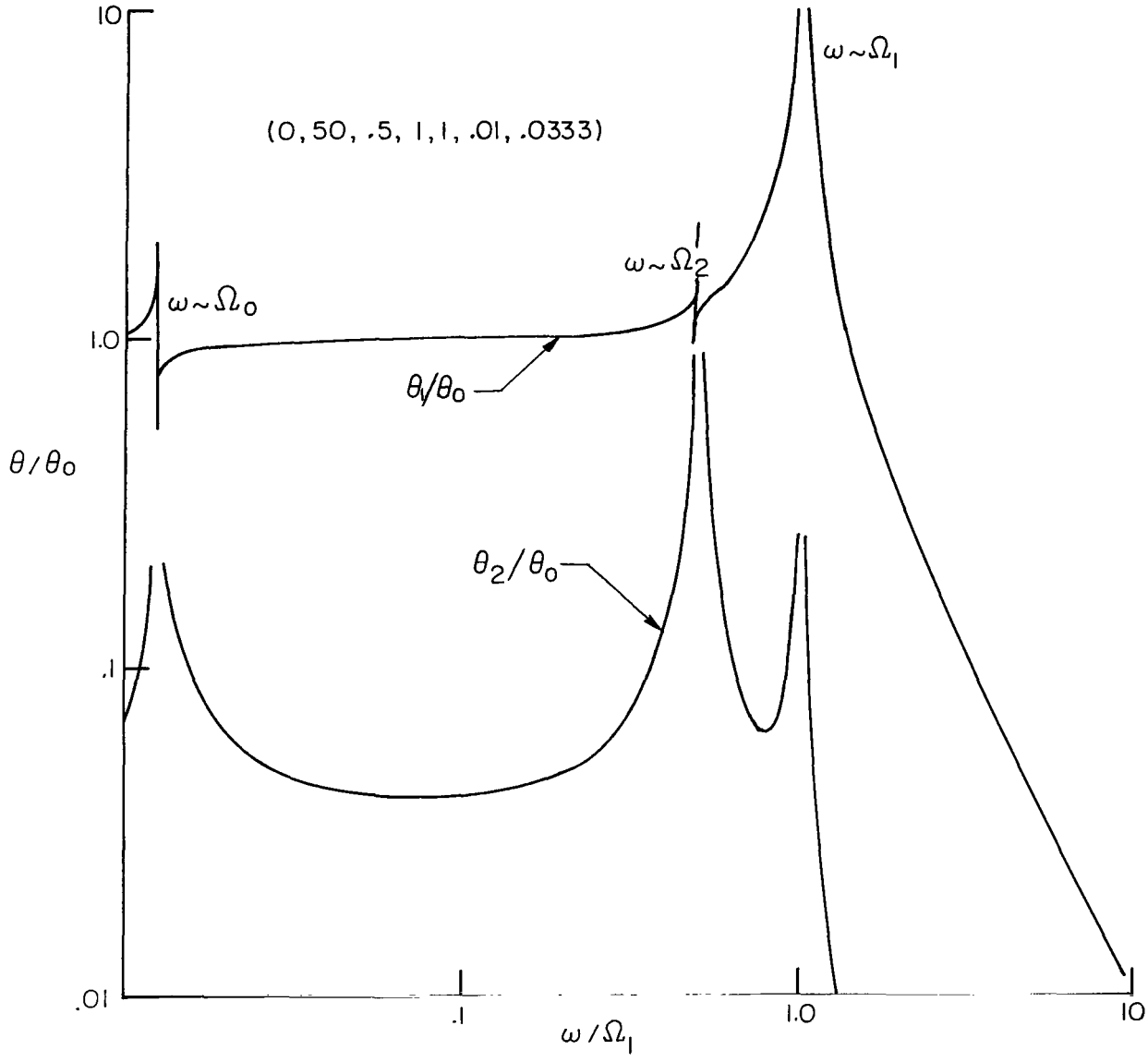

Figure 6.- Steady-state response for low counterweight frequency.

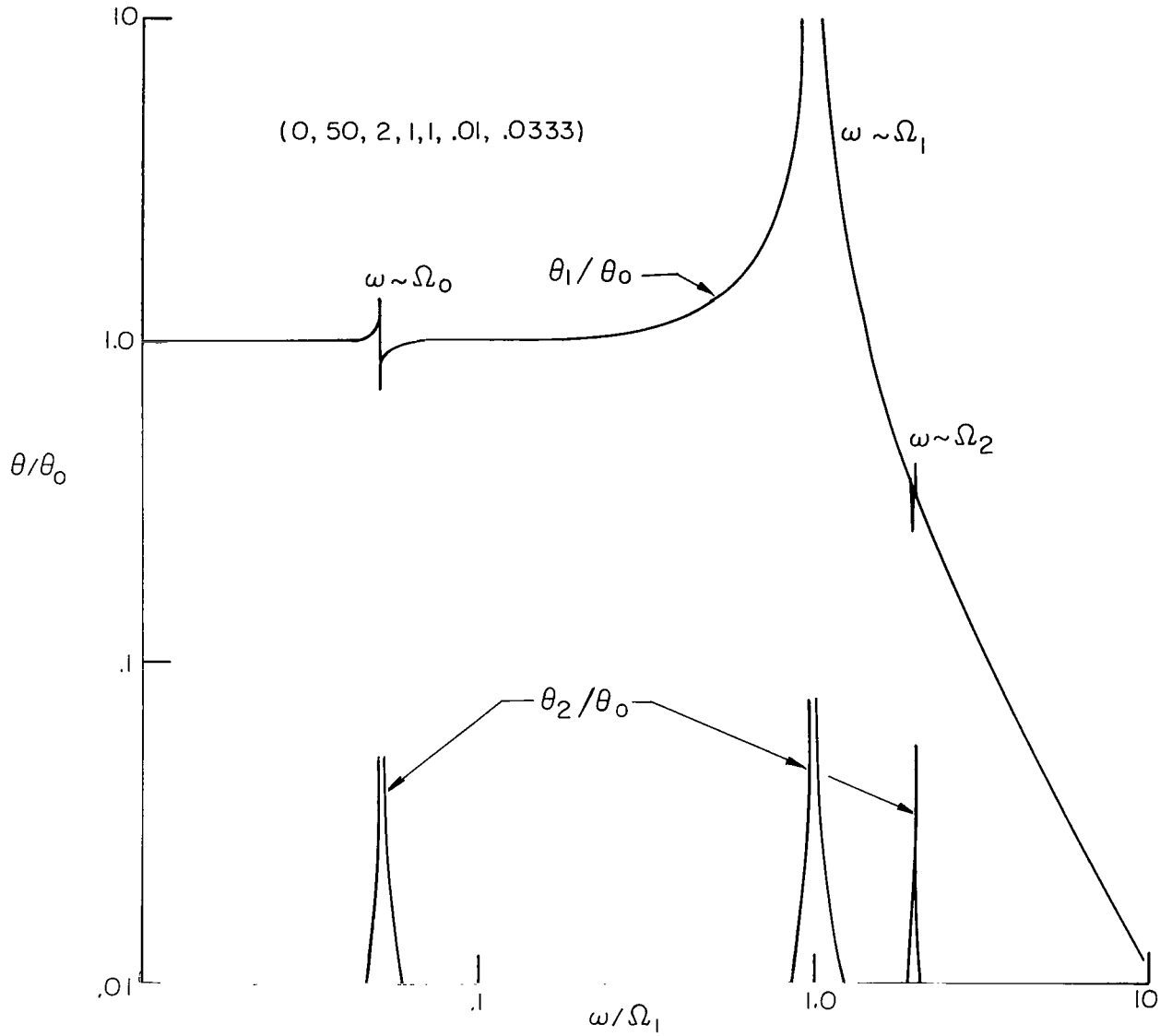

Figure 7.- Steady-state response for high counterweight frequency.

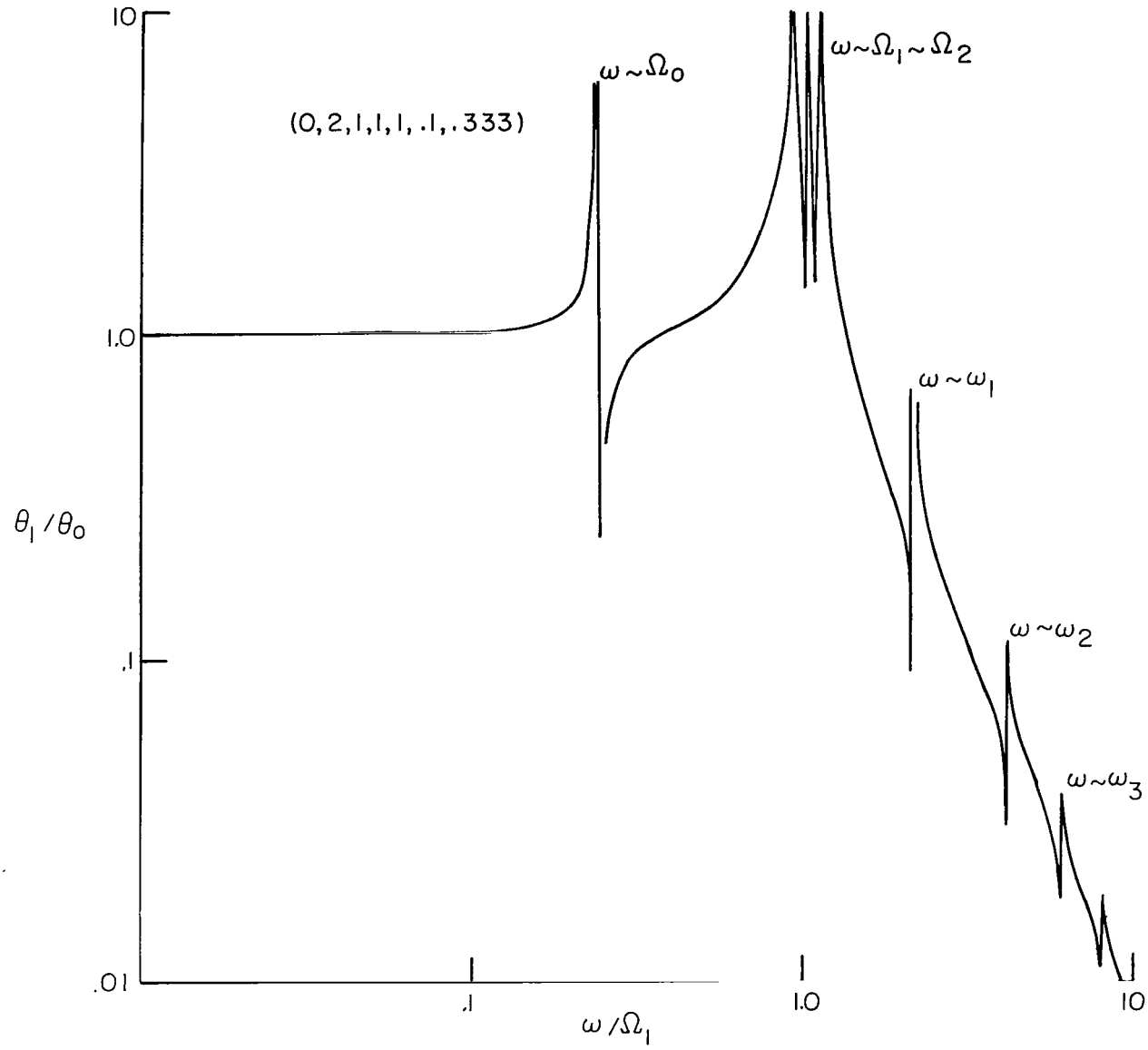

(a) Space-station attitude.

Figure 8.- Steady-state response for high cable frequency.

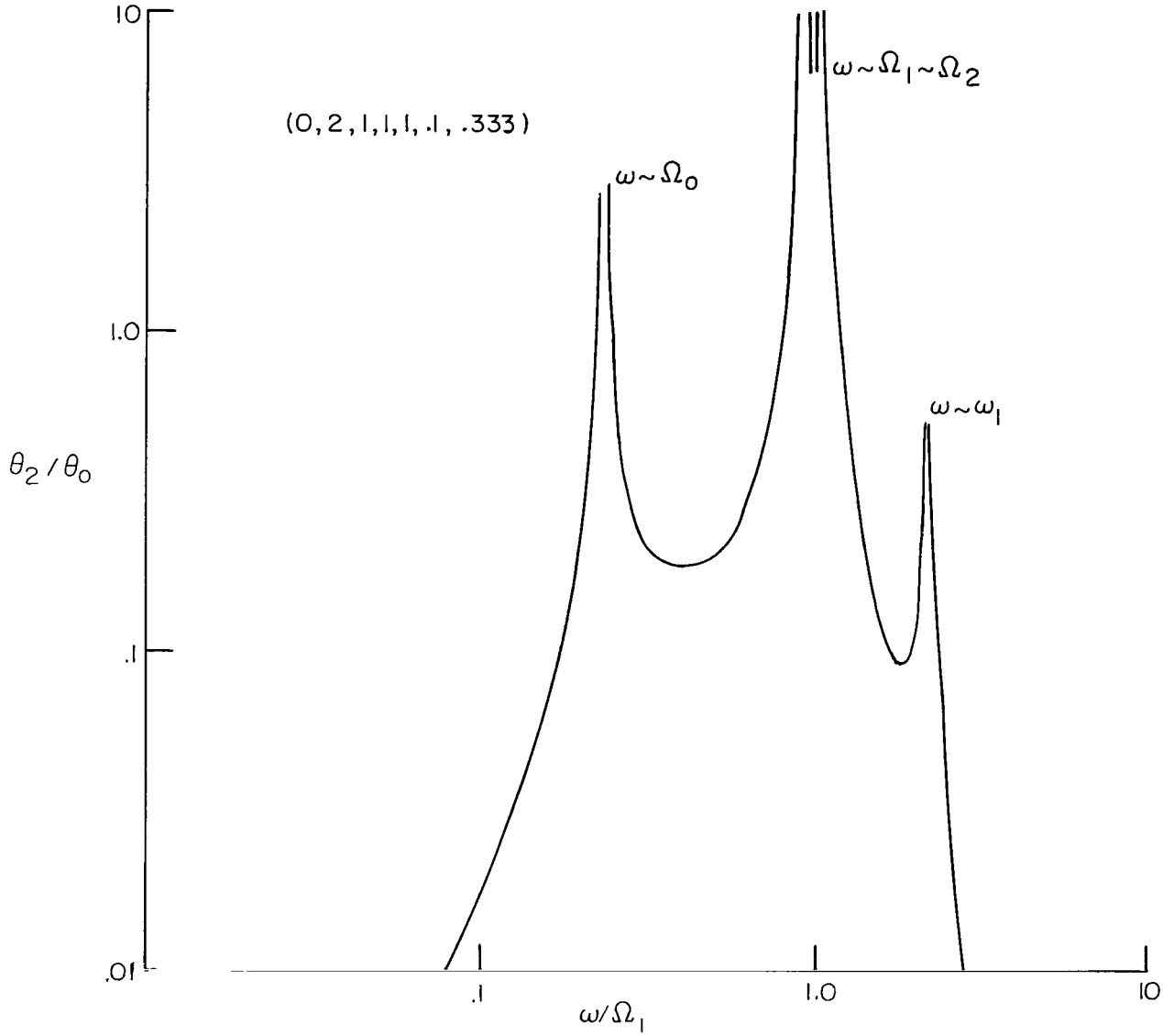

(b) Counterweight attitude.

Figure 8.- Continued.

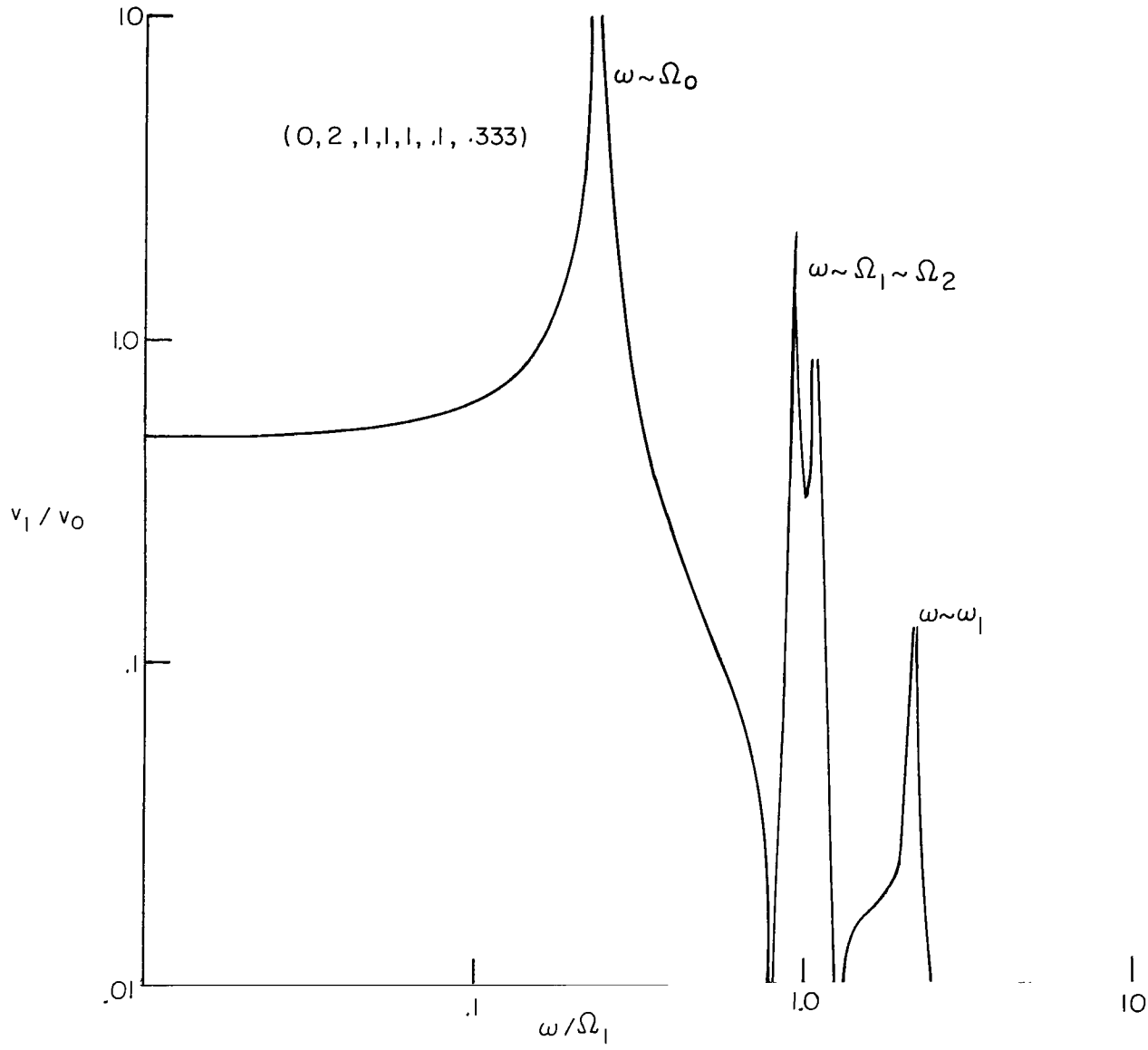

(c) Space-station translation.

Figure 8.- Continued.

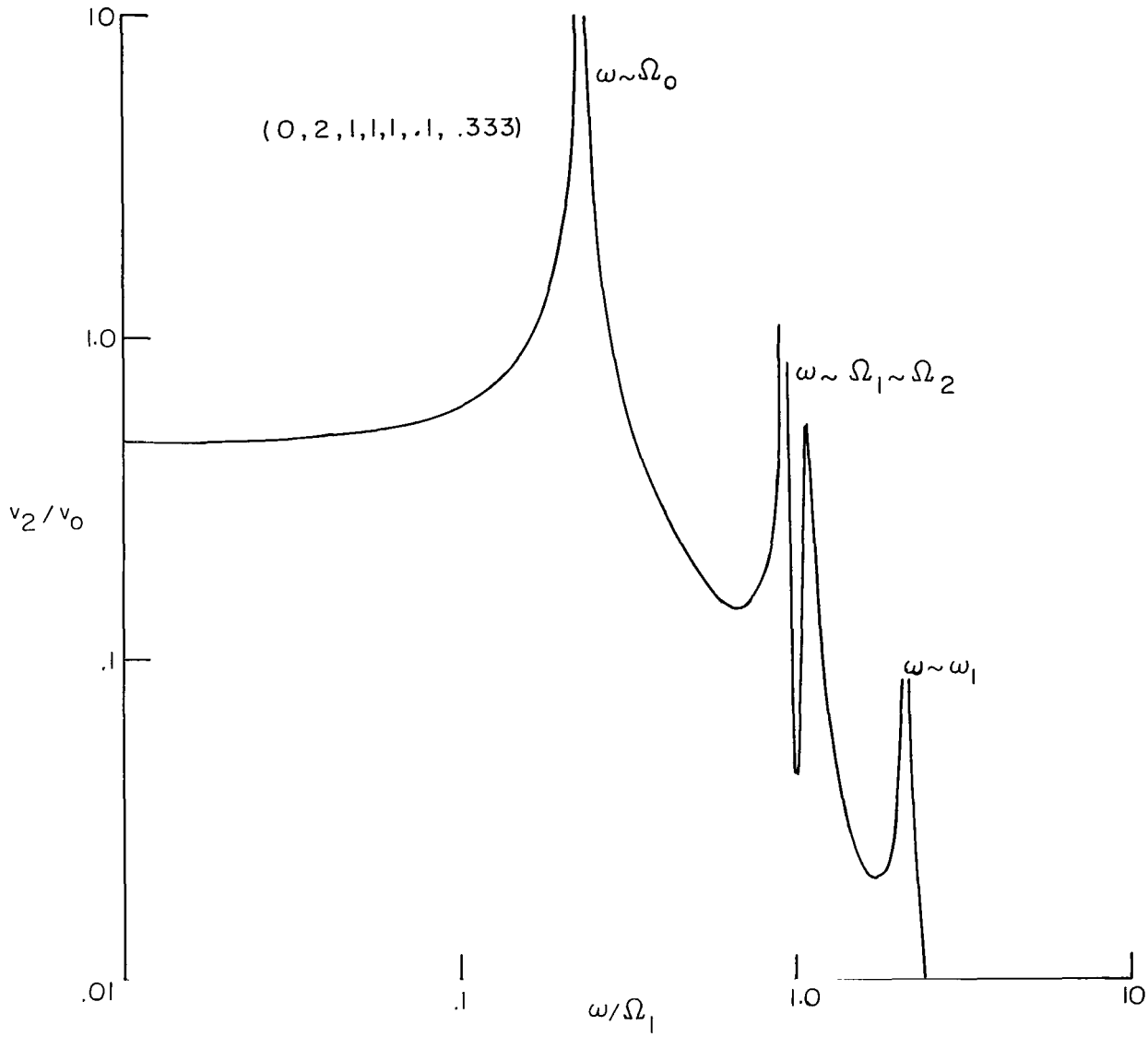

(d) Counterweight translation.

Figure 8.- Concluded.

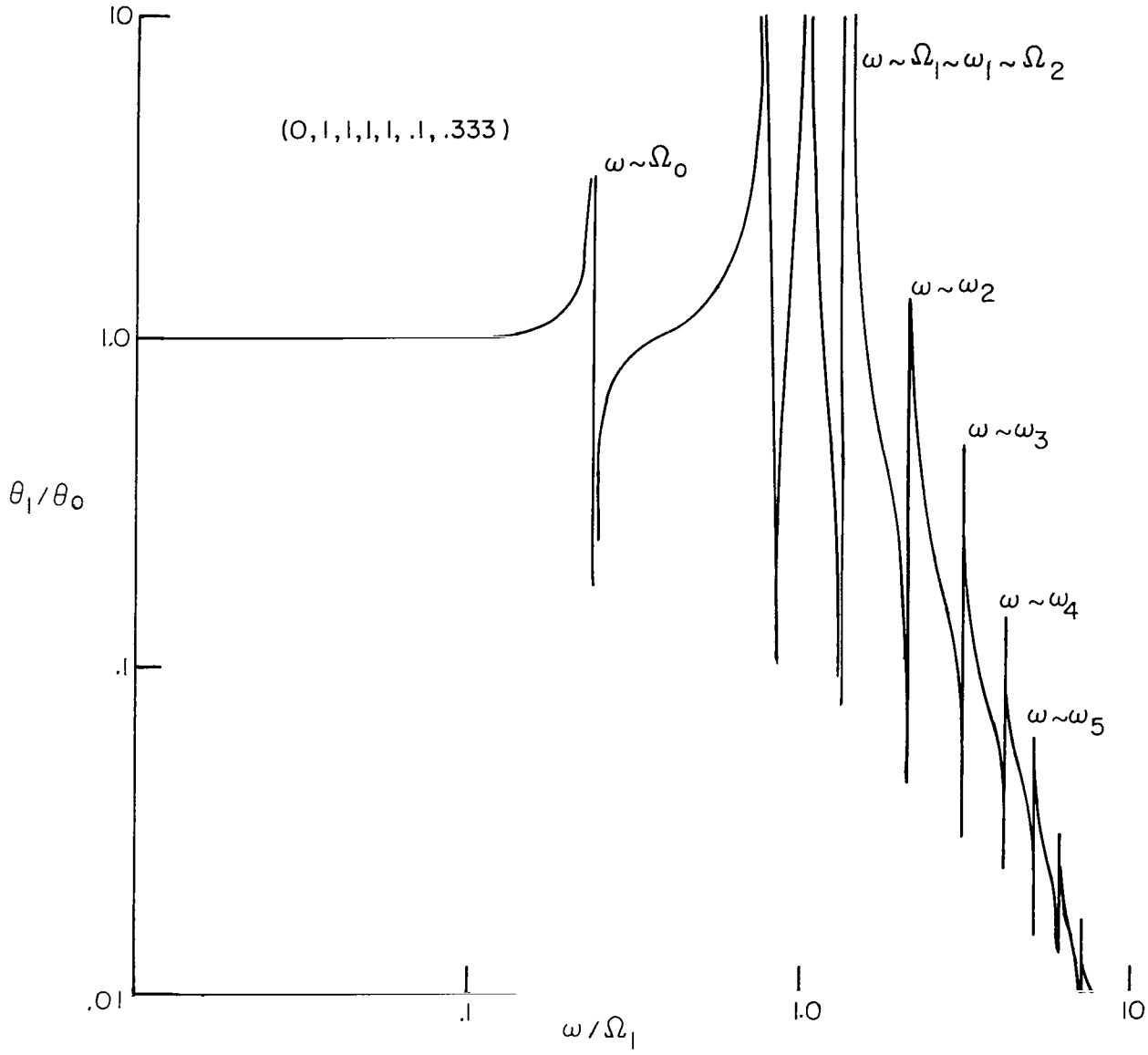

(a) Space-station attitude.

Figure 9.- Steady-state response for equal cable and space-station frequency.

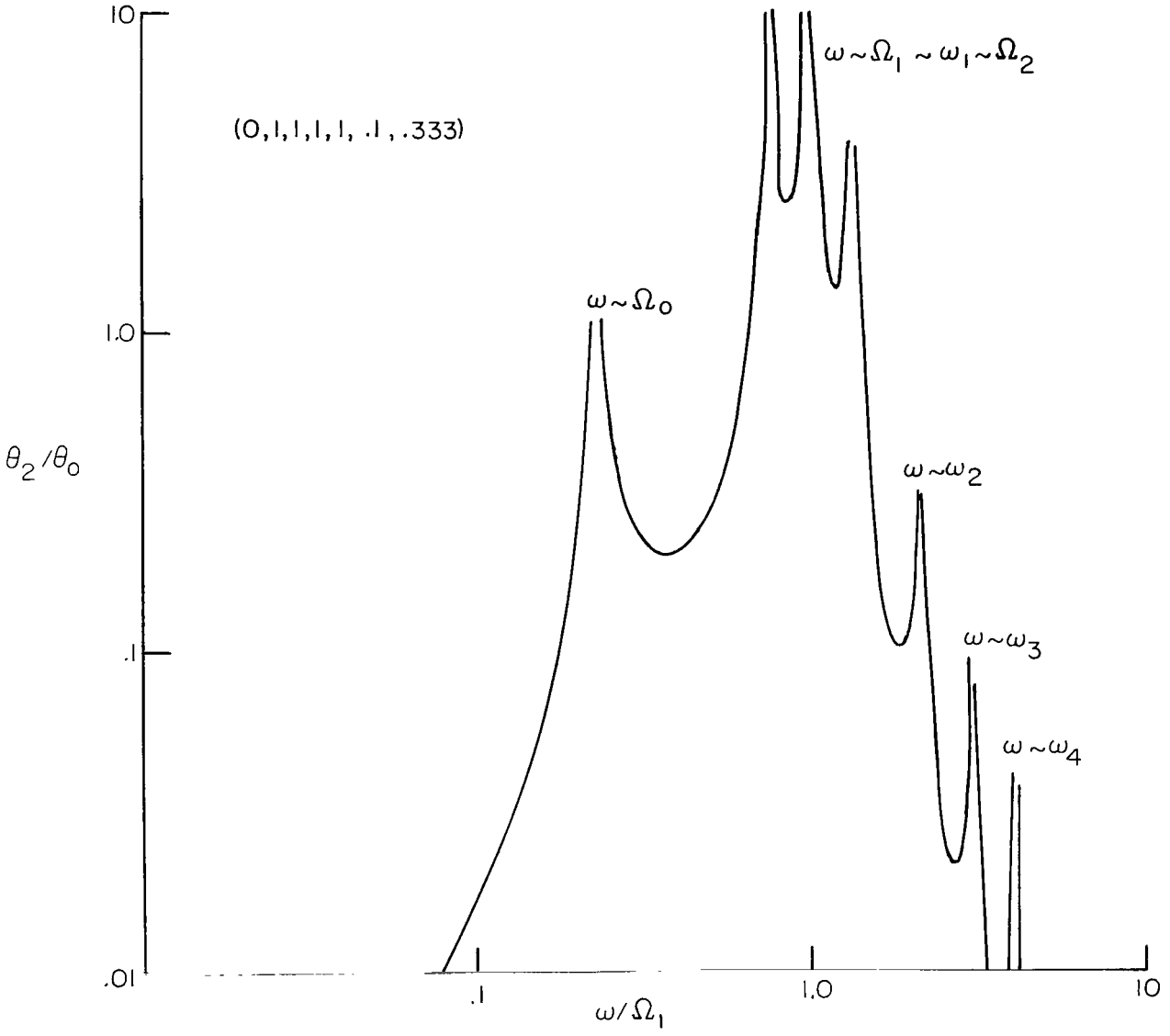

(b) Counterweight attitude.

Figure 9.- Continued.

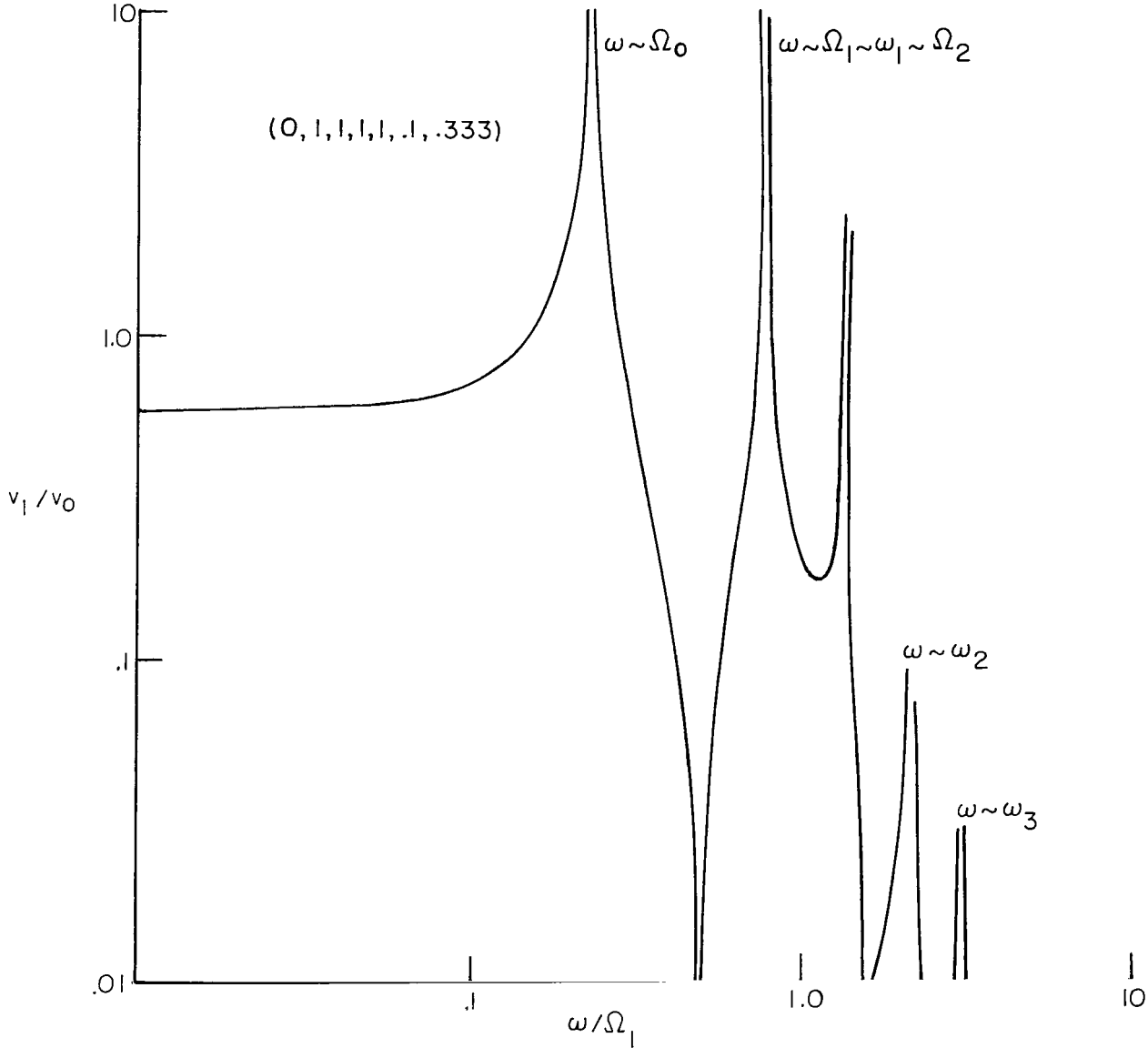

(c) Space-station translation.

Figure 9.- Continued.

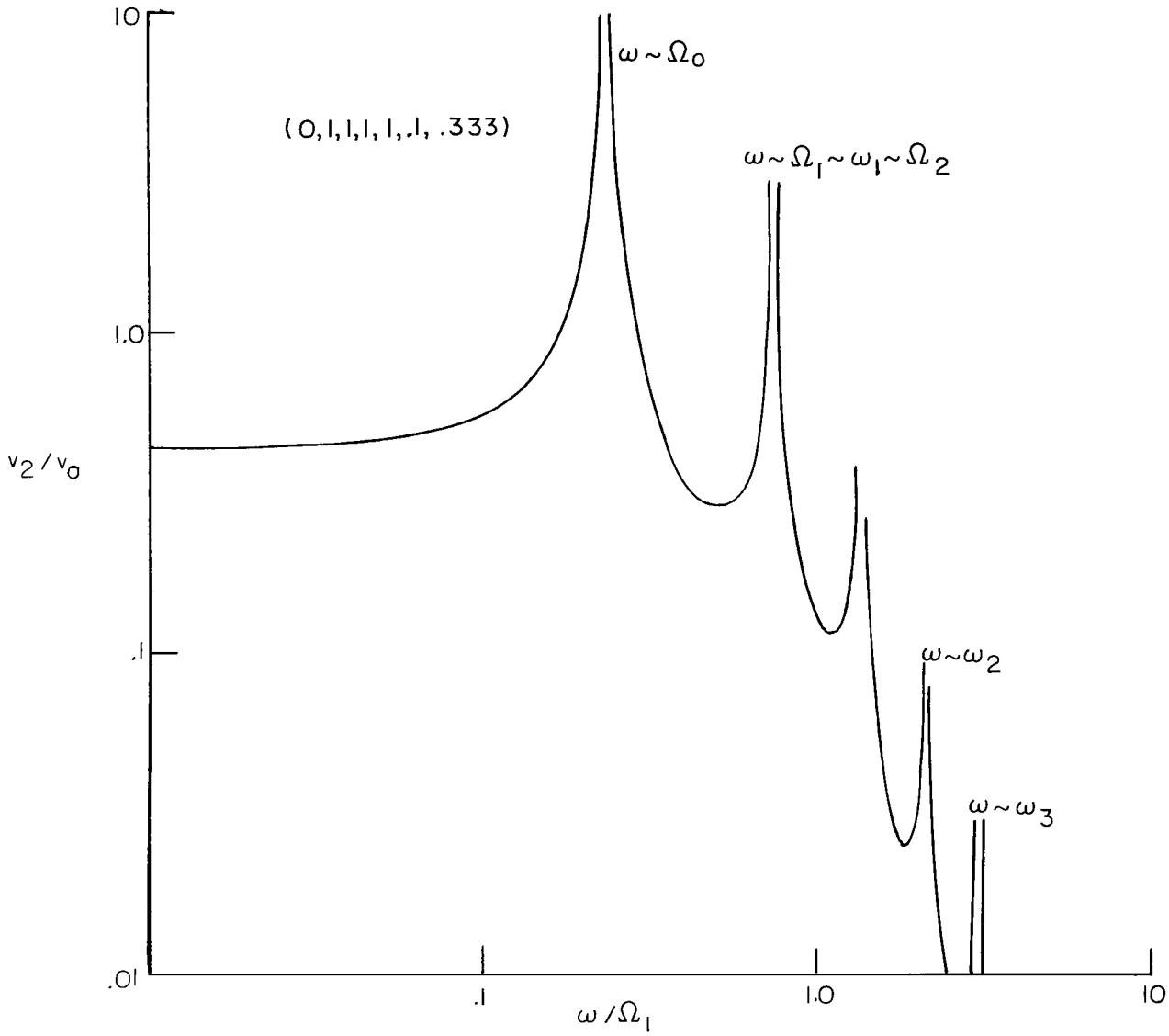

(d) Counterweight translation.

Figure 9.- Concluded.

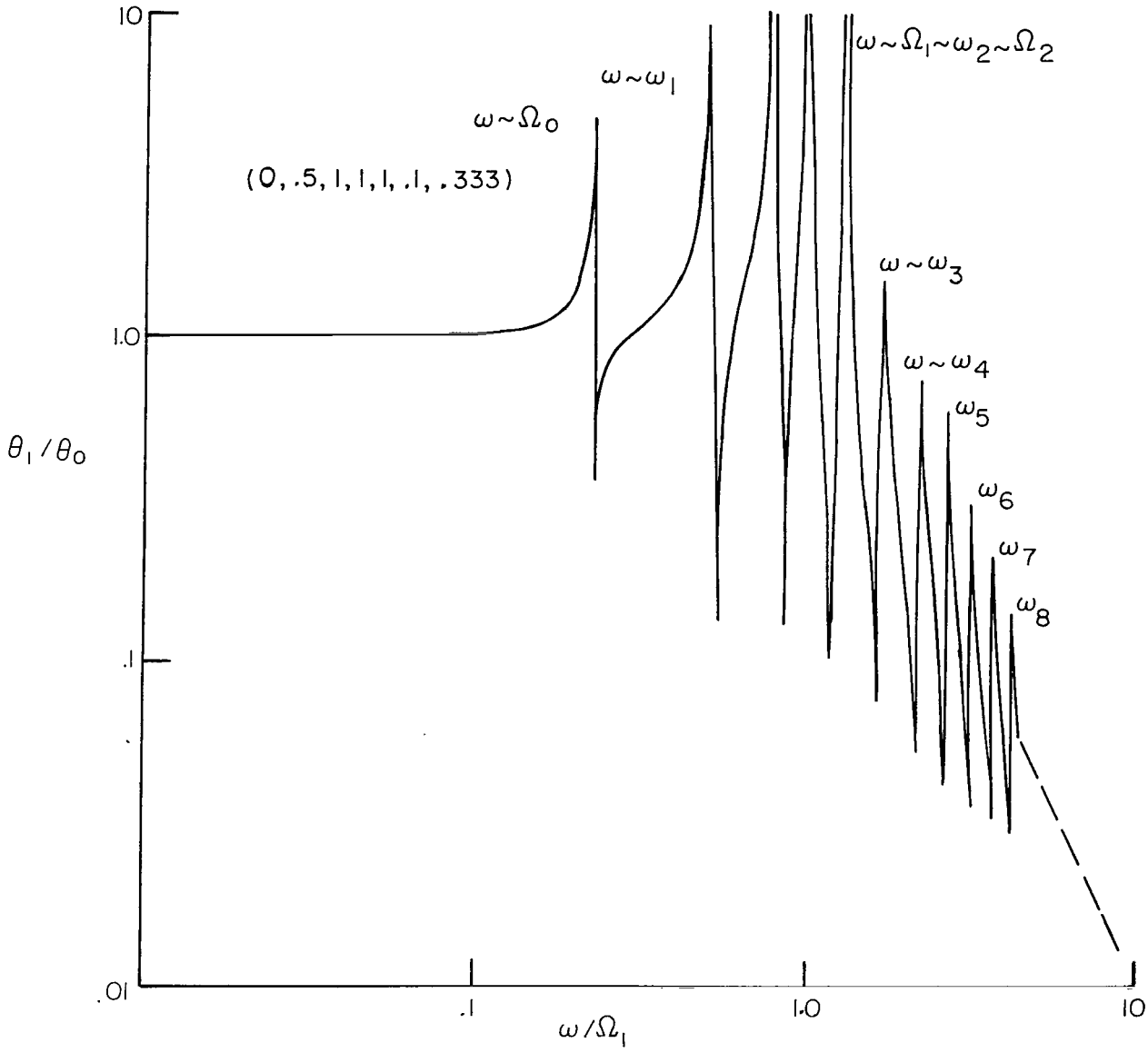

(a) Space-station attitude.

Figure 10.- Steady-state response for low cable frequency.

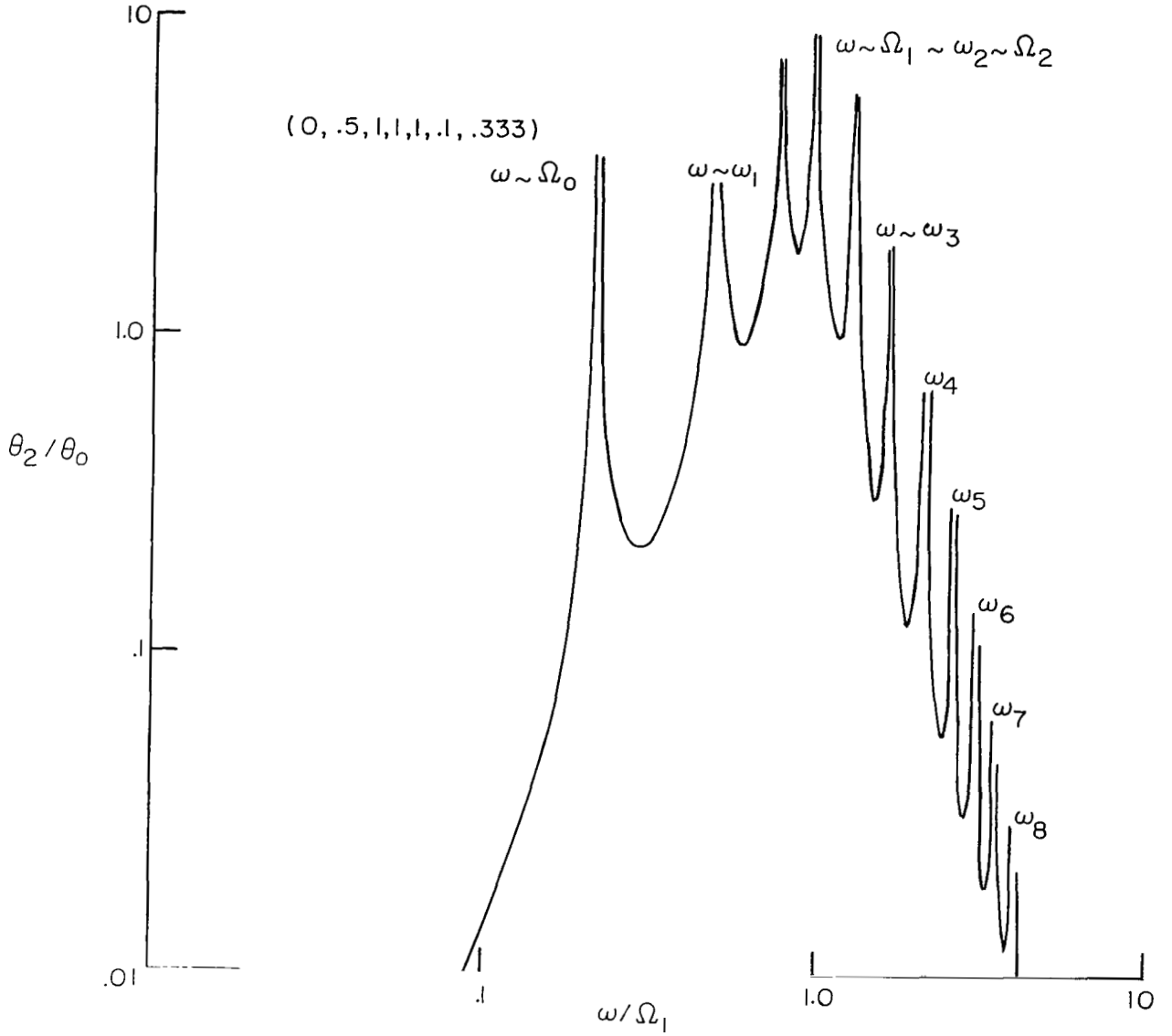

(b) Counterweight attitude.

Figure 10.- Continued.

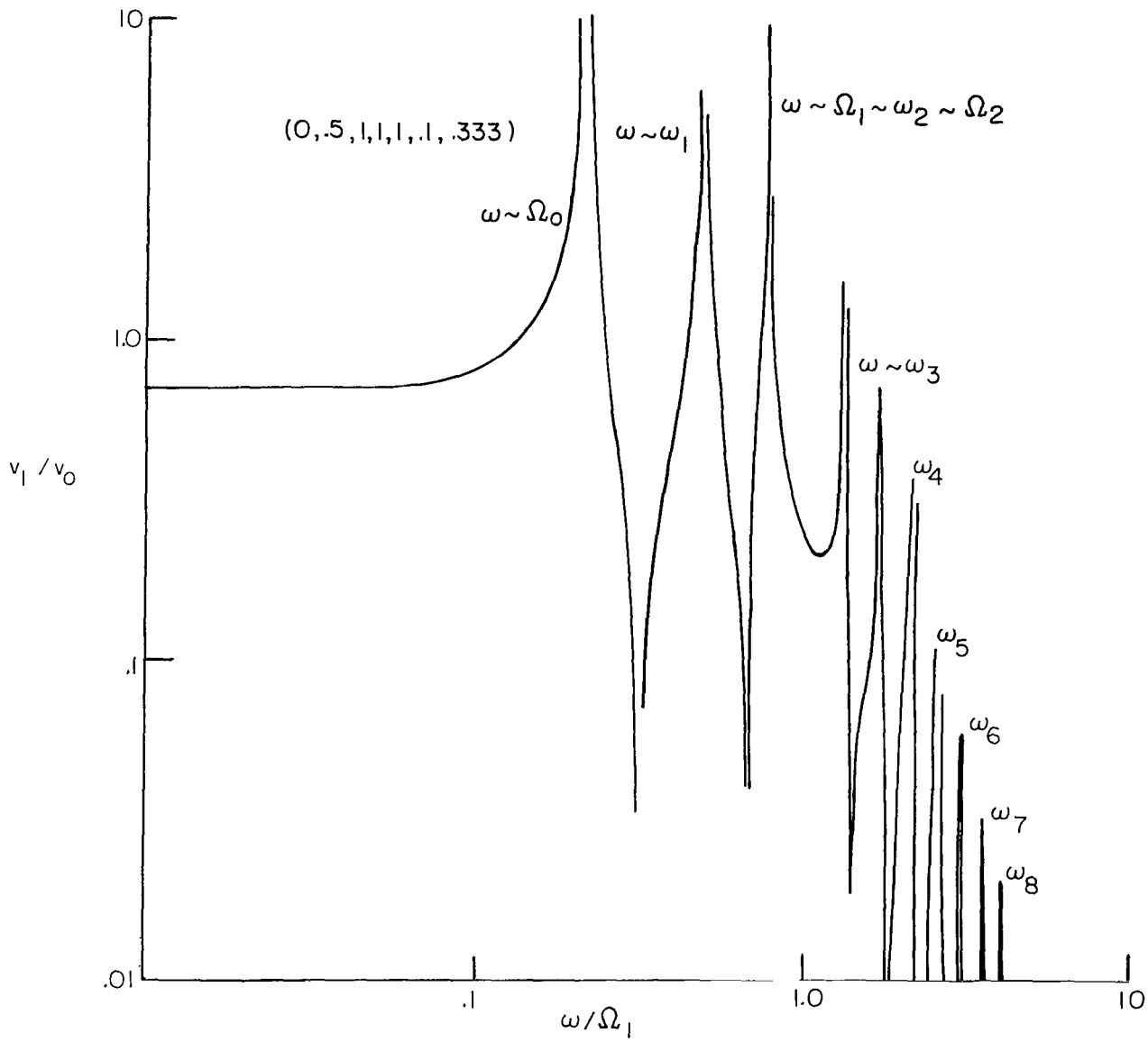

(c) Space-station translation.

Figure 10.- Continued.

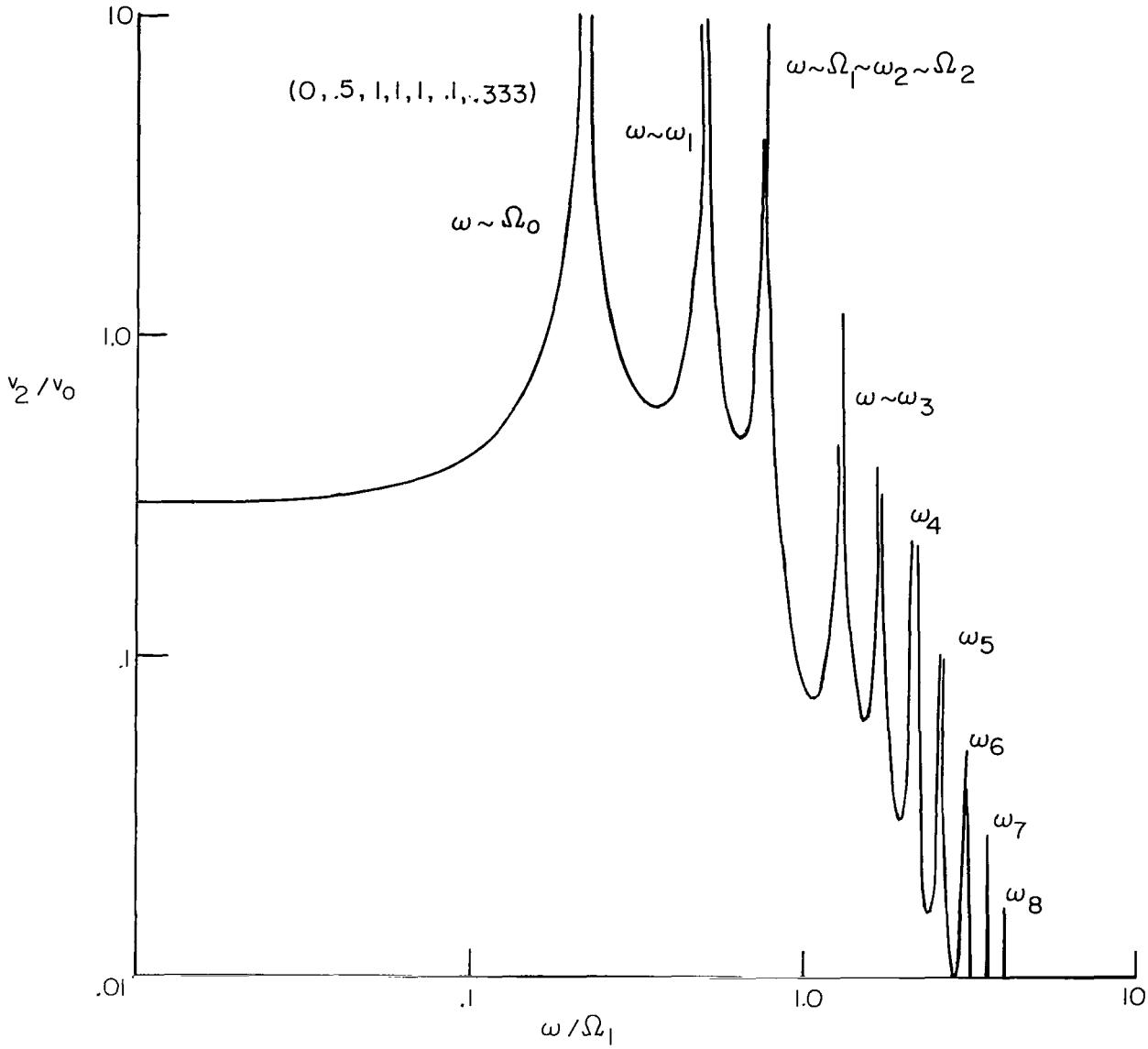

(d) Counterweight translation.

Figure 10.- Concluded.

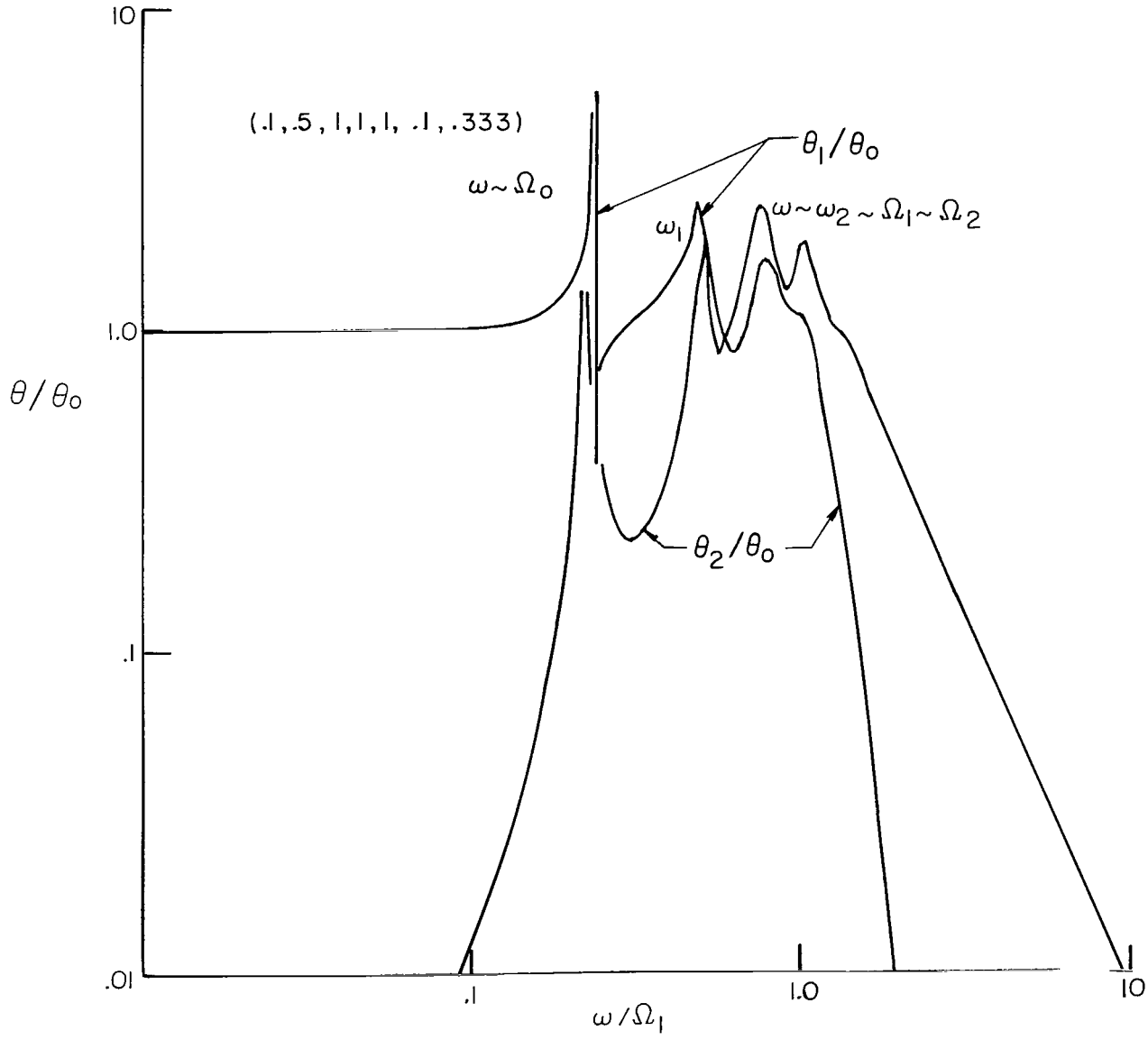

Figure 11.- Steady-state response for damped cable.

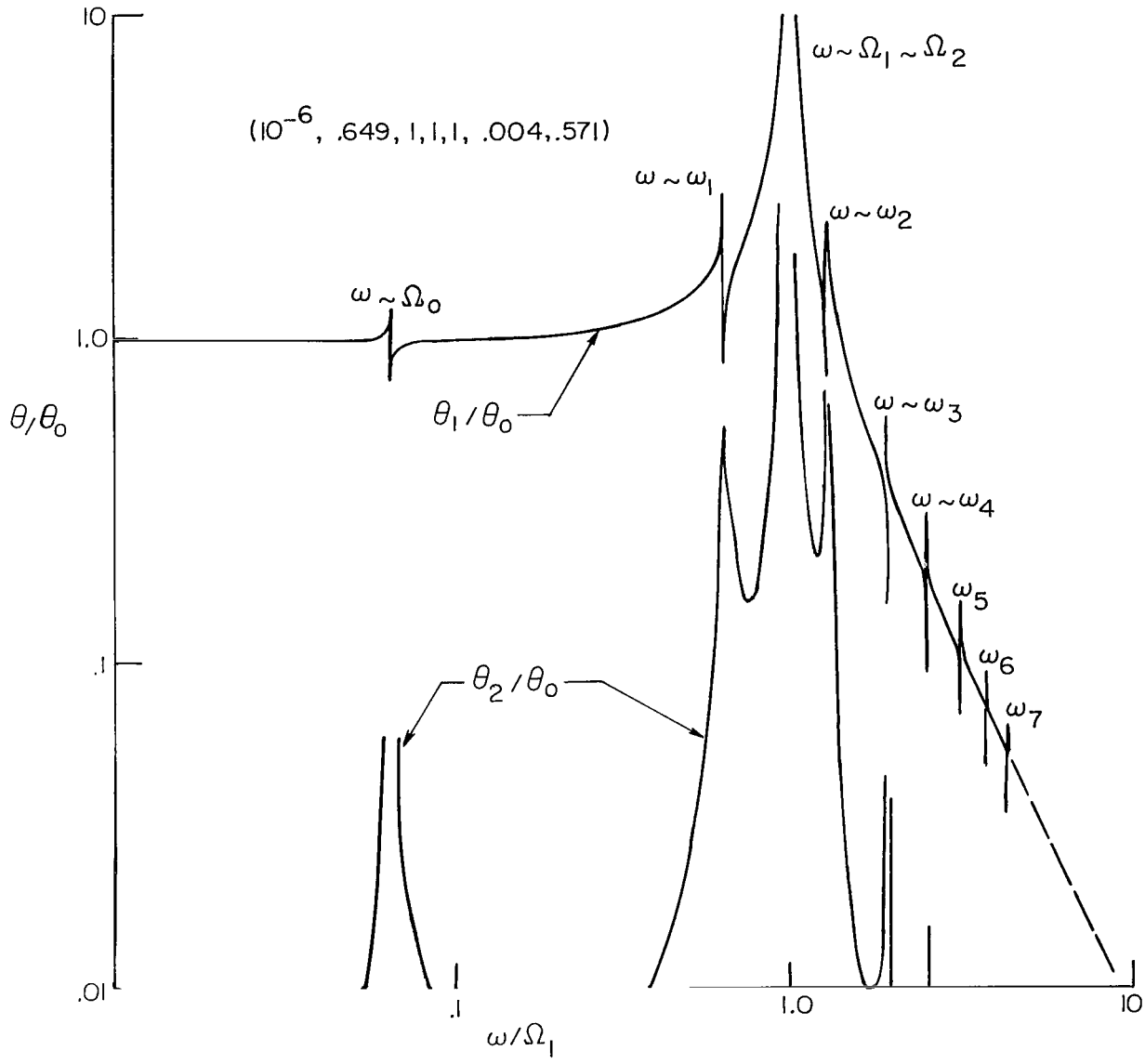

(a) Space-station and counterweight attitude.

Figure 12.- Typical system steady-state response.

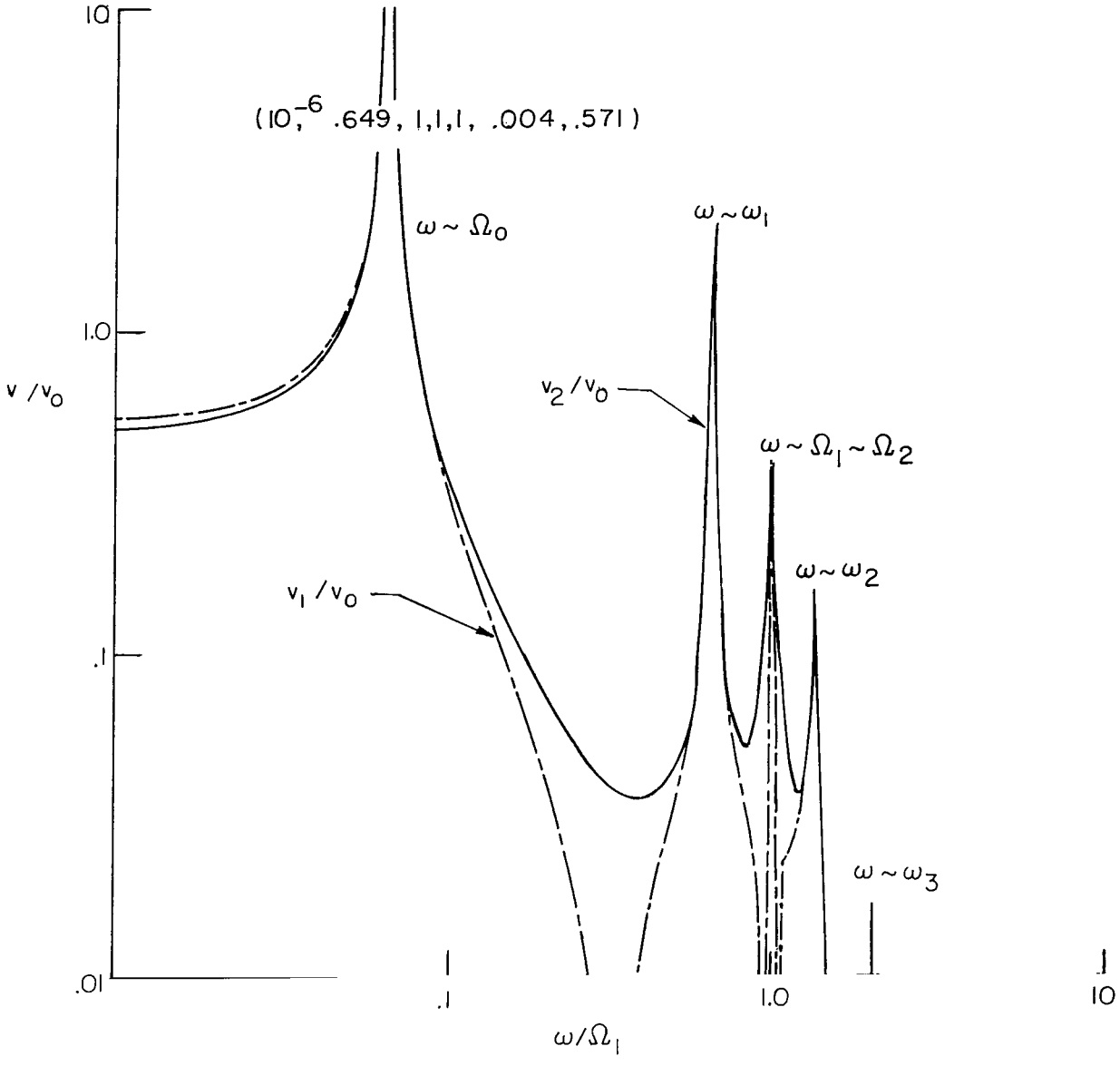

(b) Space-station and counterweight translation.

Figure 12.- Concluded.

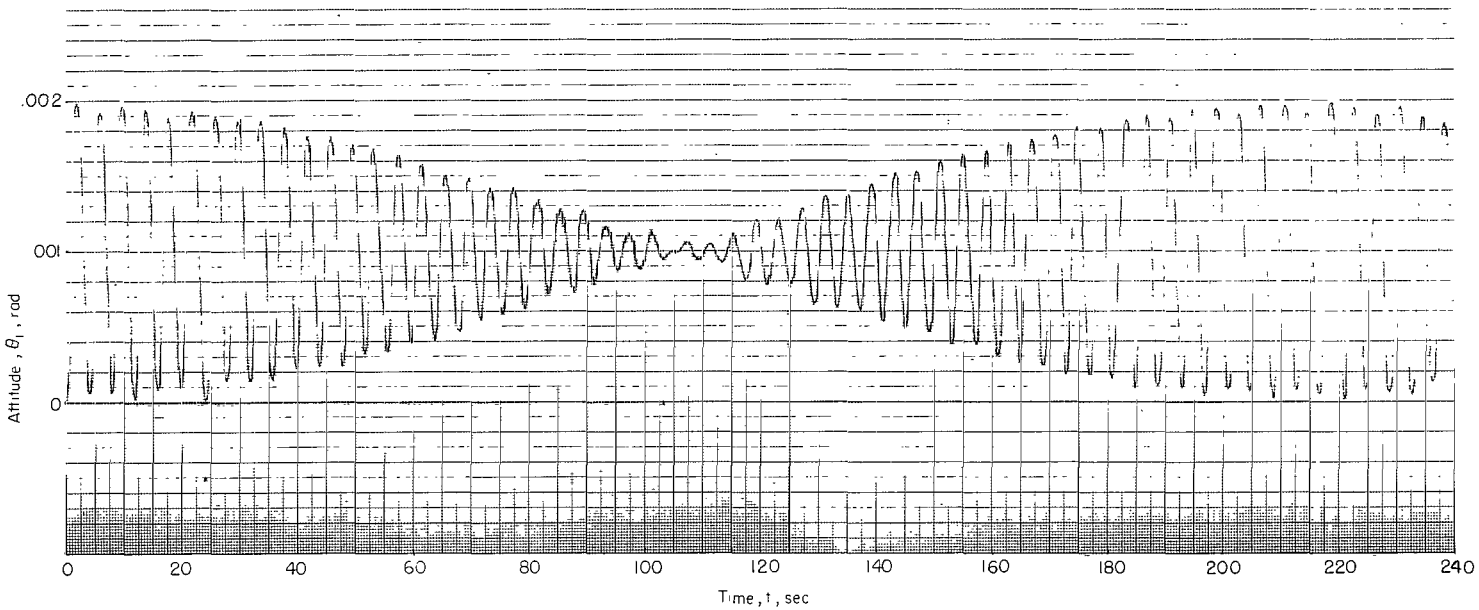

(a) Space-station attitude.

Figure 13.- Transient response to constant step input torque.

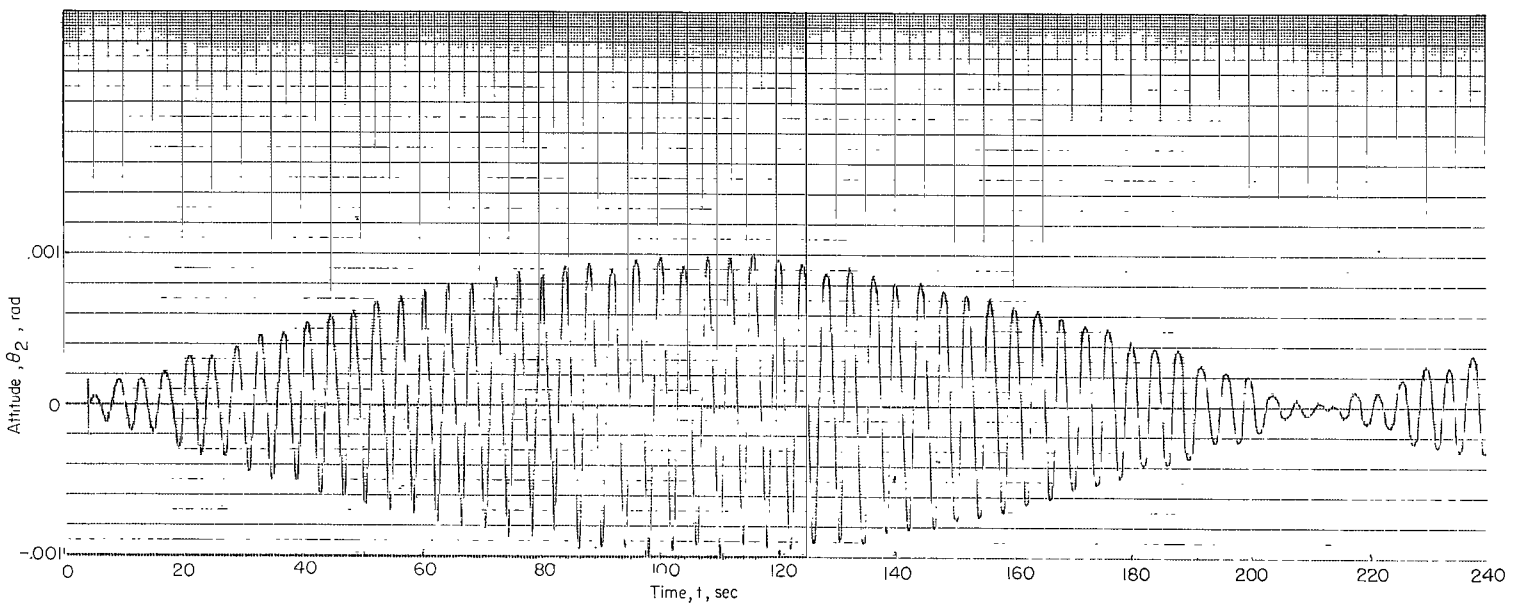

(b) Counterweight attitude.

Figure 13.- Continued.

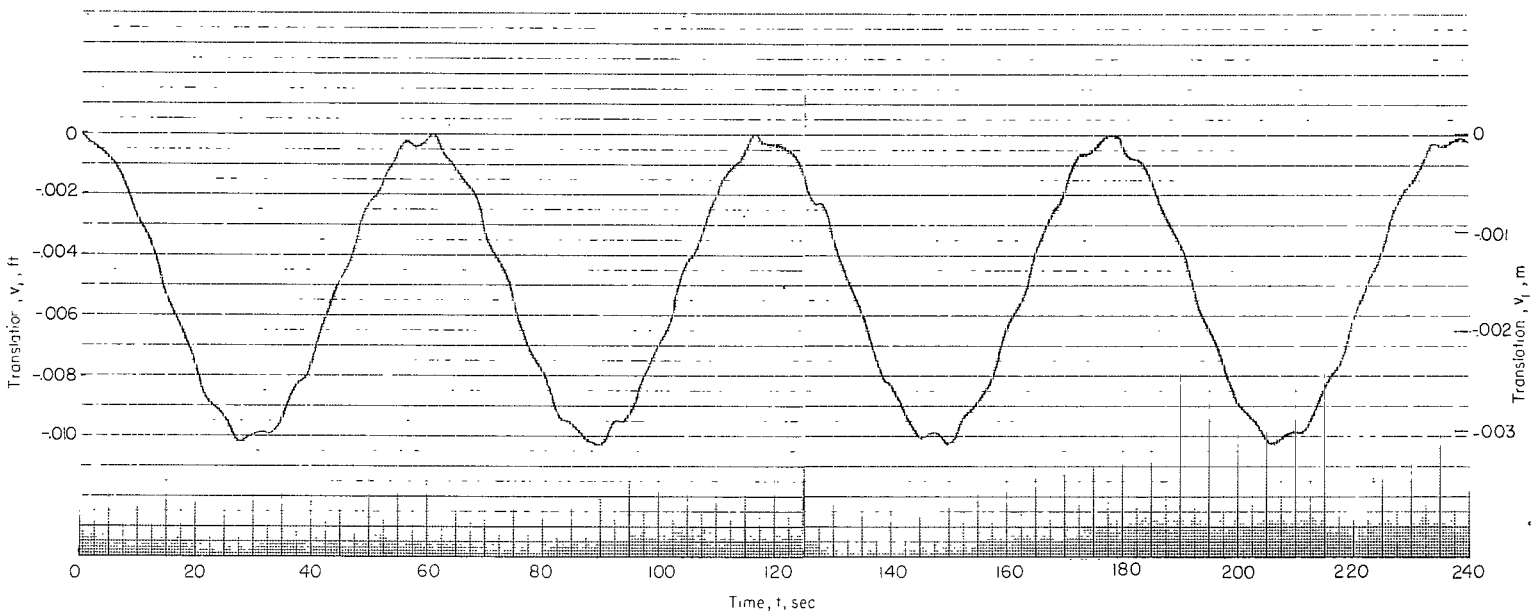

(c) Space-station translation.

Figure 13.- Continued.

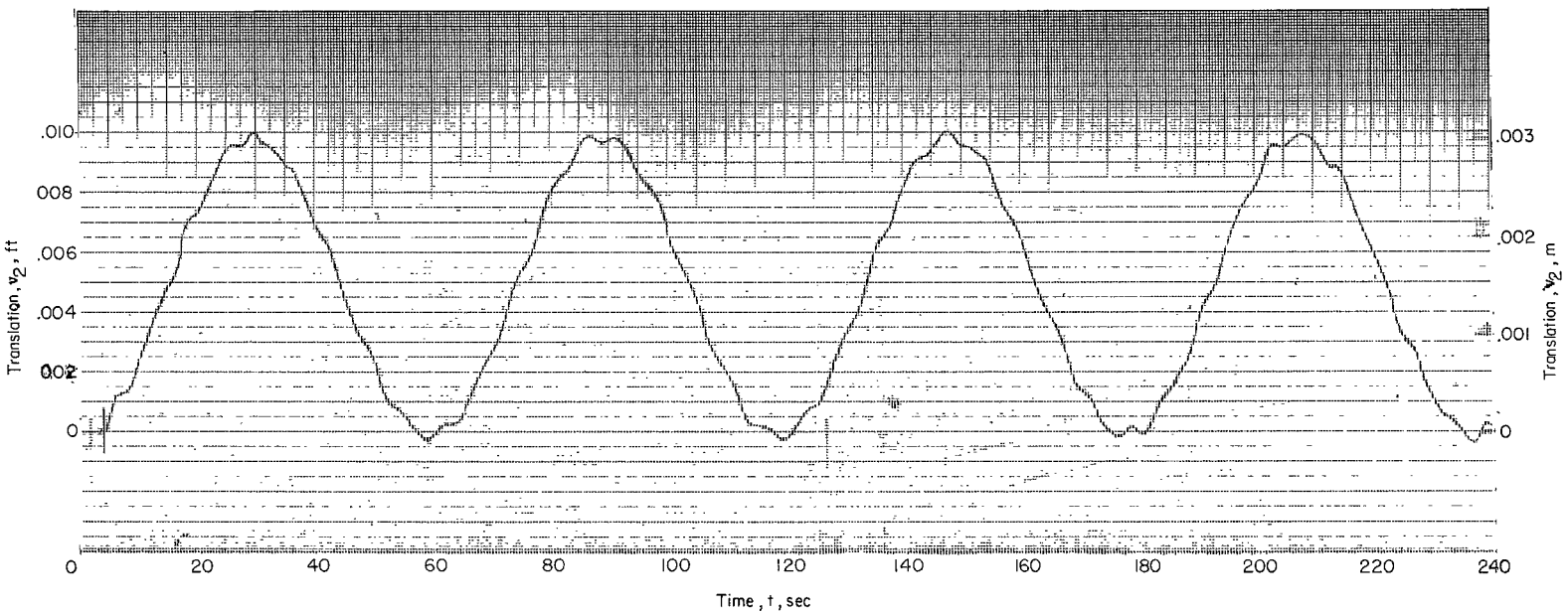

(d) Counterweight translation.

Figure 13.- Concluded.

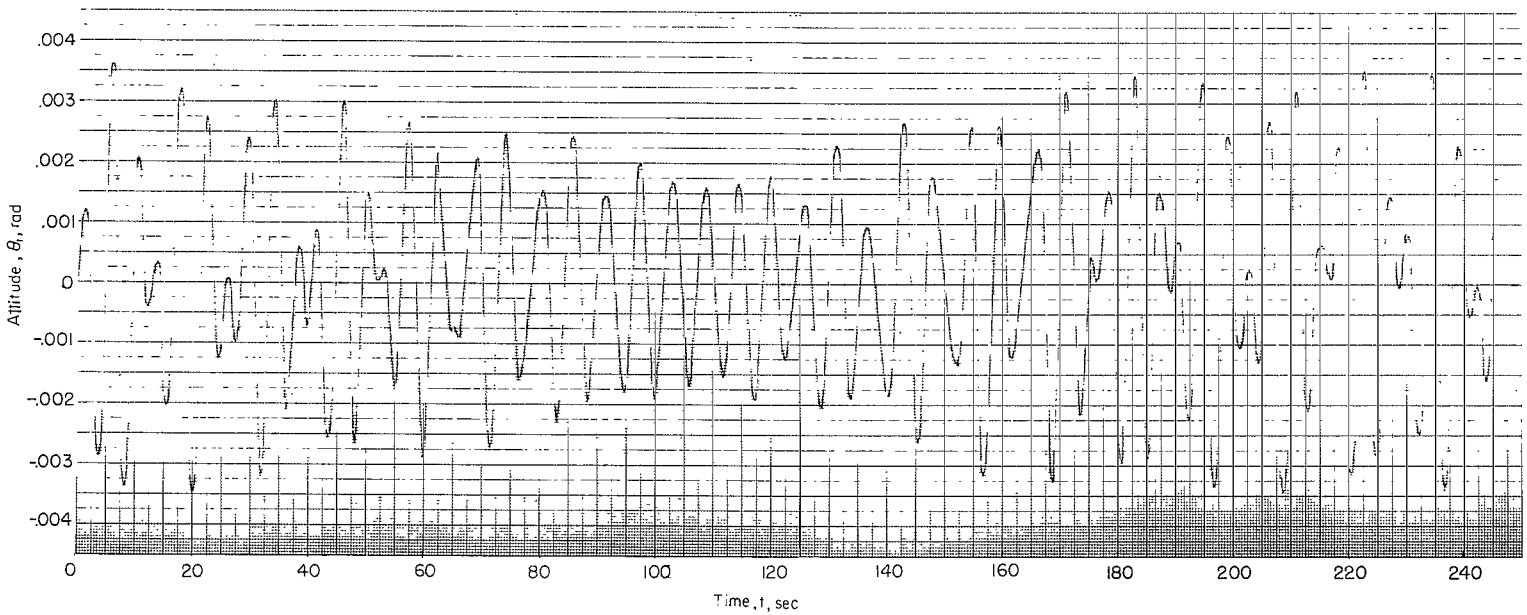

(a) Space-station attitude.

Figure 14.- Transient response to oscillatory step input torque.

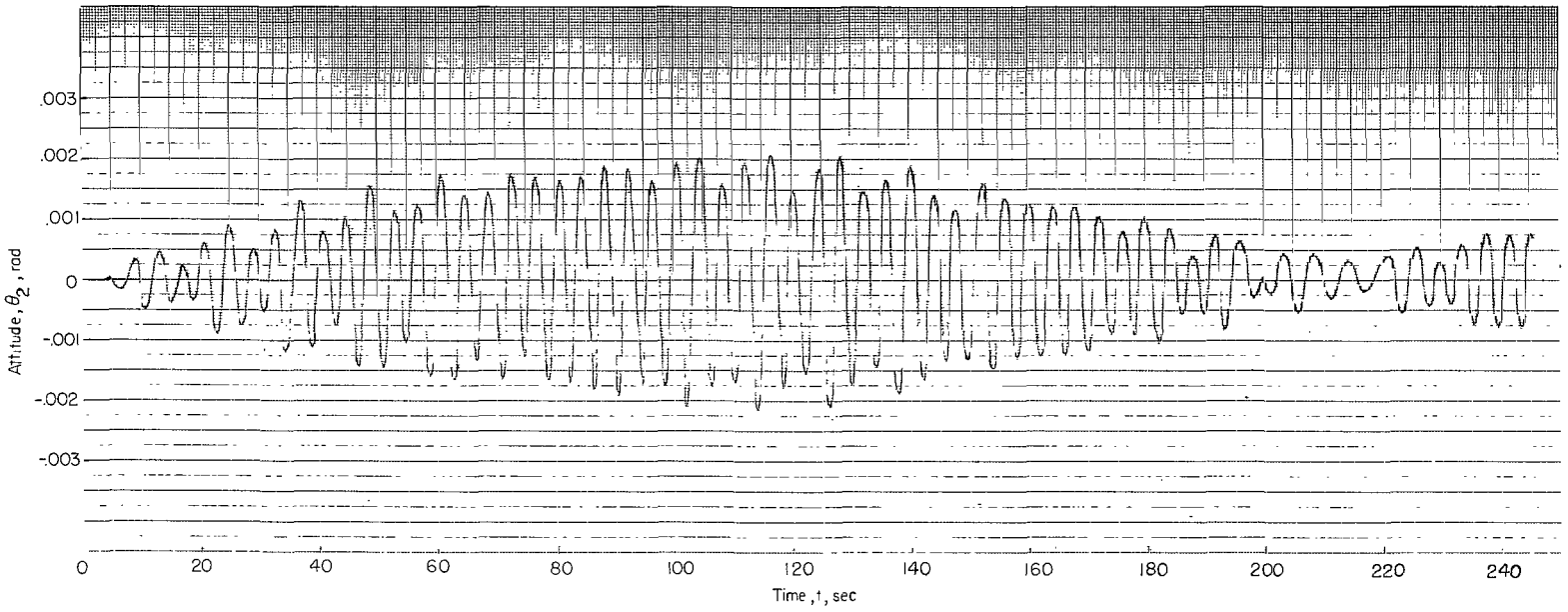

(b) Counterweight attitude.

Figure 14.- Continued.

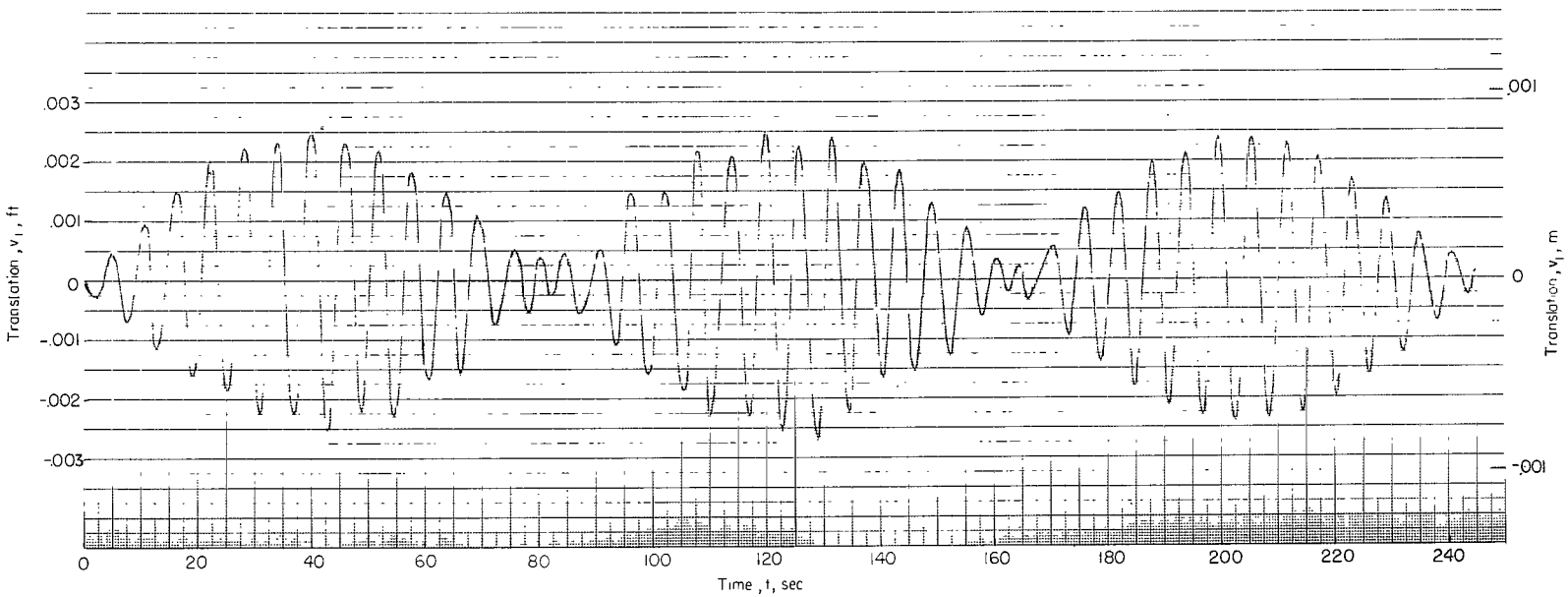

(c) Space-station translation.

Figure 14.- Continued.

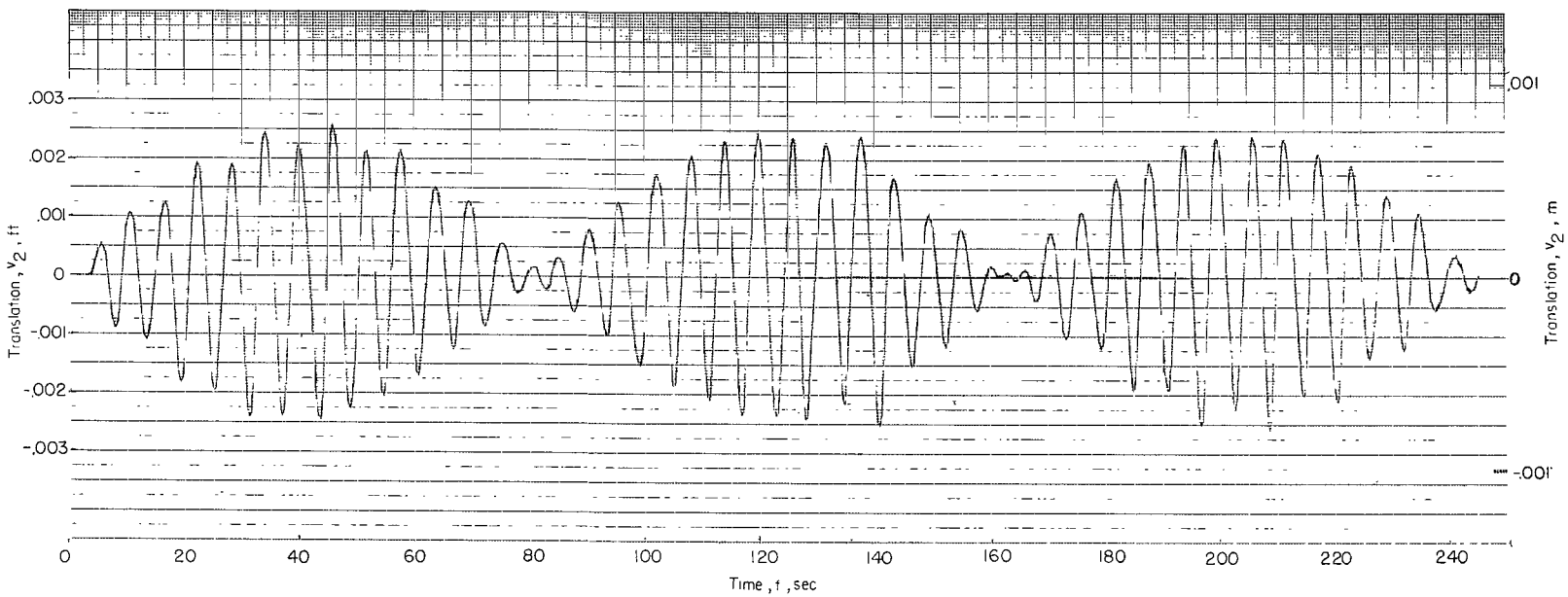

(d) Counterweight translation.

Figure 14.- Concluded.

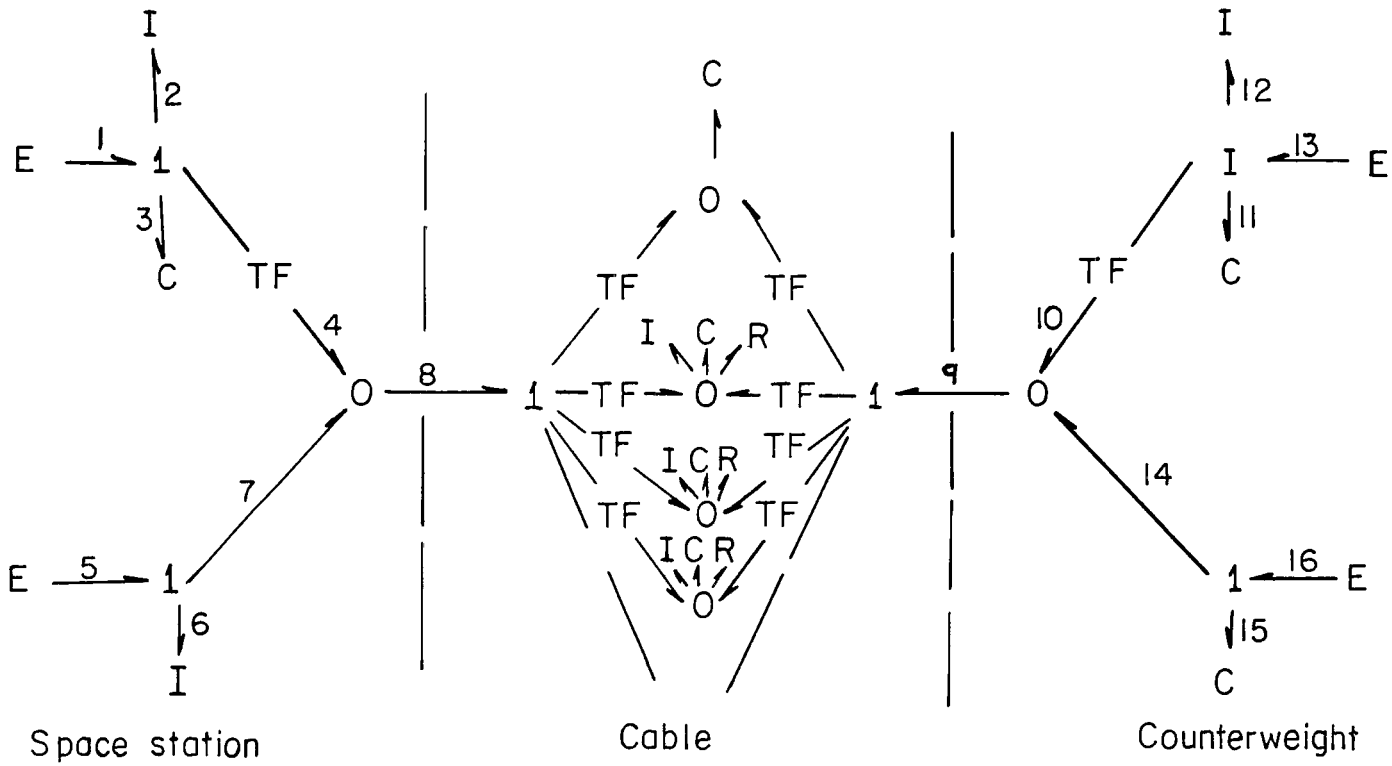

Figure 15.- Bond graph representation of system. (See appendix F for discussion of notation.)

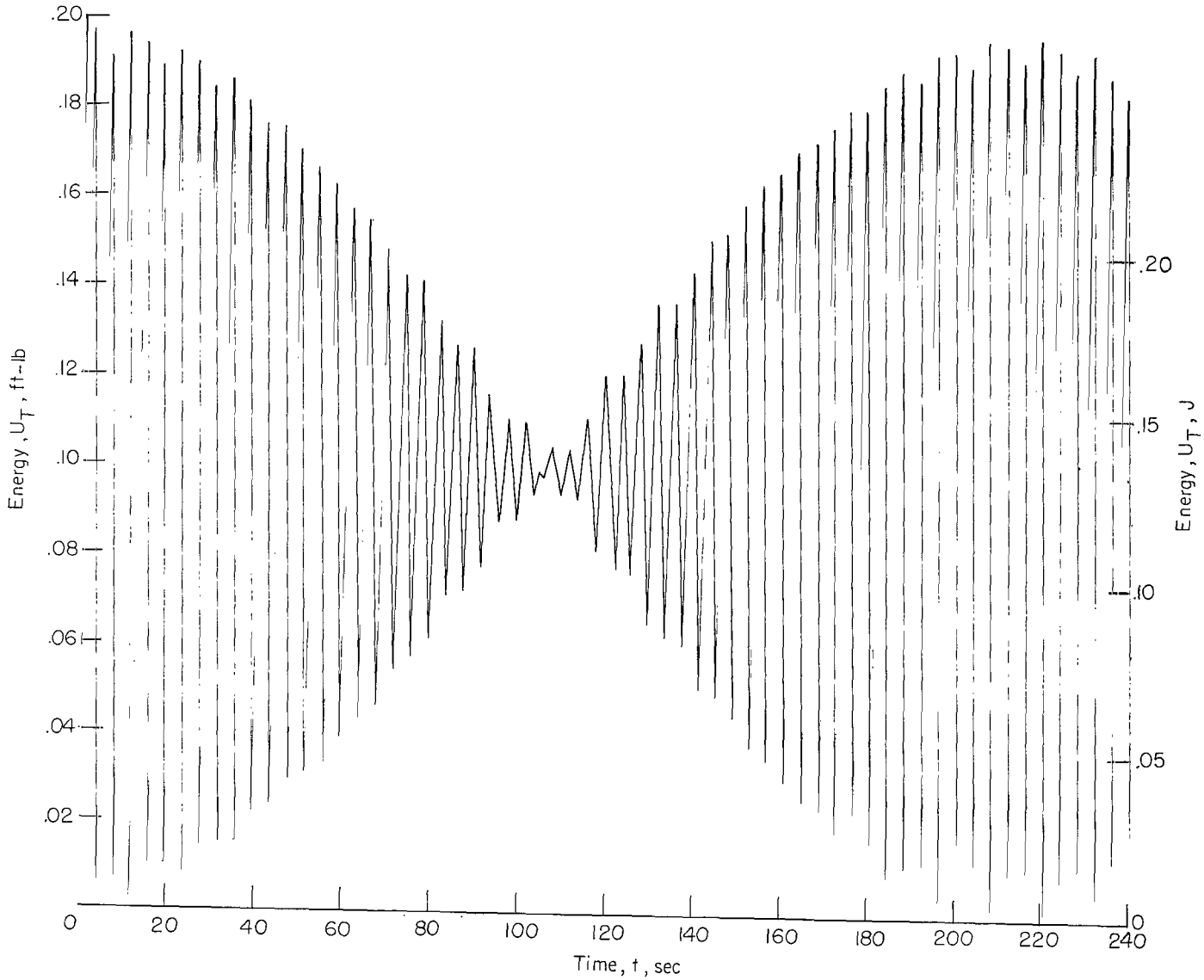

(a) Total energy.

Figure 16.- Energy flow for constant step input torque.

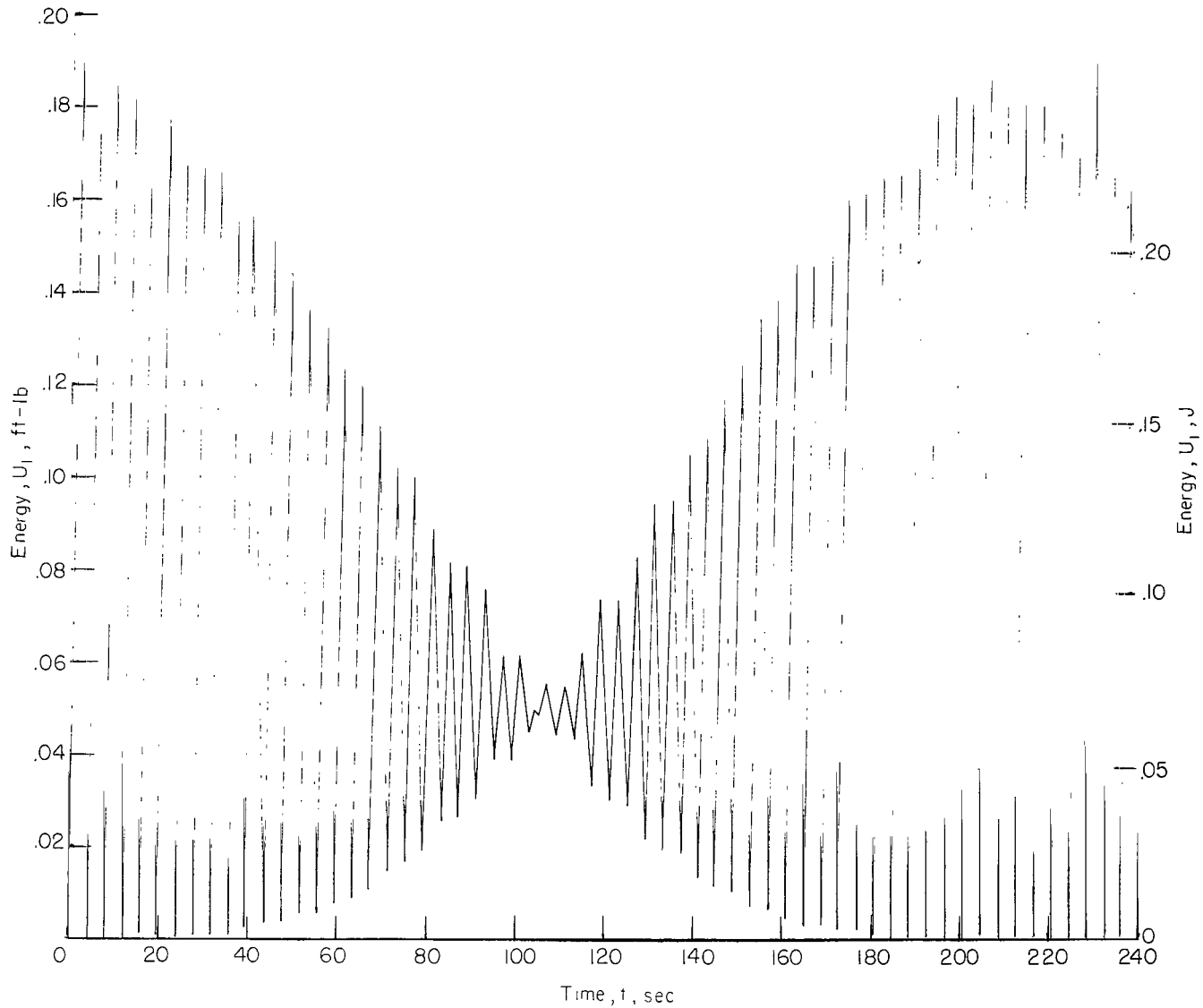

(b) Space-station energy.

Figure 16.- Continued.

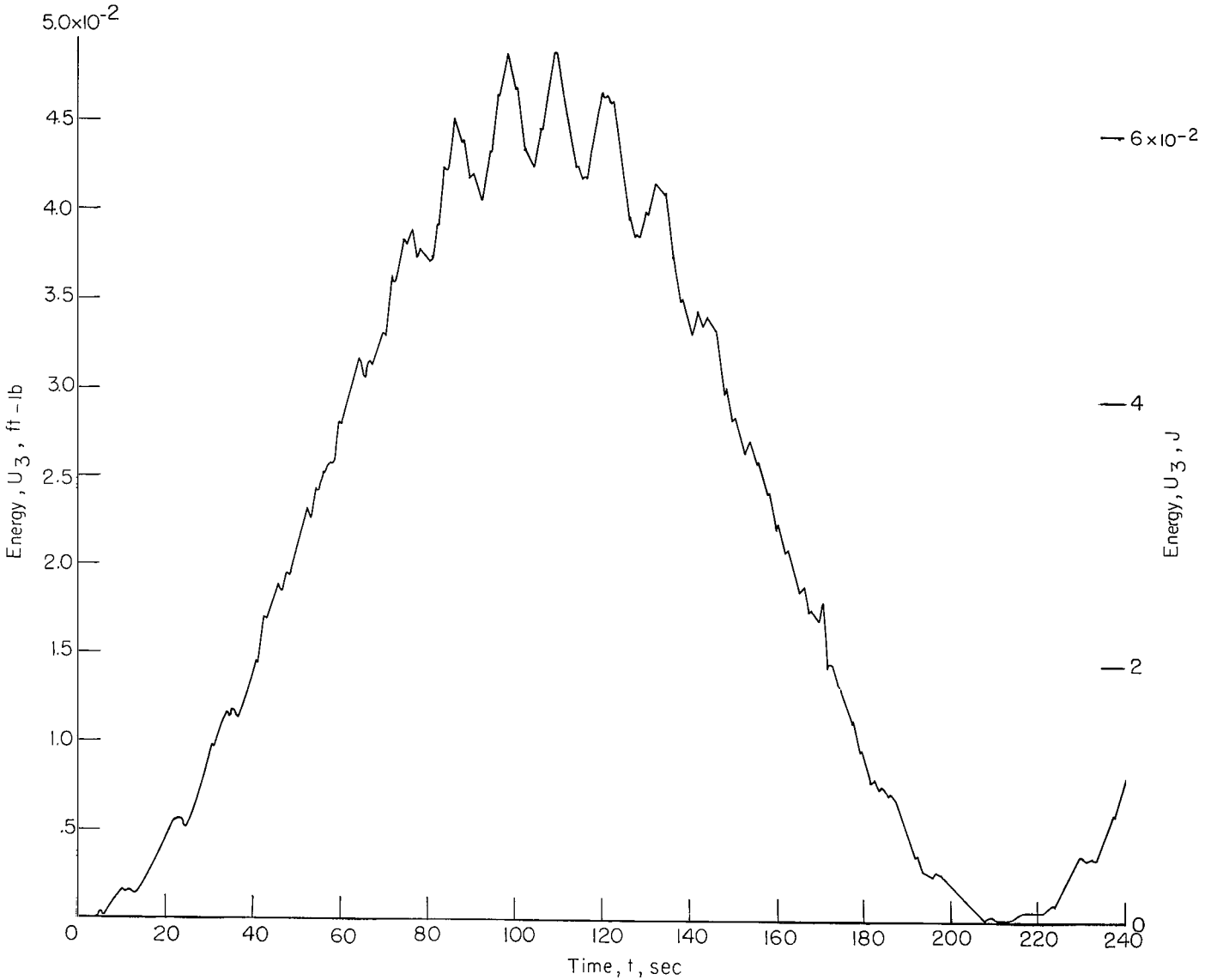

(c) Counterweight energy.

Figure 16.- Continued.

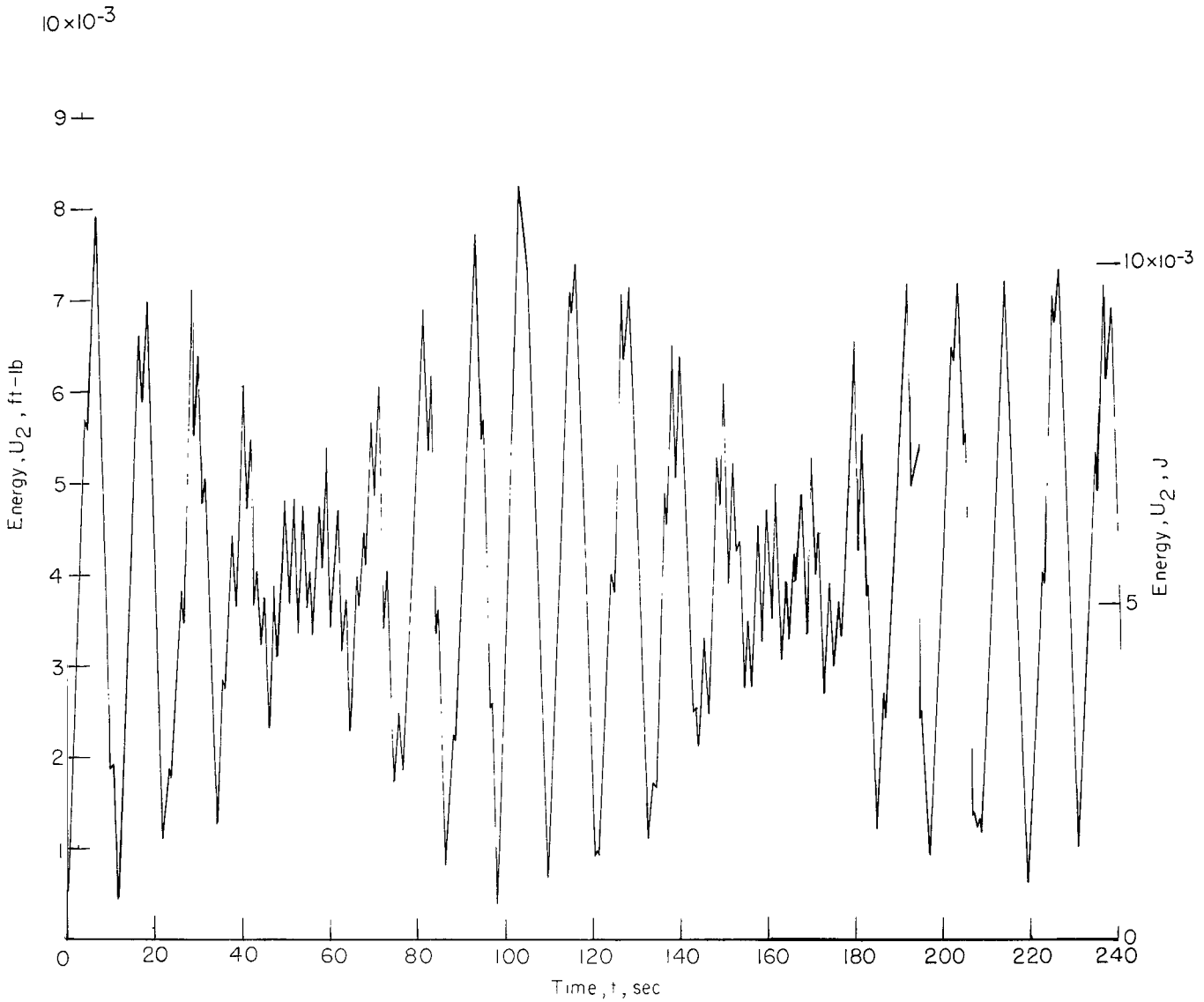

(d) Cable energy.

Figure 16.- Concluded.

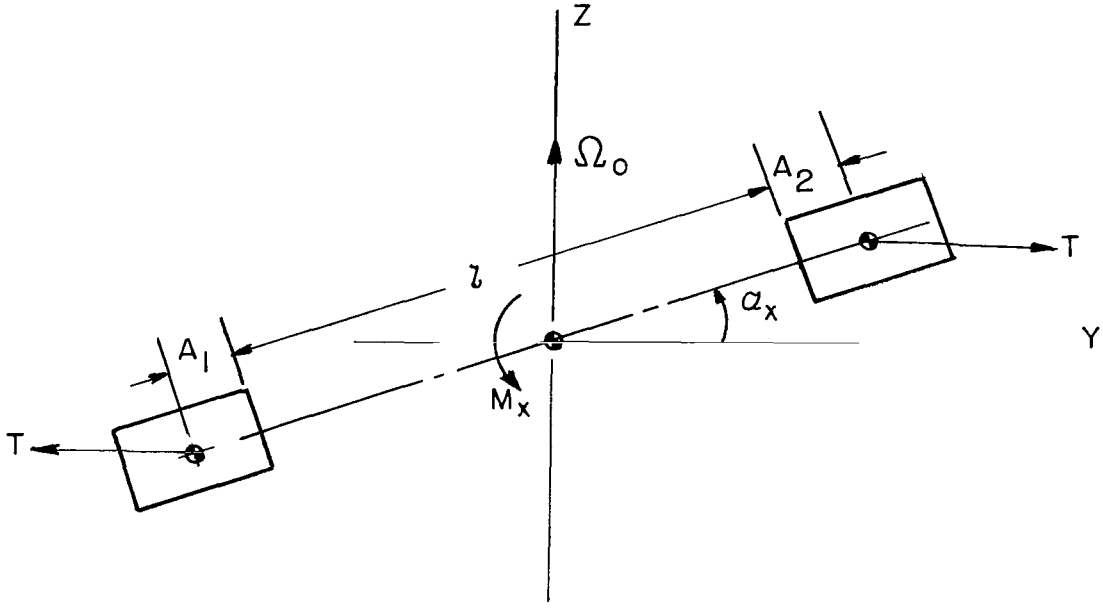

(a) Rigid-body dynamics in YZ plane.

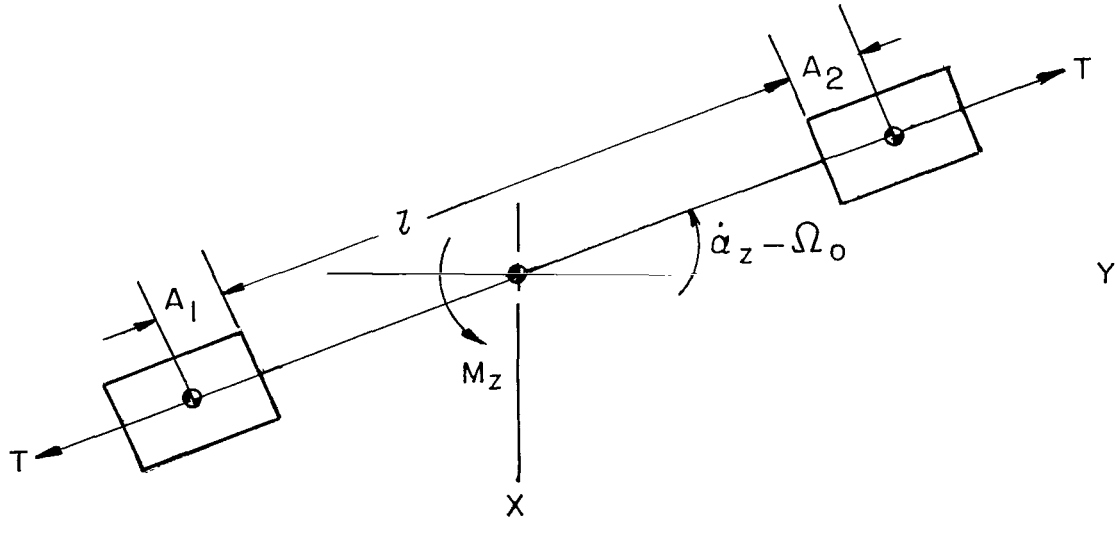

(b) Rigid-body dynamics in XY plane.

Figure 17.- Rigid-body configuration.

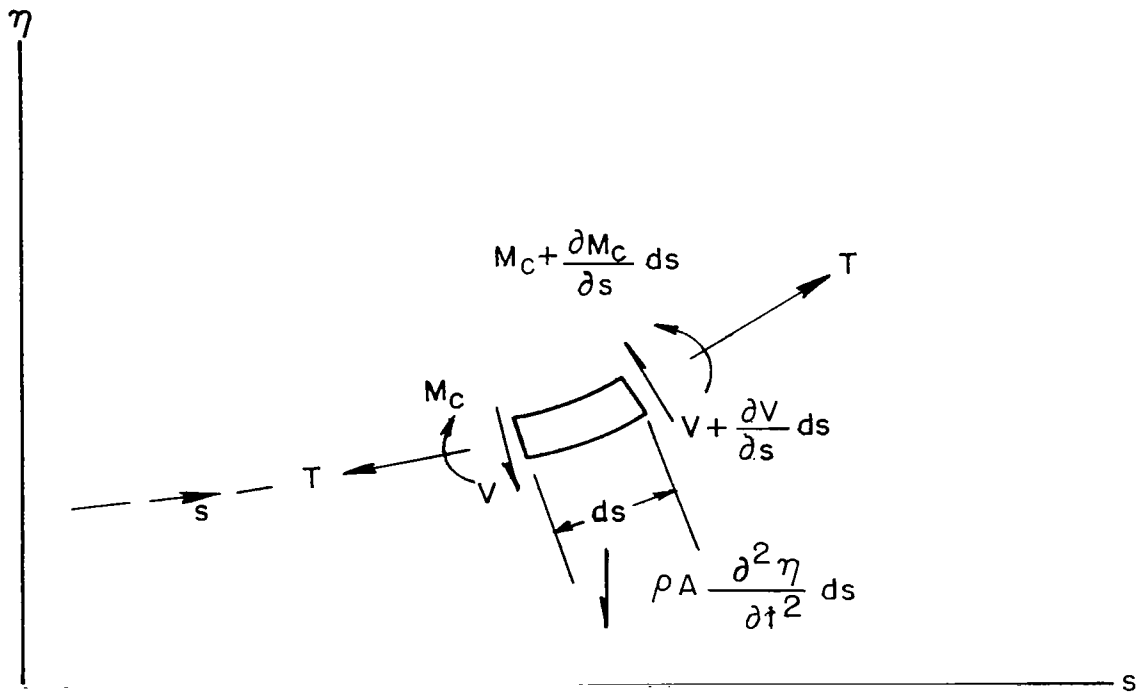

Figure 18.- Incremental cable mass equilibrium.

NATIONAL AERONAUTICS AND SPACE ADMINISTRATION
WASHINGTON, D. C. 20546

OFFICIAL BUSINESS

FIRST CLASS MAIL

POSTAGE AND FEES PAID
NATIONAL AERONAUTICS AND
SPACE ADMINISTRATION

POSTMASTER: If Undeliverable (Section 158 Postal Manual) Do Not Return

"The aeronautical and space activities of the United States shall be conducted so as to contribute . . . to the expansion of human knowledge of phenomena in the atmosphere and space. The Administration shall provide for the widest practicable and appropriate dissemination of information concerning its activities and the results thereof."

—NATIONAL AERONAUTICS AND SPACE ACT OF 1958

NASA SCIENTIFIC AND TECHNICAL PUBLICATIONS

TECHNICAL REPORTS: Scientific and technical information considered important, complete, and a lasting contribution to existing knowledge.

TECHNICAL NOTES: Information less broad in scope but nevertheless of importance as a contribution to existing knowledge.

TECHNICAL MEMORANDUMS: Information receiving limited distribution because of preliminary data, security classification, or other reasons.

CONTRACTOR REPORTS: Scientific and technical information generated under a NASA contract or grant and considered an important contribution to existing knowledge.

TECHNICAL TRANSLATIONS: Information published in a foreign language considered to merit NASA distribution in English.

SPECIAL PUBLICATIONS: Information derived from or of value to NASA activities. Publications include conference proceedings, monographs, data compilations, handbooks, sourcebooks, and special bibliographies.

TECHNOLOGY UTILIZATION PUBLICATIONS: Information on technology used by NASA that may be of particular interest in commercial and other non-aerospace applications. Publications include Tech Briefs, Technology Utilization Reports and Notes, and Technology Surveys.

Details on the availability of these publications may be obtained from:

SCIENTIFIC AND TECHNICAL INFORMATION DIVISION

NATIONAL AERONAUTICS AND SPACE ADMINISTRATION

Washington, D.C. 20546